Power-Electronics-Enabled Transient Stabilization of Power Systems

Submitted in partial fulfillment of the requirements for
the degree of
Doctor of Philosophy
in
Electrical and Computer Engineering

Miloš Cvetković

B.Sc., Electrical Engineering, University of Belgrade
M.Sc., Electrical and Computer Engineering, Carnegie Mellon University

Carnegie Mellon University
Pittsburgh, PA

December 2013

Keywords: Power Systems, Stability and Control, Transient Stabilization, Power-electronics, FACTS Devices

To my family

Abstract

Transient stability of electric energy grids is defined as the ability of the power system to remain in synchronism during large disturbances. If the grid is not equipped with controllers capable of transiently stabilizing system dynamics, large disturbances could cause protection to trigger disconnecting the equipment and leading further to cascading system-wide blackouts. Today's practice of tuning controllers generally does not guarantee a transiently stable response because it does not use a model for representing system-wide dynamic interactions. To overcome this problem, in this thesis we propose a new systems modeling and control design for provable transient stabilization of power systems against a given set of disturbances. Of particular interest are fast power-electronically-controlled Flexible Alternating Current Transmission System (FACTS) devices which have become a new major option for achieving transient stabilization.

The first major contribution of this thesis is a framework for modeling of general interconnected power systems for very fast transient stabilization using FACTS devices. We recognize that a dynamic model for transient stabilization of power systems has to capture fast electromagnetic dynamics of the transmission grid and FACTS, in addition to the commonly-modeled generator dynamics. To meet this need, a nonlinear dynamic model of general interconnected electric power systems is derived using time-varying phasors associated with states of all dynamic components. The second major contribution of this thesis is a two-level approach to modeling and control which exploits the unique network structure and enables preserving only relevant dynamics in the nonlinear system model. This approach is fundamentally based on separating: a) internal dynamics model for ensuring stable local response of components; b) system-level model in terms of interaction variables for ensuring stability of the system when the components are interconnected. The two levels can be controlled separately which minimizes the need for communication between controllers. Both distributed and cooperative ectropy-based controllers are proposed to control the interaction-level of system dynamics. Proof of concept simulations are presented to illustrate and compare the promising performance of the derived controllers. Some of the most advanced FACTS industry installations are modeled and further generalized using our approach.

Acknowledgments

This research would not be what it is without the help of those who contributed with their thoughts, advice, and words of support, among many other things. I would like to express my deepest gratitude to the following people:

To my family, who was always there to motivate and encourage me. Their support willed me through many tough moments and dead-ends during this research. I am blessed to have you.

To my academic advisor, Professor Marija Ilić, whose enthusiasm and ideas are highly contagious. I was fortunate to have an excellent mentor to guide me and to teach me what performing good research is all about. I am also grateful for her efforts and those of Dr. Ernst Scholtz from ABB in ensuring that my financial support was uninterrupted.

To Dr. Vaibhav Donde, who has been a part of this research since its beginning and has contributed greatly with his advice and insights into industry practice.

To my committee, Professor Bruno Sinopoli and Professor Erik Ydstie, who provided valuable thoughts on this research.

To Kyri Baker, for countless lunch and coffee breaks and for all the stories about careers, music, engineering, cookies, puppies and life.

To my officemates, Nikos Arechiga and Stefanos Baros, for numerous fun moments, questions, answers, scribbles on the whiteboard and classical music.

To Sanja Cvijić, for inviting me on this Ph.D. journey and for sharing happy and tough moments throughout.

To Qixing Liu and Kevin Bachovchin, for tremendous help with shaping this research into what it is now with their valuable suggestions and comments.

To the graduate students of the Electric Energy Systems Group and Porter Hall B-level, for sharing advice and conversation on engineering and everything else. My gratitude goes to Rohan Chabukswar, Tao Cui, Jonathan Donadee, Andrew Hsu, Jhi-Young Joo, Pui Siripha Junlakarn, Javad Mohammadi, Sergio Daniel Pequito, Nipun Popli, Chin Yen Tee, Yang Weng, Rui Yang, Dinghuan Zhu and others too numerous to name.

To Tijana Šestić, for many days of working together toward our graduation and for all the support she has given to me.

To Bojan Vukelić, Biljana Radojičić and Sanja Savić, for always giving me a reason to smile and for being there when I needed a word of encouragement.

To Sofija Matić, for showing me how one equation leads to another and how much dedication and hard work is needed only to write down the first one.

Finally, to Yongxu Huang, for the greatest support and understanding while I was writing these pages and for all wonderful moments which we shared and which are yet to come.

Contents

List of Figures

*

List of Tables

*

Chapter 1

Motivation

The electric power systems are currently undergoing major technological and policy-driven changes. Notably, many renewable resources, such as wind power plants, are being added to the existing grid with the hope of replacing conventional generation with cleaner resources. The integration of large amounts of intermittent renewable power could lead to previously unexperienced dynamic problems in the power systems. Of major concern is the fact that the inertia of wind power plants is considerably smaller than the inertia of large power plants, such as coal or nuclear power plants. This is mainly because wind power plants are smaller in capacity and have smaller mechanical and/or electromagnetic time constants. We recall that the capability of the system to ride through a major disturbance mostly depends on the inertia of its generators; the larger the inertia, the slower the system response to any given disturbance is. Therefore, the basic industry concern is that systems with low-inertia smaller plants would be less robust and more prone to instabilities.

Furthermore, the dynamic response of power systems to large disturbances depends on the operating conditions preceding the disturbance; heavily loaded systems generally operate closer to the stability margin and are more likely to experience transient instability when a major change happens. Efforts to increase the efficiency of the grid by operating closer to its maximal capacity often reduce its stability margin. Figure 1.1 shows how

the stability reserve, measured in terms of increment in accumulated energy, of a single generator connected to an infinite bus depends on the real power output of that generator. The horizontal axis shows the rotor angle position and the vertical axis shows the increment in accumulated energy of the generator with respect to its nominal value. When a generator is operated in its nominal working conditions, its energy is at the minimal value. If a generator is operated at a lower than normal power output (green line), the amount of energy needed to destabilize it is higher than if it is operated at a higher than normal power output (red line). This is seen in Figure 1.1 by comparing the heights of the top of the green and red hill for positive values of the rotor angle position. To summarize, the more real power a generator is producing, the lower its stability reserve is. The same can be said for interconnected electric energy grids with multiple generators [1].

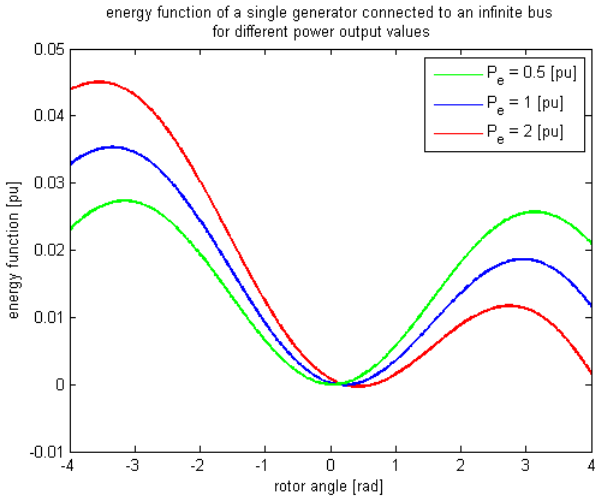

Figure 1.1: Stored energy of a single generator connected to an infinite bus for different power output values.

In today's electric energy industry, the stability of the grid during large disturbances is ensured by operating the system with sufficient stability margin [2]. This is achieved by an approach comprising the following two steps. In the first step, a system operator runs an economic dispatch optimization which is intended to maximize the social welfare using physical limits of devices in the system as the constraints. In the second step, the

system operator runs a large number of dynamic simulations in which the response of the system is analyzed for different disturbances. The disturbances are created by simulating failures of power system equipment. If a simulation shows an unstable system response for any of the disturbances, then the system operator will repeat the first step with a further constrained optimization problem. Newly added constraints are not the physical constraints of components. They are created in order to obtain stable dynamic response to all selected disturbances. The process repeats until this is achieved. Clearly, the solution of the economic dispatch problem is suboptimal because it is constrained for robustness reasons.

Additionally, large disturbances are in practice often dealt with by using Remedial Action Schemes (RAS) which rely upon removal of certain devices or parts of the system to preserve stability. Utilities, such as Southern California Edison (SCE), rely on RAS to preserve continuity of service to the load in cases of major equipment failures [3]. According to [4] RAS are usually grouped around major tie lines which deliver power to SCE from distant places. The newest trend in industry is so-called Centralized RAS (C-RAS) which makes decisions to disconnect devices based on signals gathered from different parts of the system and not only on local measurements as it is case of RAS [4]. Of course, the necessary communication infrastructure has to be put in place to enable C-RAS.

As already explained, operating the system sub-optimally in order to guarantee stability is inefficient. Also, building additional infrastructure, which only provides support in rare cases of equipment failure and faults, is very expensive. An inexpensive and efficient solution would be to use existing controllable devices equipped with advanced transient stabilizing controllers. Excitation system on generators equipped with a power system stabilizer [2] or feedback linearizing controller [5] are possible options. However, excitation system is relatively slow and relatively far from the source of disturbances. Only recently fast power-electronically-switched devices, such as FACTS devices or High Voltage Direct

Current (HVDC) lines, have been considered as possible controllable devices for transient stabilization. In nominal working conditions, FACTS devices are used to redirect active power or inject reactive power. The control logic of FACTS is at present constant-gain control [6, 7] which is used to ensure stable voltage response to small perturbations as in the case of Holly Static Synchronous Compensator (STATCOM) commissioned by Austin Energy [8], or to dampen low-frequency oscillations as in the case of the Thyristor Controlled Series Capacitor (TCSC) in the Brazilian North-South interconnection [9]. Arguably the most advanced FACTS device to date, the Convertible Static Compensator (CSC) at Marcy substation commissioned by the New York Power Authority [10], is equipped with small signal controllers only [11]. The potential of FACTS for stabilization of fast and large disturbances is significant due to their fast switching capabilities. However, FACTS can generally be used to temporarily stabilize the system, but they cannot be used to compensate for significant real power disturbances because they cannot inject or dissipate real power. In cases where FACTS are insufficient to transiently stabilize the system response to prolonged large disturbances, new fast controllers of storage devices and flywheels should be considered prior to building new transmission lines.

The benefits to be gained from using adequate stabilization methods instead of overconstraining economic dispatch for stabilization of large disturbances are substantial. First, the controllers are designed for the range of operating conditions in a way which guarantees stability during transient period with the stability margin explicitly defined by the controller logic. Second, the economic dispatch problem is constrained by the actual stability margin, and therefore, its solution is not suboptimal. Third, the time taken to find nominal generation values reduces because dynamic simulations do not have to be run every time economic dispatch problem is solved. Finally, the value of control becomes quantifiable through the offset of nominal operating point.

In order to model operating conditions-dependent responses to large disturbances it is

essential to use nonlinear dynamic models. Large disturbances excite nonlinear dynamics of the system by taking its states far from nominal values. Additionally, fault-triggered disturbances excite dynamics at all time scales. These disturbances usually spread throughout the entire grid, and therefore, only the interconnected nonlinear power system models are adequate for the analysis of the system response. Tuning of controllers against the Thevenin's equivalent can be shown to be either overly conservative or overly optimistic. Consequently, controllers used to stabilize large disturbances have to be based on nonlinear control theory of multi-input multi-output (MIMO) dynamic systems. Additionally, they have to be distributed in such a way that the need for fast communications is minimized.

Nonlinear controllers for stabilizing power system dynamics using FACTS devices were first introduced as variable structure controllers for low frequency power oscillation damping [12, 13]. Feedback Linearizing Controllers (FBLC) for FACTS followed [14, 15]. Later, nonlinear energy-based controllers were proposed for suppression of oscillations [16]. Controllers in all these references are designed on simple two bus models and are hardly generalizable to arbitrary network topologies. A transient stabilization controller for a system of arbitrary network topology was first introduced in [17] using a Control Lyapunov Function (CLF) for FACTS. The CLF used is based on a structure-preserving energy function for power system transient stability proposed in [18] and further explored in [19]. The application of the CLF in control of HVDC lines is shown in [20].

All these controllers, except of [16], are based on models which consider the fast dynamics of inductors and capacitors as instantaneous. This leads to further simplifications of the interconnected system model resulting in moderate controller performance. We show that better controller performance can be obtained using a power system model which does not neglect fast transients in the reactive components of FACTS. The proposed interconnected grid model is an ordinary differential equation model obtained using time-varying phasors [21, 22, 23]. Time-varying phasors represent the relevant fast dynamics of power-

electronically-controlled states in FACTS as well as the slower dynamics of generation units. A FACTS controller based on this model fully utilizes switching of these devices currently in the range of kHz.

One of the main premises of this thesis is that the effectiveness of energy-based control design depends to a very large extent on the selection of energy function [24]. The choice of energy function will further impact communication requirements. Based on this, much effort is put to model fast dynamics and to introduce energy functions that lend themselves to effective controller design for transient stabilization. In particular, we propose a new energy-based nonlinear control design for very fast power-electronically-controlled devices. An energy-based approach, which gives clear intuition of physical energy flows in the system, is used to design controllers. Such approach is used mainly because of its scalability to complex grid topologies with multiple controllers.

However, a straightforward energy-based controller does not exploit a priori knowledge about the system structure, and as such, its implementation is somewhat demanding. In order to exploit the system structure to build a controller easier for implementation, we introduce a two-level power system model based on the concept of interaction variables [25]. We introduce the concept of nonlinear interaction variables and use them to describe how parts of the system interact with each other. They show the propagation of disturbances as well as the impact of the controllers by modeling the dynamics of the accumulated energy and exchanged power between system components. The controller based on this model stabilizes ectropy of the system [26] and requires less communication to be implemented. The increment of energy created by large disturbances is redirected using this controller from critical devices into less stressed parts of the system [27].

The contributions of this work are in the proposed energy-based framework for transient stabilizing controller design. The framework is modular, a property obtained through the use of interaction variables, in terms of both the modeling and control-designing ap-

proaches. Modularity of the framework implies scalable implementation to an arbitrary network topology and arbitrary set of controlling devices. Also, a distributed nature of the controller follows from modular modeling. The underlying energy concept is sufficiently general to be used in response to any non-zero mean short duration disturbance. We propose more then one candidate controller for FACTS. Depending on the controller design, different communication requirements are imposed. The controllers are shown to increase the critical clearing time and the stability margin of the system.

The thesis is organized as follows. The transient stability problem is posed mathematically in Chapter 2. This chapter also reviews challenges related to transient stabilization by interpreting them in terms of dynamics of accumulated energy and exchanged power. This creates the basis for modeling and control in subsequent chapters. In Chapter 3 we derive a new physical model of a general interconnected electric power system which captures fast dynamics of interest. In Chapter 4 we introduce a controller of power system dynamics based on stabilization of system states by minimizing an energy function, thus the name energy-based control. In Chapter 5 we show how the information about the system structure and the time scales of different dynamics can be exploited to build a two-level model based on interaction variables. This two-level interaction variable-based model is controlled by: (1) stabilizing internal states of modules locally; and (2) stabilizing the interaction variables in the form of energy by using an ectropy-based controller proposed in Chapter 6. Chapter 7 shows how the interaction variables and the ectropy-based controller can be used to dimension FACTS controllers. All models and controllers in this thesis are illustrated in some detail on a three-bus system example, while the IEEE 14-bus system is used to illustrate their performance on a larger, more general system.

Chapter 2

The Problem of Transient Stabilization

The stability of power systems is a highly complex problem, whose complexity is a result of various factors.

First, an exact dynamic model of a power system is hard to define. The topological structure of the system is constantly changing; starting from the load profile variables contributed by different dynamic behavior of consumers, through the configuration of the transmission system dictated by markets and reliability requirements, to the economic dispatch-dependent generation changes and unexpected equipment failures. The number of possible topological and structural combinations of interest is very high and most of the time the exact dynamic models are not known.

Second, the range of operating conditions is wide due to economic reasons. Economic dispatch of power generators is done every 15 minutes or each hour in anticipation of predictable system load component. A stable equilibrium of the system must correspond to the desired operating condition. Controllers must meet this requirement. As conditions vary, the nonlinearities in the system dynamics may result in multiple stable and unstable equilibria [28].

Third, system dynamics could have multiple stable and/or unstable equilibria. Transient response of an interconnected electric energy system is affected by vastly different rates of response of different components (power plants, loads, T&D equipment). Economic dispatch generally changes the set points of the controllable equipment for predicted load. The interaction of different components around system equilibria results in dynamic phenomena ranging from low frequency oscillations to high frequency fluctuations and loss of synchronism.

Fourth, if the operating constraints are violated the protection schemes will act to prevent malfunction of equipment. Therefore, any violation of operating constraints will cause a topological change in the system and cause dynamic response at multiple rates.

From everything said, the stability problem of power systems can be described as an interconnected system-wide problem of high complexity. An effective controller has to be able to keep system response transiently stable during both equipment failures and/or sudden input disturbances.

In what follows in this chapter we first review the transient stabilization problem as defined by the power engineering community. Next, we rethink the problem taking into consideration that the grid is evolving and adopting new technologies. Finally, we propose an approach to solving transient stabilization problem for general interconnected power systems with new technologies.

2.1 Transient Stability Problem

Transient stability is a type of stability specific to the power system operation. The state space of a power system contains large number of stable and unstable equilibria. Each asymptotically stable equilibrium has its own Region of Attraction (ROA). If a disturbance is large enough it will perturb the states causing them to leave ROA of a pre-disturbance equilibrium. If a post-disturbance state is outside of ROA of a desired (or in more general

case any) equilibrium point, then the system will not return to a viable operating point. In this case further actions usually taken by the protection devices are necessary to keep the system stable.

A simple example of a transient stability problem is the problem caused by a short circuit of a transmission line to the ground. The system states are perturbed from the pre-fault equilibrium by the short circuit. The protection reacts moments after the fault and removes the faulted line from the rest of the grid. All post-fault equilibria are clearly different from the pre-fault equilibrium. The time evolution of states in the post-fault system depends on the time of fault duration. If the state trajectories remain inside the ROA of a viable stable equilibrium we say that the system is transiently stable for this particular fault and this particular duration of the fault.

Another example would be a faulted generator removed from the system by protection actions in response to unacceptable voltage or frequency changes. Clearly, without a backup generator taking the place of a faulted generator or without an instantaneous load shedding, the balance between generation and demand will not exist for a certain time after the protection has acted. A post-fault equilibrium will not exist either. In this case, the system is transiently unstable because of the nonexistence of a post-fault equilibrium.

In conclusion, a transient stability problem is defined for a particular fault and not for a particular post-fault equilibrium point. A pre-fault equilibrium point and duration of the fault are both needed to determine the state trajectory following fault clearing. Therefore, the transient stability problem needs to be defined for a certain set of operating conditions. Finally, the existence of at least one post-fault equilibrium is a necessary but not sufficient condition for the system to be transiently stable. This is because the system may not return to a post-fault equilibrium even when such equilibrium exists.

The time interval from the beginning of the fault until the moment the states leave the pre-fault equilibrium's ROA is known as the Critical Clearing Time T_{cct}. Critical clearing

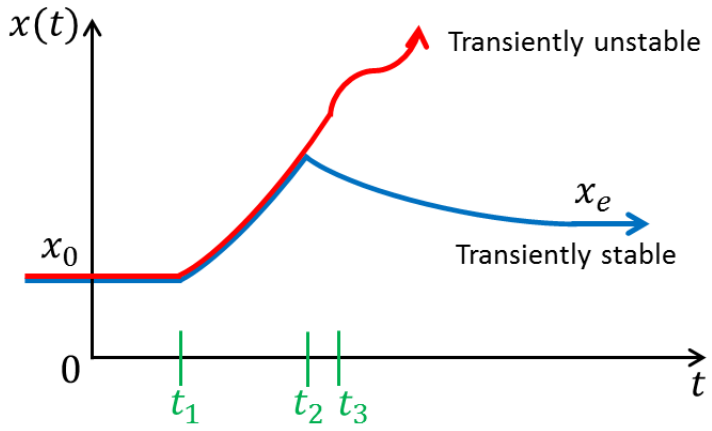

Figure 2.1: Sequence of events and transient stability.

time is often used as a measure of transient stability margin. The longer this time is, the greater the ROA of the pre-fault equilibrium is [1]. Figure 2.1 illustrates qualitatively different possible response of system states after the fault is cleared. The system is at equilibrium x_0 at time zero and the fault occurs at time t_1. If the fault is cleared after $t_2 - t_1 < T_{cct}$, where T_{cct} is the critical clearing time, then the system states settle in a post-fault equilibrium x_e. If the fault is cleared after $t_3 - t_1 > T_{cct}$ then the system trajectory will diverge, and the system becomes *transiently unstable*.

2.2 Dynamic Response of Power Systems to Large Disturbances

Dynamic response of power systems is extremely rich. Different devices contribute to the system dynamics at different rates and their contribution is often operating conditions-dependent. In this section we elaborate on dynamical behavior of evolving power systems and describe commonly made assumptions and approaches to their modeling.

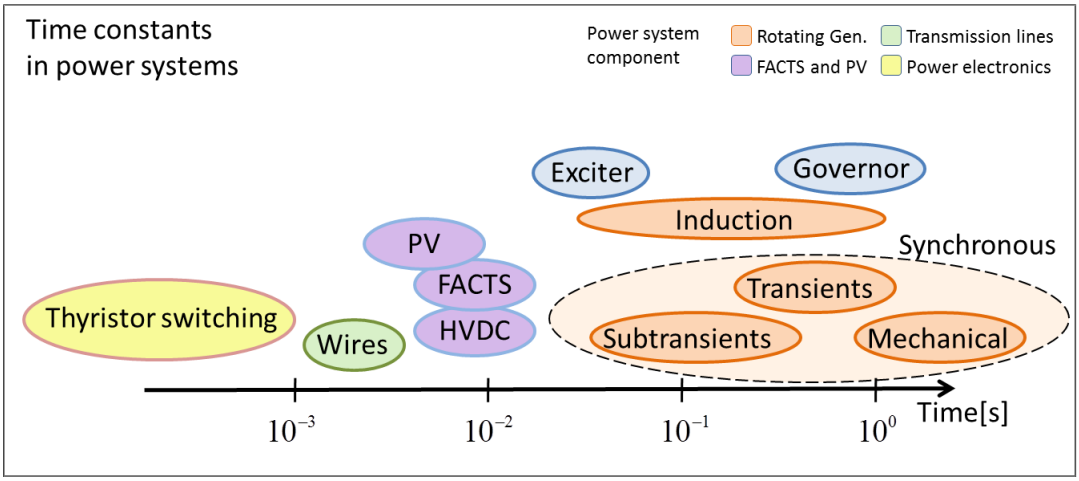

Figure 2.2: Time constants in power systems.

2.2.1 State-of-the-Art Approach to Modeling and Control

Typical bulky power systems are composed of large synchronous generators, transmission lines and aggregated loads, as shown in Figure 2.3. As the generator dynamics are dominant and critical for transient stability in AC electric power systems, the generators were the only system components whose dynamics was modeled. The simplest power system dynamical models are second order Ordinary Differential Equations (ODEs) representing rotation of the generator shafts [29, 30]. These dynamics have time constants in the range of seconds. Figure 2.2 shows typical time scales of different devices in power systems.

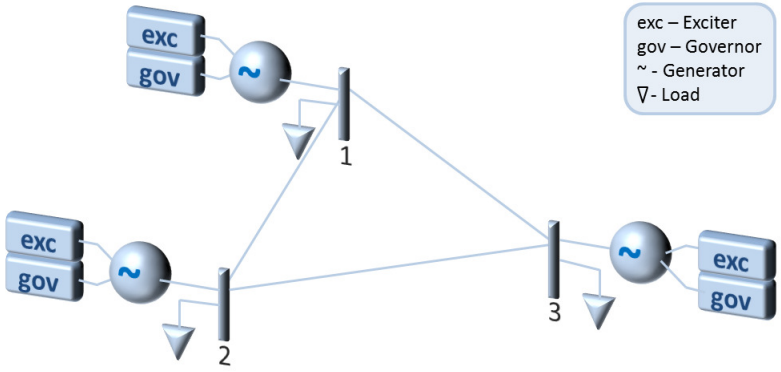

Figure 2.3: An electric power system comprising conventional components.

Somewhat faster time constants are associated with the dynamics of generator rotor

windings. These time constants are in the range of 0.1 second, which is smaller than those of the rotation. The power system dynamic models which include electromagnetic dynamics of rotor windings and mechanical dynamics of rotation are known as the two-axis and the one-axis (flux-decay) models [30, 31]. The difference between the two is in the number of details they describe. The first represents dynamics of the damper and the excitation windings while the second one captures only dynamics of the excitation winding. The dynamics of the damper windings are usually faster than the one of the excitation winding which is due to the relative difference in their sizes. Therefore, it is often stated that the first model represents subtransients and transients while the second model represents only transients.

The dynamics of generator stator windings, transmission lines and loads are usually considered instantaneous in typical dynamic studies. The reason for this is the significant difference between the time scales of rotor and stator windings for typical generator parameters. A full dynamic generator model captures dynamics on this fast time scale of milliseconds as well [30, 32], but this model is more commonly used for analysis and not synthesis of controllers.

Inductive and capacitive wires in transmission system have dynamics on the same time scale of milliseconds. The transmission system is sometimes modeled as dynamic for power system analysis purposes. However, these cases are rare [23, 33, 34]. On the other hand, it is a common practice not to model transmission system as dynamic for control purposes. This is because it is assumed that controllers have slow time constants themselves in comparison to the transmission system time constants. For example, the dynamics of excitation control are slower than that of a transmission line. Therefore, vary fast transients in wires are taken as instantaneous. Of course, the necessary underlying assumption is that the fast dynamics of the transmission system are always stable.

FACTS devices are traditionally deployed in power systems to redirect power flows or

inject reactive power in steady state. As their key purpose is to improve nominal working conditions, they are rarely modeled as dynamic in transient stability studies. Instead, they are modeled as variable impedances with no dynamics of their own [13].

2.2.2 Newly Proposed Approach to Modeling and Control

Power systems are undergoing a major transformation in recent years as the grid evolves toward adopting smart, distributed and renewable technologies as shown in Figure 2.4. The newly adopted technologies contribute to the system dynamics in various ways. The renewable generation, often distributed and of small power, adds to the power system dynamics on fast time scales. Although their individual impact to the bulky grid might be small, their combined effect cannot be neglected. Power-electronically-controlled FACTS devices and HVDC lines, equipped with very fast switching capability, give the opportunity to control dynamics on both slow and fast time scales. Finally, Phasor Measurement Units (PMU) are sensors whose measurements could enable closing the control loops and utilizing the fast switching of FACTS to control interconnected system behavior.

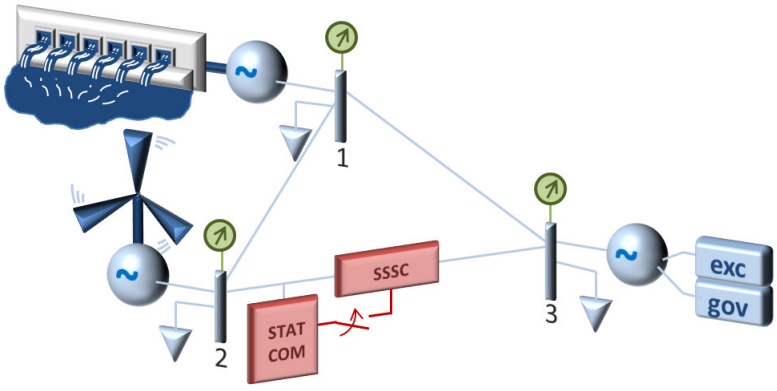

Figure 2.4: An electric energy system comprising new technologies.

We recognize that richness in dynamics of today's electric energy systems comes from both the conventional components and the newly added technologies. Therefore, the traditional approach to modeling and control for transient stabilization is insufficient to guar-

antee interconnected system stability and the new approach is needed.

In the first part of this thesis, namely in Chapter 3, we propose a dynamic model of general interconnected power systems whose all components are modeled as dynamic. This model provides sufficient accuracy to design transient stabilizing controllers.

The assumption of instantaneous transmission system dynamics is not made in our approach. Instead, this dynamics is modeled using time-varying phasors. Time-varying phasors have routinely been used in generator and interconnected system modeling for software analysis [23] but they have traditionally rarely been deployed for dynamic controller design for interconnected system stability [21, 35] due to the increased complexity they bring to the dynamic model by introducing additional states.

FACTS devices can also be modeled using the time-varying phasor-based models [22]. These models are developed for the stand-alone analysis of FACTS and have only been deployed for the analysis of interconnected power system dynamics. In this thesis, we use them to design dynamic controllers.

Modeling of transmission system and FACTS as dynamic brings benefits in two ways. First, a more accurate picture of power system dynamics is obtained and the newly derived dynamic model resembles reality in a more truthful way. Second and more important for controller design is the fact that dynamic states have memory. In other words, the energy accumulated in a dynamic system is determined by its dynamic states, while algebraic states do not carry any additional information about the accumulated energy.

In Chapter 4, we design a FACTS controller using the model introduced in Chapter 3. The controller is based on the idea described in Figure 2.5. The increment of energy created by a disturbance is accumulated inside the generator in the uncontrolled system, while the energy of FACTS and transmission system remains almost unchanged. As a consequence, the generator will accelerate. If the disturbance is large enough, its states will leave the region of attraction, moving away from a viable equilibrium. The basic goal of

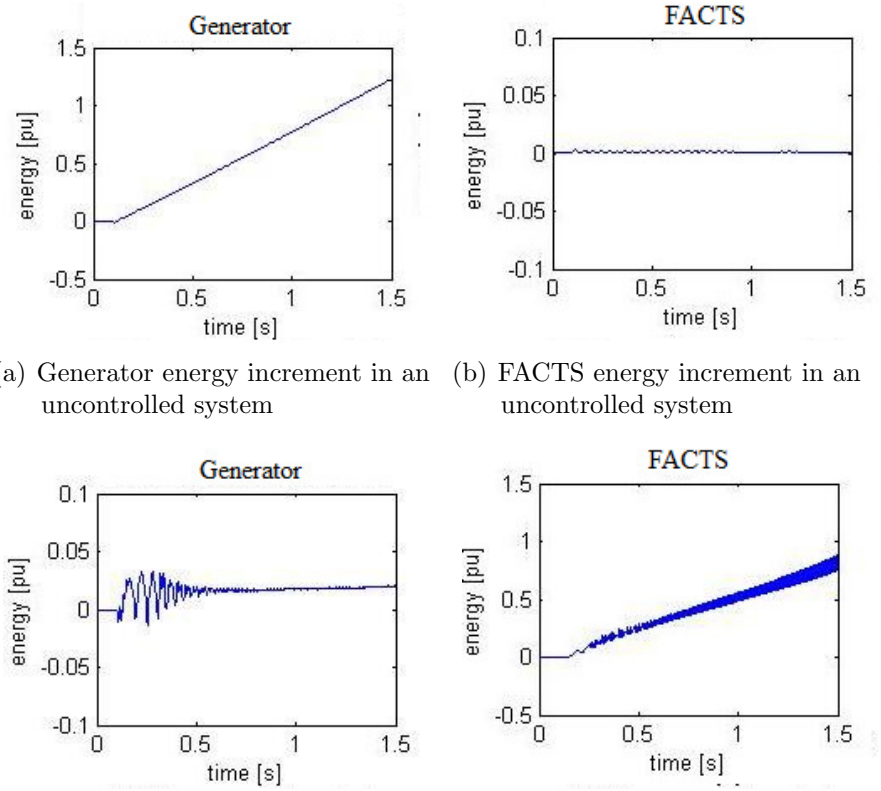

(a) Generator energy increment in an uncontrolled system

(b) FACTS energy increment in an uncontrolled system

(c) Generator energy increment in a controlled system

(d) FACTS energy increment in a controlled system

Figure 2.5: The increment in the accumulated energy caused by a fault.

our FACTS controller is to assure that the states of the generator remain inside the region of attraction. In other words, the accumulated energy of the FACTS and transmission system should increase while the generator energy level decreases (remains unchanged relative to its pre-fault value) as shown in Figure 2.5.

This controller defers from all other controllers of FACTS as it is based on the idea that FACTS can store excessive amounts of energy for very short periods of time. Therefore, the effects of FACTS controllers in response to large disturbances can be significantly larger than what was shown in the literature.

2.2.3 Two-level Approach to Modeling and Control

Although the newly introduced model captures relevant dynamics for transient stabilization, its complexity is overwhelming. This causes serious implementation issues as the number of states grows very quickly for large systems.

In the second part of this thesis, in Chapter 5 in particular, we propose a two-level approach to modeling and control of power systems. The proposed approach is focused on modeling of the accumulated energy dynamics as this variable is an essential indicator of interconnected system stability. Additionally, our approach captures this energy in terms of dynamical states. This form is suitable not only for power system analysis but also for synthesis of dynamic controllers.

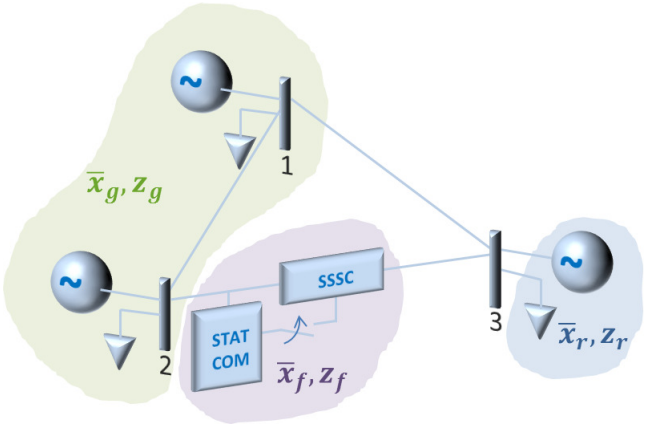

Figure 2.6: Modular approach to power system representation.

To understand why rate of change of energy is an important indicator of stability, we look at the energies of three generators shown in Figure 2.7. The generators are a part of the three-bus system given in Figure 2.6 and the energies are plotted with no controllers acting to stabilize disturbance.

At the beginning of the simulation, the system is at an equilibrium. At the time of fault $t_f = 0.1s$ the energies of generators start to change. If the fault is cleared before the system has accumulated sufficient amount of energy to become unstable ($t_c = 0.33s$), the states will converge to a post-fault equilibrium and so will the accumulated energy. If the

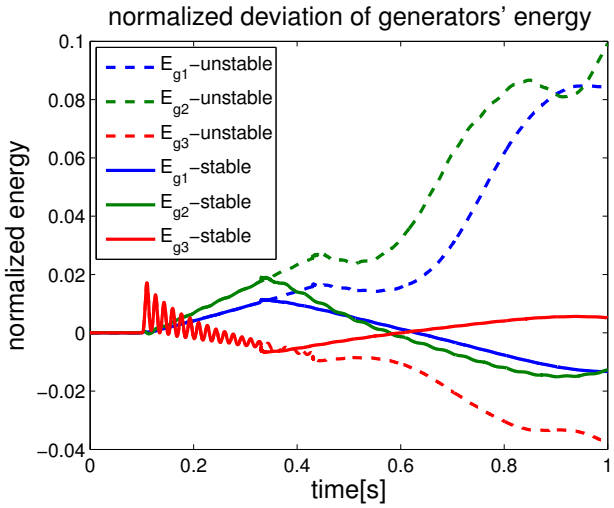

Figure 2.7: Energies of three generators plotted as $(E_{gi} - E_{gi0})/E_{gi0}$.

fault has injected too much energy into the system, the system states and the accumulated energy will not return to an equilibrium after the fault is cleared ($t_c = 0.43s$). The rate at which the accumulated energy increases/decreases depends on the location and the type of fault, the pre-fault conditions in the grid, and the most important, of the exchange of energy with different components. It is clear that managing accumulated energy of generators and other components plays important role in transient stability of the system.

The modeling approach proposed in Chapter 5 is based on the concept of interaction variables. Interaction variables show how different components of the system interact. We choose accumulated energy of each component as its interaction variable z_i and rewrite the system model as

$$\dot{\bar{x}}_i = \bar{f}_i(\bar{x}_i, y_i, z_i, u_i, d_i), \quad \bar{f}_i(\bar{x}_{i0}, z_{i0}, y_{i0}, u_{i0}, 0) = 0 \tag{2.1}$$

$$\dot{z}_i = p_i(\bar{x}_i, z_i, y_i, u_i, d_i), \quad p_i(\bar{x}_{i0}, z_{i0}, y_{i0}, u_{i0}, 0) = 0 \tag{2.2}$$

where subscript i denotes different components. In this model, states $\bar{x}_i$ are the internal states of components and states z_i are the interaction variables. Inputs u_i and disturbances d_i are internal for each device, although they still affect dynamics of interactions. Coupling

vector y_i contains states on ports of all other components connected to component i. Therefore, this vector captures the rate of change of energy between components.

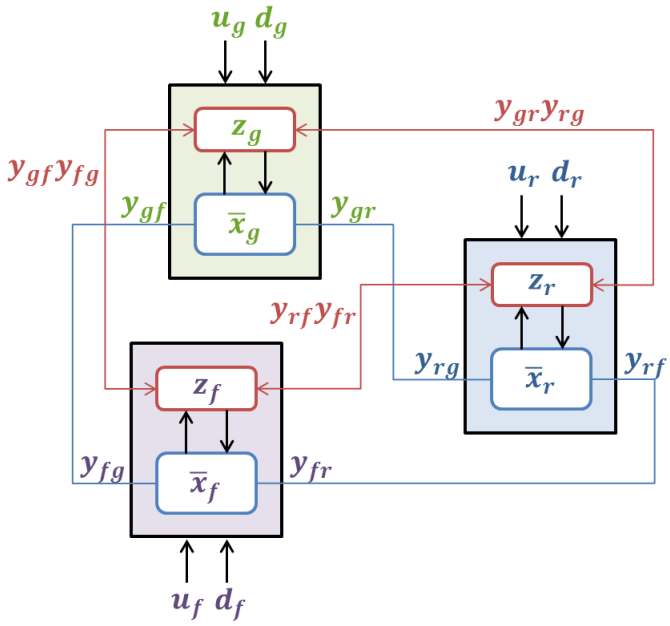

Figure 2.8: Two-level approach to modeling and control.

This framework lends itself to separating the requirements for internal device stability and interconnected system stability in a two-level approach. Figure 2.8 graphically illustrates this separation. The internal dynamics of components, given in Equation (2.1), can be stabilized locally using controllers u_i. The interaction variable dynamics, given in Equation (2.2), has to be stabilized at the interconnected level for all components. This ensures that the exchange of excessive energy between components will be minimized and that the interconnected system will reach an equilibrium.

In Chapter 6 we propose an ectropy-based controller which stabilizes interaction-level dynamics. This controller requires minimal communication as it stabilizes the exchange of energy between devices while the internal device dynamics are stabilized locally. The controller can be posed as distributed or cooperative as shown in Figure 2.9. If posed as distributed, each module will stabilize its own interaction variable. We focus our efforts on

cooperative control as this formulation fits well with using FACTS controllers for transient stabilization of synchronous generators.

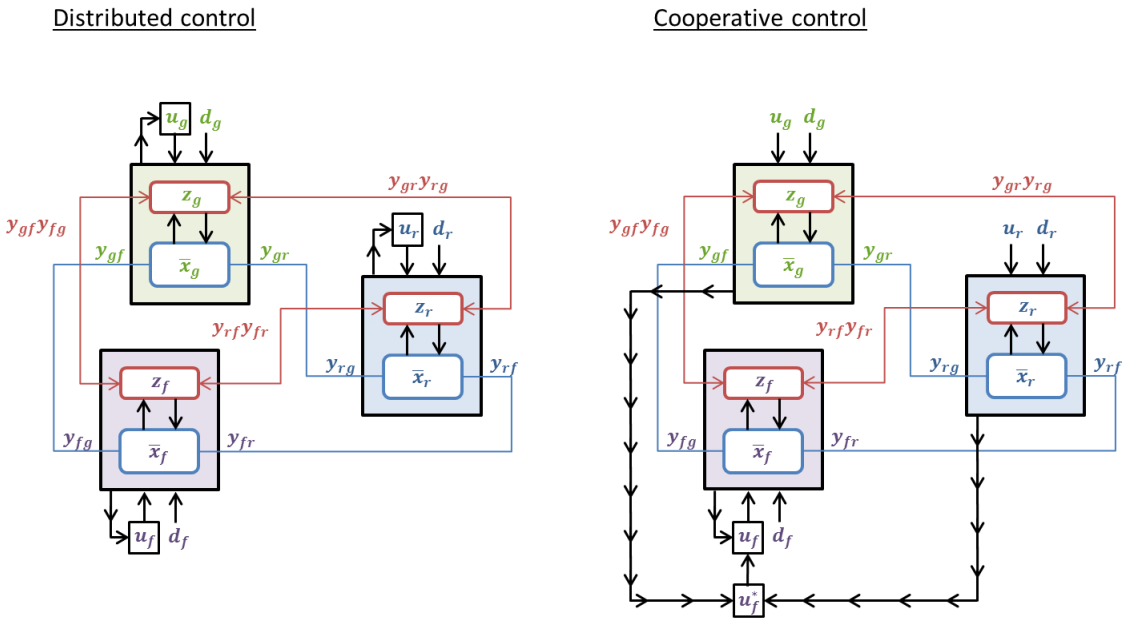

Figure 2.9: Distributed and cooperative ectropy-based controller.

A cooperative ectropy-controller consists of two parts as shown in Figure 2.9. The first part is a local controller of active power which controls the active power at the terminals of a module. This power is controlled toward a reference which is given by the second part of the controller. The second part is the ectropy-based controller of the interconnected system dynamics. The ectropy-based controller provides the reference for the active power controllers and the reference is computed to ensure that the dynamics of the interconnected modules stay stable. These two parts together form a composite controller. This thesis is organized in a way in which active power controllers are introduced first in Section 3.2.1. The ectropy-based controller and the detailed explanation on how the two parts of the controller fit together are introduced later in Chapter 6.

The approach to modeling and control presented in this thesis can be used on general interconnected power systems of arbitrary size and topology which are composed of various components. For illustration purposes, we demonstrate all concepts on a simple three-bus

system such as the one in Figure 2.6.

Part I

Modeling Dynamics for Very Fast Switching Control

Chapter 3

Dynamic Modeling of Power Systems

Modeling of power systems for control using FACTS has previously suffered from two major shortcomings which reflect in the number of details captured by the model.

On one side, the conventional power system models which are used to design transient controllers usually assume that FACTS devices have instantaneous dynamics [13]. This approximation is justified by the time scale separation between fast FACTS dynamics and slow generator rotation dynamics and it leads to the controllable impedance model of FACTS. Although this approach to modeling captures the transients of generators, which are needed to be controlled to maintain transient stability, it does not capture dynamics of the FACTS which are to be used as controlling devices. And in order to control system dynamics successfully using FACTS, it is not sufficient to model only the rotation of generators as it has been done in the past.

On the other side, FACTS are commonly modeled as dynamic when they are used to control a local variable, such as power flow through the line or nodal voltage. In this case, they are often modeled in time domain using a lot of details, while the rest of the power system is represented as a current or voltage source [7]. These models fail to capture the response of interconnected systems to large disturbances, and therefore, cannot be used for transient stabilization.

A combination of the two previously described approaches is needed in order to obtain best results. We show that modeling FACTS and the transmission grid as dynamic components, in addition to already dynamically modeled generators, leads to an ODE model of interconnected power systems. This model is essential to represent the dynamic exchange of energy between the generator and the capacitors/inductors of the FACTS devices.

In this chapter we introduce a dynamic model of a general interconnected power system with all components modeled as dynamic using time-varying phasors. Although this model has been used in the past to analyze power system dynamic behavior in presence of disturbances [23] and to design low-frequency oscillation damping controllers for systems of simple topologies [16], it has never been used to design transient stabilizing FACTS controllers for general grid topologies. There are a few reasons for this. First, time-varying phasors increase the complexity of the dynamic model by adding dynamic states which would otherwise be considered algebraic. Second, most of the controllers for transient stabilization used in the past, such as the excitation system on synchronous generators, have slower time constants than wires. Third, no real time synchronized measurements on the fast time scales of kHz were available in the past. Today, the latter two technical issues are solved with the use of power-electronic controllers and PMU sensing. The first issue can be resolved by using systematic model reduction based on singular perturbation. At any rate, in our approach the complexity of the model is an acceptable price to pay for ensuring the stability of the power grid at all time scales and against very fast and large disturbances.

An important benefit of representing the fast dynamics of wires and FACTS using time-varying phasors is that they provide a way to model active power in reactive elements of these devices, namely capacitors and inductors. Active power of capacitors and inductors is zero in steady state. Representing the reactive elements using time-varying phasor dynamics allows us to capture the active power during transients. This property is exploited

later to design controllers.

We consider FACTS devices, generators, transmission lines and loads as integral parts of interconnected power systems. A dynamic model of the interconnected system is obtained by combining the dynamic models of these devices. Only balanced three-phase system modeling is considered.

3.1 Time-varying Phasors

A time-varying phasor is a vector rotating in a complex plane at near constant frequency, with time-varying magnitude and phase angle as shown in Figure 3.1.

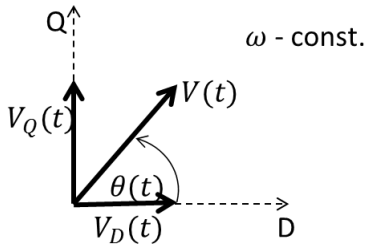

Figure 3.1: A time-varying phasor.

The assumption of near constant frequency proves to be true for power systems for most of its operating conditions. The dynamics that governs electrical frequency in power systems are slow because of the large inertia of big generators. In addition, the electrical frequency is kept in a close range of the desired value using governor control. Therefore, sinusoidal time-domain voltage $v(t)$ and current $i(t)$ can be transformed into their time-varying phasor equivalents

$$\begin{aligned} v(t) = V\sqrt{2}sin(\omega t + \theta) \quad &\rightarrow \quad V_D + jV_Q = Ve^{j\theta} \\ i(t) = I\sqrt{2}sin(\omega t + \psi) \quad &\rightarrow \quad I_D + jI_Q = Ie^{j\psi} \end{aligned} \tag{3.1}$$

where the time-varying phasor form is given in both Cartesian, (V_D, V_Q) and (I_D, I_Q), and

polar, (V, θ) and (I, ψ), coordinates. Subscripts D and Q are used to denote direct (real) and quadrature (imaginary) component of a phasor. Both coordinate systems are used interchangeably.

The time domain differential equations of many common devices in power systems (e.g. synchronous and induction machines, transmission lines, loads) can be written as time-varying phasor differential equations if all variables are near-sinusoidal and the frequency is near constant. We start by showing this transformation on an example of a capacitor and an inductor.

An inductor of constant inductance L and a capacitor of constant capacitance C are described with the following dynamic equations in time domain

$$v(t) = L\frac{di(t)}{dt} \quad , \quad i(t) = C\frac{dv(t)}{dt} \tag{3.2}$$

These two equations transferred into time-varying phasor domain are

$$\begin{aligned} \dot{I}_D &= \frac{1}{L}V_D + \omega I_Q \quad , \quad \dot{V}_D = \frac{1}{C}I_D + \omega V_Q \\ \dot{I}_Q &= \frac{1}{L}V_Q - \omega I_D \quad , \quad \dot{V}_Q = \frac{1}{C}I_Q - \omega V_D \end{aligned} \tag{3.3}$$

in Cartesian coordinates, or equivalently

$$\begin{aligned} \dot{I} &= \frac{1}{L}Vcos(\theta - \psi) \quad , \quad \dot{\psi} = \frac{1}{LI}Vsin(\theta - \psi) - \omega \\ \dot{V} &= \frac{1}{C}Icos(\psi - \theta) \quad , \quad \dot{\theta} = \frac{1}{CV}Isin(\psi - \theta) - \omega \end{aligned} \tag{3.4}$$

in polar coordinates. Note that frequency ω is the electrical frequency in the grid and it is assumed constant in this derivation.

Steady state equations which describe AC circuits are obtained from (3.3) or (3.4) if the derivatives are set to zero.

3.1.1 Energy Function in the Time-varying Phasor Domain

The time-varying phasor modeling is not compatible with instantaneous power and accumulated energy. Thus, the appropriate definitions of accumulated energy and power for the time-varying phasor domain have to be found in order to proceed with the controller derivation. References [21] and [25] introduce expressions for power of inductors and capacitors in time-varying phasor domain. We review these and then we define expressions for accumulated energy of inductors and capacitors in time-varying phasor domain.

Instantaneous power $p_L(t)$ and instantaneous accumulated energy $e_L(t)$ of the inductor are equal to

$$\begin{aligned} p_L(t) &= v(t)i(t) = Li(t)\frac{di(t)}{dt} \\ e_L(t) &= \int_0^t p(t)dt = \frac{1}{2}Li^2(t) \end{aligned} \tag{3.5}$$

If the current through the inductor is $i(t) = I\sqrt{2}sin(\omega t + \psi)$ and, additionally, frequency ω is assumed constant as with time-varying phasors, then instantaneous power from (3.5) can be rewritten as

$$\begin{aligned} p_L(t) = LI\dot{I}(1 - cos(2\omega t + 2\psi)) \\ + LI^2 sin(2\omega t + 2\psi)(\omega + \dot{\psi}) \end{aligned} \tag{3.6}$$

where $\dot{I} = \frac{dI}{dt}$ and $\dot{\psi} = \frac{d\psi}{dt}$. Now, the active power P_L and reactive power Q_L of this inductor in time-varying phasor domain can be defined according to [25] as

$$\begin{aligned} P_L &= LI\dot{I} \\ Q_L &= LI^2(\omega + \dot{\psi}) \end{aligned} \tag{3.7}$$

In steady state, the active power P_L represents the average power of the inductor over the nominal frequency cycle while the reactive power Q_L represents the magnitude of the

zero-mean oscillations.

Next, we propose a definition of accumulated energy in time-varying phasor domain. Based on Equation (3.5) energy of an inductor can be rewritten as

$$\begin{aligned} e_L(t) &= LI^2 sin^2(\omega t + \psi) \\ &= \frac{1}{2}LI^2 - \frac{1}{2}LI^2 cos(2\omega t + 2\psi) \end{aligned} \tag{3.8}$$

In steady state, the average energy of the inductor is $\frac{1}{2}LI^2$, because the second term in (3.8) results in zero after averaging over the nominal frequency cycle. On the other hand, average of $cos(2\omega t + 2\psi)$ over one period is not zero during transients because phase angle ψ changes over time. Therefore, the accumulated energy of an inductor cannot only be defined as $\frac{1}{2}LI^2$, but the change in phase angle ψ has to be taken into consideration as well.

In order to find a valid energy function for an inductor represented in the time-varying phasor domain we rewrite (3.8) as

$$\begin{aligned} e_L(t) &= \frac{1}{2}LI^2 - \frac{1}{4}LI^2(e^{j(2\omega t+2\psi)} + e^{-j(2\omega t+2\psi)}) \\ &= |E_L| - \frac{1}{2}\hat{E}_L e^{j\omega t} - \frac{1}{2}\hat{E}_L^* e^{-1\omega t} \end{aligned} \tag{3.9}$$

where $\hat{E}_L$ is defined as

$$\hat{E}_L = \frac{1}{2}LI^2 e^{j2\psi} \tag{3.10}$$

Function $\hat{E}_L$ is not positive for all values of ψ, and therefore, cannot be used as an energy function of an inductor. However, it is the basic unit-function of inductor's energy and its stabilization will mean the stabilization of instantaneous inductor energy as well. Therefore, we use $\hat{E}_L$ to propose energy function ν_L of an inductor in time-varying phasor domain.

An intuitive way to find a candidate for an energy function is to multiply $\hat{E}_L$ by its conjugate. The product of the two is an always positive function.

$$\nu_L = \sqrt{\hat{E}_L \hat{E}_L^*} = \frac{1}{2} L I^2 = E_L \tag{3.11}$$

The first derivative of such energy function is

$$\dot{\nu}_L = \dot{E}_L = L I \dot{I} = P_L \tag{3.12}$$

Similarly, capacitor's energy function is given as

$$\nu_C = \sqrt{\hat{E}_C \hat{E}_C^*} = \frac{1}{2} C V^2 = E_C \tag{3.13}$$

and the first derivative of this function is

$$\dot{\nu}_C = \dot{E}_C = C V \dot{V} = P_C \tag{3.14}$$

By looking at the proposed energy functions E_L, E_C and their derivatives we see that the change in energy magnitudes is directly controlled by the active power P_L and P_C applied to the inductor/capacitor. However, the proposed energy functions do not depend on the current and voltage phase angles ψ and θ. Therefore, stabilization of such energy function only guarantees stability of magnitudes of phasors I and V, while phase angles ψ and θ are allowed to move freely.

Energy functions (3.11) and (3.13) are convenient for stabilization of active power in the system, but not for stabilization of reactive power. Therefore, we consider a different energy function by looking at the first derivative of $\hat{E}_L$.

The first derivative of $\hat{E}_L$ is

$$\begin{aligned}\dot{\hat{E}}_L &= LI\dot{I}e^{j2\psi} + jLI^2\dot{\psi}e^{j2\psi} \\ &= LI\dot{I}e^{j2\psi} + j(LI^2(\omega+\dot{\psi}) - LI^2\omega)e^{j2\psi} \\ &= (P_L + j(Q_L - Q_{L0}))e^{j2\psi}\end{aligned} \tag{3.15}$$

Using the same approach as in (3.11) to construct an energy function, we get

$$\begin{aligned}\nu_L &= \frac{1}{2}\dot{\hat{E}}_L\dot{\hat{E}}_L^* \\ &= \frac{1}{2}(P_L^2 + (Q_L - Q_{L0})^2)\end{aligned} \tag{3.16}$$

This energy function depends on both, current magnitude I and phase angle ψ. Its stabilization leads to stabilization of the inductor's current.

Another advantage of this energy function is that it consists of two parts which could be controlled independently. In other words, a controller which stabilizes only active or only reactive power can be designed using this energy function.

A similar approach can be used to derive the active and reactive power expressions of a capacitor

$$\begin{aligned}P_C &= CV\dot{V} \\ Q_C &= -CV^2(\omega + \dot{\theta})\end{aligned} \tag{3.17}$$

and the expression for capacitor's energy function

$$\nu_C = \frac{1}{2}(P_C^2 + (Q_C - Q_{C0})^2) \tag{3.18}$$

It follows from (3.7) and (3.17) that the active power of inductors/capacitors is different from zero only if the magnitude of their current/voltage is changing over time. The reactive

power, on the other hand, always exists. This is best illustrated on Figure 3.2 which compares active and reactive power of an inductor if the voltage across it changes in a stepwise manner.

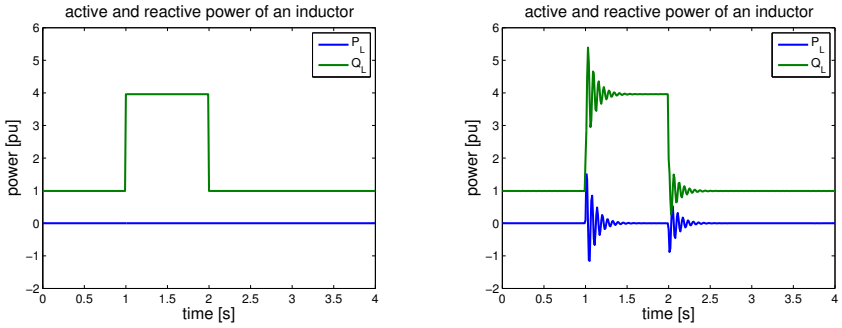

(a) Instantaneous inductor dynamics (b) Time-varying phasor model

Figure 3.2: Comparison of active and reactive power of an inductor modeled as static vs. dynamic using time-varying phasors.

The reactive elements, capacitors and inductors, have active power equal to zero when the system is in steady state. The steady state here refers to the constant magnitudes, phase angles, and frequencies of all sinusoidal signals in the system. Therefore, additional energy can be stored in FACTS devices only if their states are changing over time and do not reach steady state.

3.2 Time-varying Phasor Modeling of Devices

Dynamic models of different devices which compose an electric power system are presented in this section. As parts of electric energy systems, we consider generators, transmission lines, loads and FACTS devices. Although we focus our attention on these devices, dynamic models of other devices/controllers can easily be added to the interconnected system model.

All of the models presented here are either based on time-varying phasors or compatible with time-varying phasor modeling.

3.2.1 FACTS Devices

FACTS devices are located in the transmission part of the electric grid. They are primarily used to redirect line flows if they are connected in series or to provide voltage support to the grid if they are connected in shunt [36, 37].

The main part of a FACTS device is the reactive element: the capacitor and/or inductor. A connection with the grid is made through a set of interconnected thyristor switches. The fundamental characteristic of such a device is its ability to actively change its own equivalent impedance as seen from the network side. This happens on the relatively fast time scales due to the switching speed of thyristors, which is in the range of a few kHz [38].

The overall behavior of a FACTS device is set by controlling firing angle α of the thyristor switch [39]. The firing angle controls the time thyristor switch stays closed allowing the current to flow through the branch. The switch can be either open ($\alpha = 0$) or closed ($\alpha = 1$). Due to the fast time scale of thyristor switching, which is much faster than any other time scale in the system, the firing angle can be thought of as a continuous signal between zero and one. Different values in this range can then be implemented using pulse width modulation. This is a common control strategy used to achieve desired behavior of power electronic devices [40, 41].

FACTS devices come in two major groups [36, 37]. The group which was developed first contains FACTS devices whose core component is a Thyristor Controlled Reactance (TCR). A TCR is a series connection of an inductor and a thyristor switch. As its name say, the thyristor is used to control the reactance of the inductor as seen by the rest of the grid. Different FACTS devices are created by combining TCR branches with inductors and capacitors and we will refer to all of them as TCR-based FACTS devices.

Another big group of FACTS devices are converter-based FACTS devices. These devices contain a capacitor which is separated from the grid by the network of thyristor switches.

The thyristors convert AC voltage of the grid to a unipolar voltage at the internal FACTS capacitor. The voltage at the capacitor can be considered as DC voltage when power system is in steady state.

It is important to mention similarities and differences between the two groups of FACTS devices. Both groups are used to provide reactive power and voltage support, and to redirect active power flow through the grid. The difference comes from the way they are implemented which will determine how they are modeled and controlled. The TCR-based FACTS are usually modeled as variable impedances and their controllers are designed accordingly. The converter-based FACTS are typically modeled as ideal controllable voltage sources.

In this thesis, we propose a modeling approach which does not look at them strictly as variable impedances or ideal voltage sources. Instead, our proposed model captures their internal dynamics allowing us to design advanced controllers for FACTS capable of stabilizing transients. We define the models and design controllers by using active power and energy expressions for inductive and capacitive elements obtained in Section 3.1.

TCR-based FACTS Devices

A parallel connection of a capacitor and an inductor connected in series with a thyristor switch is used as the basic TCR-based FACTS unit. This unit, shown in Figure 3.3, is known as a Thyristor Controlled Series Capacitor (TCSC) if connected in series with a transmission line or Static Var Compensator (SVC) if connected in shunt to a transmission line [36]. We proceed with derivation thinking about it as a TCSC unless stated otherwise.

The states of the TCSC in Figure 3.3 are voltage across the capacitor $v(t)$ and current through the inductor $i(t)$. The firing angle α of the thyristor switch is used as the control input.

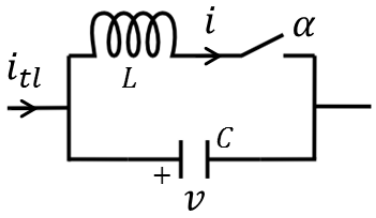

Figure 3.3: Typical structure of a TCR-based FACTS device.

The time domain dynamic equations of the TCSC given in Figure 3.3 are

$$\begin{aligned} \dot{v}(t) &= \frac{1}{C}\left(i_{tl}(t) - i(t)\right) \\ \dot{i}(t) &= \frac{\alpha(t)}{L} v(t) \end{aligned} \tag{3.19}$$

The equations can be rewritten using time-varying phasor representation of each variable.

$$\begin{aligned} \frac{d}{dt}(V(t)cos(\omega t + \theta(t))) &= \frac{1}{C}[I_{tl}(t)cos(\omega t + \psi_{tl}(t)) - I(t)cos(\omega t + \psi(t))] \\ \frac{d}{dt}(I(t)cos(\omega t + \psi(t))) &= \frac{\alpha(t)}{L} V(t)cos(\omega t + \theta(t)) \end{aligned} \tag{3.20}$$

After we introduce trigonometric identities we can remove the carrier functions $sin(\omega t)$ and $cos(\omega t)$ by grouping the terms next to each of them. Dependence of time has been omitted for simplicity.

$$\begin{aligned} \frac{d}{dt}(Vcos\theta) &= \frac{1}{C}(I_{tl}cos\psi_{tl} - Icos\psi) + \omega Vsin\theta \\ \frac{d}{dt}(Vsin\theta) &= \frac{1}{C}(I_{tl}sin\psi_{tl} - Isin\psi) - \omega Vcos\theta \\ \frac{d}{dt}(Icos\psi) &= \frac{\alpha}{L}(Vcos\theta) + \omega Isin\psi \\ \frac{d}{dt}(Isin\psi) &= \frac{\alpha}{L}(Vsin\theta) - \omega Icos\psi \end{aligned} \tag{3.21}$$

And the final form of the TCSC/SVC time-varying phasor model in Cartesian coordinates

becomes

$$\begin{aligned}
\dot{V}_D &= \frac{1}{C}\left(I_{tl_D} - I_D\right) + \omega V_Q \\
\dot{V}_Q &= \frac{1}{C}\left(I_{tl_Q} - I_Q\right) - \omega V_D \\
\dot{I}_D &= \frac{\alpha}{L} V_D + \omega I_Q \\
\dot{I}_Q &= \frac{\alpha}{L} V_Q - \omega I_D
\end{aligned} \tag{3.22}$$

where subscripts D and Q indicate direct (real) and quadrature (imaginary) component of a phasor, respectively.

A similar derivation as the one presented here has been used in [22, 42] to introduce a model of the same circuit based on the first coefficients of Fourier analysis. One version of this model, which preserves sufficient accuracy for purposes of transient stabilization, is the one in Equation (3.22).

To ease the notation, Equation (3.22) will be referred to as

$$\dot{x}_f = f_f(x_f, y_f, u_f) \tag{3.23}$$

where $x_f = [V_D\ V_Q\ I_D\ I_Q]^T$ is the vector of TCSC states. Vector $y_f = [I_{tlD}\ I_{tlQ}]^T$ is the coupling vector with the transmission line current. Input $u_f = \alpha$ is the firing angle of TCSC and it is used as the input for the transient stabilization control.

The proposed controllers are energy-based. Therefore, we introduce energy functions for each of the devices starting with the energy function of TCSC.

An energy function of the TCSC described by the model in Equation (3.22) is composed by combining energy functions of inductor in 3.11 and capacitor in 3.13 as

$$E_f = \frac{1}{2}L(I_D^2 + I_Q^2) + \frac{1}{2}C(V_D^2 + V_Q^2) \tag{3.24}$$

TCR-based FACTS as a short-term energy accumulation device

A TCR-based FACTS accumulates energy in its inductor and capacitor by controlling the thyristor switch. The switch is controlled in such a way that the stored energy is cycling between the inductor and capacitor allowing the FACTS to temporarily generate/consume active power. We try to illustrate the process of energy accumulation in this subsection.

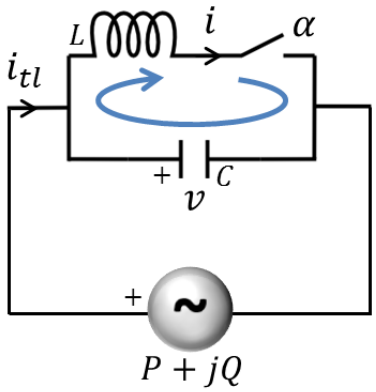

Figure 3.4: A TCR-based FACTS device connected to a controllable power source.

Let us assume that a source of external active and reactive power is attached to the FACTS device as shown in Figure 3.4. The external source of active and reactive power is

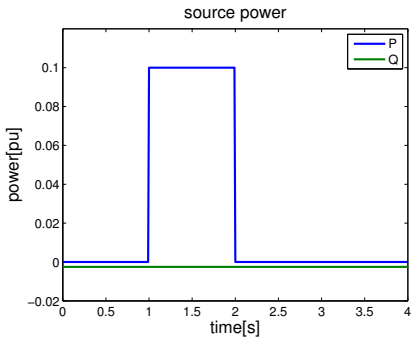

Figure 3.5: Power of the controlled source.

only used for this illustration as such device will not be attached to the FACTS in real-world installations. However, it is a useful concept to show how a FACTS device will behave if controlled to accumulate energy. In this subsection the thyristor switching of FACTS is

kept constant while only the power of the source is modified. The source is generating active and reactive power as shown in Figure 3.5. The reactive power is unchanged in this simulation while only the active power is modified.

The response of the FACTS is shown in Figure 3.6. The current and the voltage of FACTS increase during the time active power is controlled to be different than zero. During the same period, energy of the inductor and capacitor of FACTS grows.

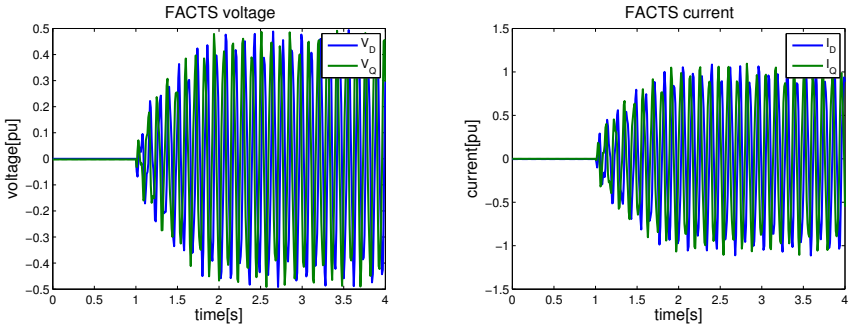

(a) Capacitor voltage

(b) Inductor current

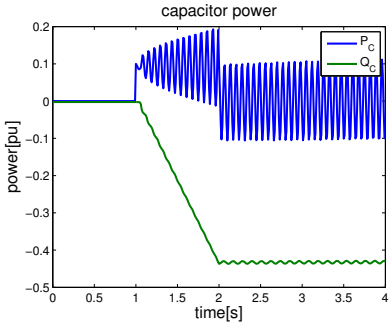

(c) Capacitor power

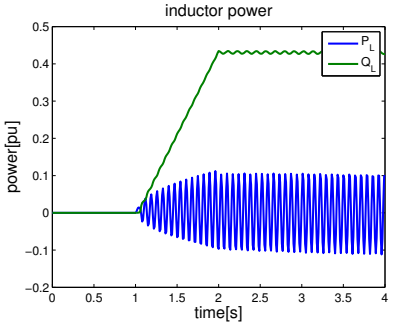

(d) Inductor power

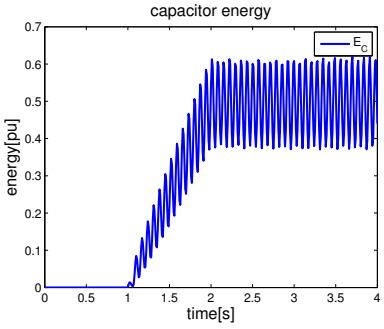

(e) Capacitor energy

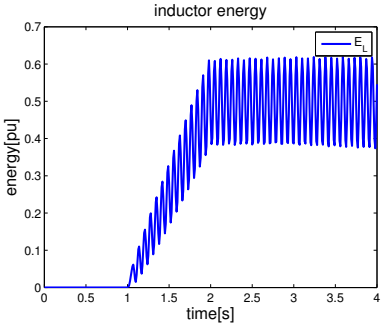

(f) Inductor energy

Figure 3.6: FACTS device as an energy accumulation device.

The additional energy, injected into FACTS by the non-zero active power coming from

the source, is cycling between inductor and capacitor as we can see from Figures 3.6(a) and 3.6(b). In this example, the FACTS devices is taking all the energy supplied by the source. In the following subsection we derive an expression for an active power controller which uses thyristor switching to control how much energy is stored in the FACTS.

Control of active power through TCR-based FACTS

The main reason we model FACTS devices as dynamic is to be able to inject or extract energy from them by controlling the active power through the device. In this subsection we derive the controller of active power through the TCR-based FACTS device. This controller is used in the following chapters to design a controller for transient stabilization of interconnected systems.

The TCR-based FACTS model is given in Equation (3.22). The goal of the controller is to switch the thyristor on and off so that the active power through the TCSC device is equal to power reference P_f^*. This is accomplished by using a control Lyapunov function-like controller. The theory of the Control Lyapunov Function (CLF) is given in Appendix 3. We choose the following control Lyapunov function

$$\nu(x_f) = \frac{1}{2}(P_f - P_f^*)^2 \tag{3.25}$$

where

$$P_f = V_D I_{tlD} + V_Q I_{tlQ} = P_L + P_C \tag{3.26}$$

is the active power through the TCSC. This function satisfies the first two properties of CLF: $\nu(x_f) \geq 0,\ \forall x_f \in \mathcal{R}^4$ and $\nu(x_f) = 0,\ P_f = P_f^*$. The controller which guarantees the third property of the CLF, $\dot{\nu}(x_f) \leq 0,\ \forall x_f \in \mathcal{R}^4$, is derived next.

Combination of the active and reactive power expressions of an inductor given in (3.7)

yields

$$P_L = Q_L \frac{1}{\omega + \dot{\psi}} \frac{\dot{I}}{I} \tag{3.27}$$

The first derivative of this expression is

$$\dot{P}_L = \dot{Q}_L \frac{1}{\omega + \dot{\psi}} \frac{\dot{I}}{I} - Q_L \frac{\dot{\omega} + \ddot{\psi}}{(\omega + \dot{\psi})^2} \frac{\dot{I}}{I} + Q_L \frac{1}{\omega + \dot{\psi}} \frac{\ddot{I} I - \dot{I}^2}{I^2} \tag{3.28}$$

The second derivatives of current magnitude I and current phase angle ψ can be found by taking the derivative of the differential equations of the model in Equation (3.22), translated into polar coordinates. Once these derivatives are found, the first derivative of active power through FACTS becomes

$$\dot{P}_f = \dot{P}_C + \frac{\dot{Q}_L}{Q_L} P_L + \frac{P_L^2 + Q_L^2}{Q_L} \left(-(\omega + \dot{\theta}) + \frac{\alpha Q_L}{L I^2} \right) \tag{3.29}$$

If the controller is chosen as

$$\alpha = \frac{L I^2}{Q_L} \left[(\omega + \dot{\theta}) - \frac{Q_L}{P_L^2 + Q_L^2} \left(\frac{\dot{Q}_L}{Q_L} P_L + \dot{P}_C + \beta \right) \right] \tag{3.30}$$

then Equation (3.29) reduces to

$$\dot{P}_f = -\beta \tag{3.31}$$

Finally, the first derivative of the CLF follows

$$\dot{\nu}(x_f) = -(P_f - P_f^*)\beta \tag{3.32}$$

The term β is specified by the designer and it depends on the choice of the control

logic. For a CLF type controller, β is

$$\beta = K_P(P_f - P_f^*) \tag{3.33}$$

where $K_P > 0$ is the gain of the controller.

In this case, the controller from (3.30) together with (3.33) will enable the active power through TCSC to approach reference P_f^* as long as the switching signal α does not reach saturation. Further analysis has to be made to determine the type of disturbance this controller is capable of handling without reaching saturation. In other words, this becomes the problem of dimensioning FACTS components to ensure transient stabilization for a given set of disturbances.

Control performance on a two-bus system

This simulation is performed to show that FACTS devices can have active power different from zero even if they are made of only reactive elements.

A TCSC with the active power controller from Equation (3.30) is simulated in a two bus power system on Figure 3.7. The generator at Bus 1 is producing 90% of the total generation of $1.5MW$. The flow of power through the transmission line with TCSC is 30% while the flow of power through the parallel line is 70% of the total power transfered from Bus 1 to Bus 2.

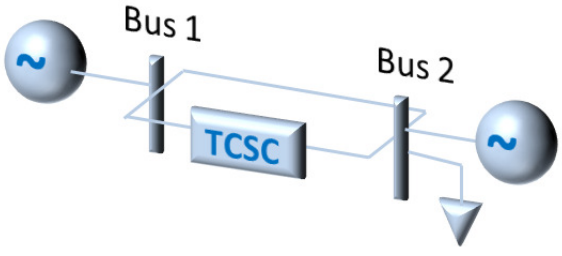

Figure 3.7: Two generator test system.

The TCSC is controlled to have reference power of $P_f^* = 0.001MW$ across its ends for duration of $T = 0.125s$. The resulting plots are show in Figure 3.8 for two different sets of parameters of the TCSC. TCSC is considered large in terms of compensation it provides for one set of parameters and small for the other. In both cases, TCSC reacts fast and controls active power across its ends. This can be best seen by looking at the plots of the accumulated energy on the inductor. Both plots show increase in this energy during time T. This is a conclusion hard to make only by looking at the plots of the active power of the inductor, because these have too many spikes created by thyristor switching. Finally, the large inductor TCSC and the small inductor TCSC differ in their behavior. The TCSC with a smaller inductor is accumulating energy with a slower pace.

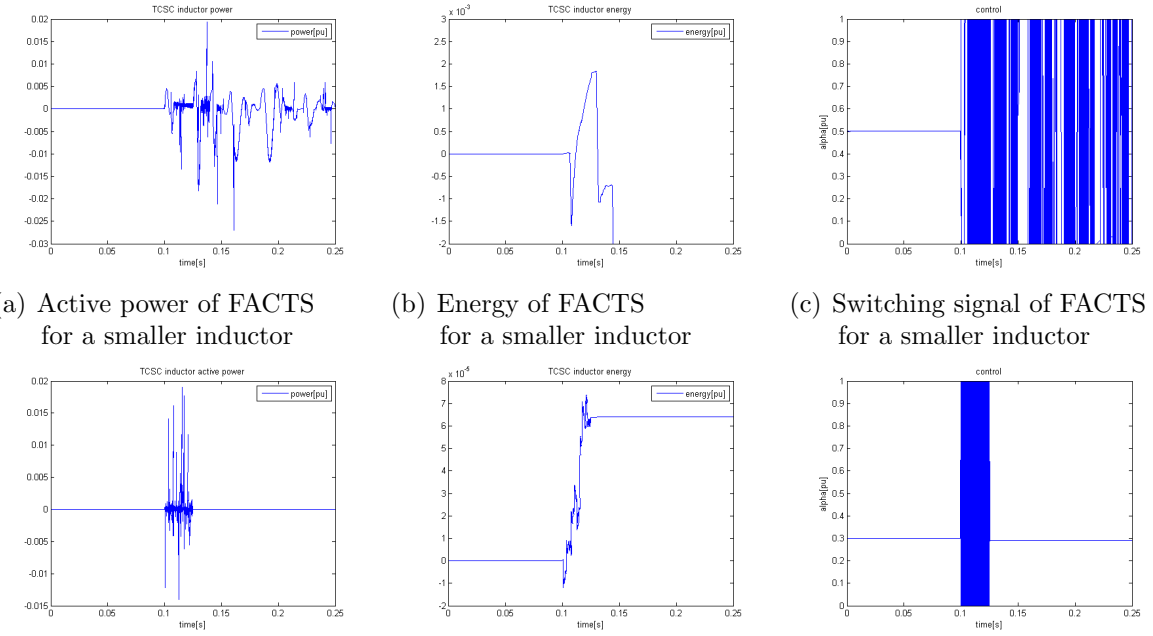

(a) Active power of FACTS for a smaller inductor

(b) Energy of FACTS for a smaller inductor

(c) Switching signal of FACTS for a smaller inductor

(d) Active power of FACTS for a bigger inductor

(e) Energy of FACTS for a bigger inductor

(f) Switching signal of FACTS for a bigger inductor

Figure 3.8: Two generator test system simulation results for active power control on TCSC.

Converter-based FACTS Devices

Converter-based FACTS devices are recently becoming more popular as they are smaller in size compared to TCR-based FACTS. A Convertible Synchronous Compensator (CSC) commissioned by New York Power Authority (NYPA) at Marcy substation, one of the most advanced power-electronically-controlled devices in the grid to date, has the ability to operate in ten different regimes controlling voltage at the bus and active and reactive power through two transmission lines [10, 11].

We consider a simplified Marcy-like Convertible Synchronous Compensator (CSC) made of two identical DC to AC converters which can be interconnected through a shared DC bus. The structure of the CSC is taken from [10] but its set of functionalities is reduced for this illustration. According to this reference, one converter is connected in series with the transmission line acting like a Synchronous Static Series Compensator (SSSC), while the other converter is connected in shunt with the bus acting like a Synchronous Static Compensator (STATCOM). If the two converters are internally connected via a shared bus then the CSC device is acting like a Unified Power Flow Controller (UPFC) as shown in Figure 3.9.

For steady state or small signal stability applications, it is safe to assume that these converters can be modeled as ideal AC voltage sources. However, this assumption does not hold if we wish to use converters for stabilization of large disturbances as these disturbances might require excessive amounts of energy to stabilize. Therefore, we introduce a new model of converter-based FACTS device which captures their dynamics and their limitations.

We start by assuming that a converter is modeled as a non-ideal voltage source whose magnitude and phase angle are controllable using a network of thyristor switches, but whose energy is supplied by the internal FACTS capacitor. The voltage of this capacitor is not assumed constant as it is usually done when looking at the steady state. Therefore, we avoid using the term *DC* and instead refer to this capacitor as the FACTS capacitor.

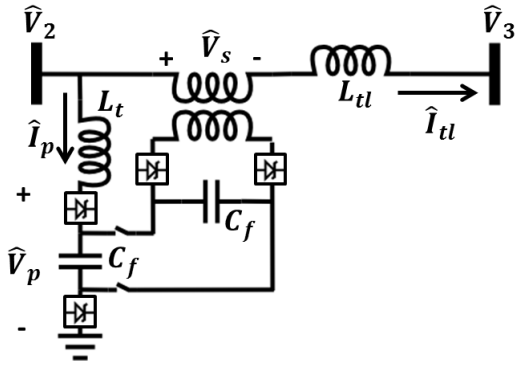

Figure 3.9: Unified Power Flow Controller.

We model dynamics of the FACTS capacitor C_f which supplies the SSSC voltage V_s as

$$\dot{V}_f = \frac{1}{C_f} I_f \tag{3.34}$$

where subscript f refers to FACTS variables and parameters on the internal side of the converter, which we avoid calling DC for already mentioned reasons.

Assuming negligible converter losses and negligible size of harmonics we can claim that $V_f I_f = P_f = P_{sssc} = V_s I_{tl} cos(\theta_s - \psi_{tl})$ and rewrite

$$\dot{V}_f = \frac{1}{C_f} \frac{V_s I_{tl} cos(\theta_s - \psi_{tl})}{V_f} \tag{3.35}$$

where V_s, I_{tl}, θ_s and ψ_{tl} refer to the phasor of voltage and current on the AC side of the converter. The last equality is obviously an approximation as some of the energy will go into harmonics or will be dissipated by the losses of thyristor switches. Further work is needed to accurately model these losses of energy in Equation (3.35).

If the CSC is used as a UPFC then the two FACTS capacitors are connected in parallel giving the dynamical model of the CSC as

$$\dot{V}_f = \frac{1}{2C_f} \frac{V_s I_{tl} cos(\theta_s - \psi_{tl}) + V_p I_p cos(\theta_p - \psi_p)}{V_f} \tag{3.36}$$

In some practical applications, the converter is operated in a phase-locked loop with certain reference voltage/current in the grid. This practically means that the converter achieves its objective by controlling the magnitude of the AC source while its phase is locked and determined by the phase of the reference. In the case of large disturbances, locking the phase of the controllable source to a freely moving reference in the grid might prove to be, if not harmful, then at least non-beneficial for the system stability. Therefore, we assume that voltages of the two converters V_s, θ_s, V_p and θ_p are controllable.

However, an additional condition on the control input has to be met. Namely, controlled voltage magnitudes V_s and V_p have to stay inside the range of the voltage of the internal FACTS capacitor

$$\begin{aligned} 0 < V_p < K_{sw_p} V_f \\ |V_s| < \frac{1}{2} K_{sw_s} V_f \end{aligned} \tag{3.37}$$

where $0 < K_{sw_p}, K_{sw_s} < 1$ is a constant which depends on the topology of the converter's switches. This condition can be interpreted in terms of size of the FACTS capacitor. Namely, the bigger the capacitor, the higher nominal voltage V_f can be.

To ease the notation, Equation (3.36) will be referred to as

$$\dot{x}_f = f_f(x_f, y_f, u_f) \tag{3.38}$$

where $x_f = [V_f]^T$ is the vector of CSC states. Vector $y_f = [I_{tlD}\ I_{tlQ}\ I_{pD}\ I_{pQ}]^T$ is the coupling vector with the transmission line and the STATCOM current. Input vector $u_f = [V_s\ \theta_s\ V_p\ \theta_p]^T$ contains voltages injected to the grid by the CSC and it is used as the input for the transient stabilization control.

An energy function of the CSC described by the model in Equation (3.36) is

$$E_f = \frac{1}{2} C_f V_f^2 \tag{3.39}$$

Control of active power through converter-based FACTS

We derive expressions for the controllers of converter-based FACTS on the example of the CSC. Similarly as in the case of the TCR-based FACTS, we wish to control active power through SSSC to obtain desired reference P_f^*.

The phase angle of the converter's voltage is controlled as

$$\theta_s = arccos(\frac{1}{V_s I_{tl}} P_f^*) + \psi_{tl} \tag{3.40}$$

where P_f^* is an arbitrary reference for SSSC power. Control signal from (3.40) is used until

$$|\frac{1}{V_s I_{tl}} P_f^*| > 1 \tag{3.41}$$

If this condition is met, the controller will not be able to provide required power just by controlling the phase angle θ_s. Therefore, we introduce the expression for control of AC voltage of the converter as

$$V_s = \frac{1}{I_{tl} cos(\theta_s - \psi_{tl})} P_f^* \tag{3.42}$$

Of course, V_s can reach saturation defined by (3.37). If this happens, the controller is supplying/absorbing the largest amount of energy under given conditions in the network.

Next, we introduce the controller of the internal dynamics of FACTS, namely internal voltage V_f. This voltage is controlled by using the STATCOM converter. The goal is to ensure that the converter-based FACTS will be internally stable while at the same time,

it is helping to transiently stabilize the system. The phase angle of this converter is

$$\theta_p = arctan(\frac{-K_f(V_f - V_{f0}) - y(V_f)I_{pD}}{y(V_f)I_{pQ}}) \tag{3.43}$$

while the voltage magnitude of this converter V_p is given as

$$V_p = \frac{1}{cos(\theta_p)} y(V_f) \tag{3.44}$$

where $y(V_f) = V_{2D} + L_t(\omega I_{pQ} + K_I I_{pD} + K_f(V_f - V_{f0}))$. As in the case with the SSSC, this controller can reach saturation as V_p reaches its limit given in (3.37).

The main difference between TCR-based FACTS and converter-based FACTS is that the first accumulate energy only on average per cycle while the second can accumulate energy for infinite time in theory. This additional energy is stored as electric charge at capacitor C_f. The physical characteristics of the capacitor will determine how much energy can be stored in it. In other words, this becomes the problem of dimensioning converter capacitors to obtain guaranteed performance.

3.2.2 Transmission line

To avoid dealing with algebraic states, all transmission lines are represented using a lumped parameter π model. Next, their lumped-parameter representation is modeled using time-varying phasors. The derivation of this model is the same as the derivation of the time-varying phasor model for FACTS and it is omitted here due to limited space. Only the final form of this model is given.

The time-varying phasor model of a transmission line which is connecting two nodes in the grid, in this particular case nodes 1 and 2 as shown in Figure 3.10, is given by the

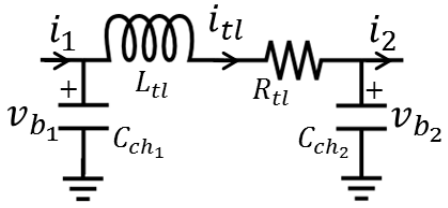

Figure 3.10: Transmission line π representation.

following two sets of equations

$$\begin{aligned}
\dot{V}_{b_1D} &= \frac{1}{C_{ch_1}}\left(I_{1_D} - I_{tlD}\right) + \omega V_{b_1Q} \\
\dot{V}_{b_1Q} &= \frac{1}{C_{ch_1}}\left(I_{1_Q} - I_{tlQ}\right) - \omega V_{b_1D} \\
\dot{V}_{b_2D} &= \frac{1}{C_{ch_2}}\left(I_{tl_D} - I_{2D}\right) + \omega V_{b_2Q} \\
\dot{V}_{b_2Q} &= \frac{1}{C_{ch_2}}\left(I_{tl_Q} - I_{2Q}\right) - \omega V_{b_2D}
\end{aligned} \tag{3.45}$$

$$\begin{aligned}
\dot{I}_{tlD} &= \frac{1}{L_{tl}}(V_{b_1D} - V_{b_2D} - R_{tl}I_{tlD}) + \omega I_{tlQ} \\
\dot{I}_{tlQ} &= \frac{1}{L_{tl}}(V_{b_1Q} - V_{b_2Q} - R_{tl}I_{tlQ}) - \omega I_{tlD}
\end{aligned} \tag{3.46}$$

where (I_{tlD}, I_{tlQ}) is the current through the transmission line. Voltages (V_{b_1D}, V_{b_1Q}) and (V_{b_2D}, V_{b_2Q}) are the voltages of two nodes on each side of the transmission line. Currents (I_{1D}, I_{1Q}) and (I_{2D}, I_{2Q}) are the currents injection into the line between nodes 1 and 2. In an interconnected network, these currents will be equal to the sum of currents of all transmission lines, generators and loads connected to that node excluding current (I_{tlD}, I_{tlQ}). If a series FACTS device is located at the transmission line, then Equation (3.46) would take the following form

$$\begin{aligned}
\dot{I}_{tlD} &= \frac{1}{L}(V_{b_1D} - V_{b_2D} - V_D - RI_{tlD}) + \omega I_{tlQ} \\
\dot{I}_{tlQ} &= \frac{1}{L}(V_{b_1Q} - V_{b_2Q} - V_Q - RI_{tlQ}) - \omega I_{tlD}
\end{aligned} \tag{3.47}$$

where (V_D, V_Q) is the FACTS capacitor voltage from the model given in Equation (3.22).

To ease the notation, transmission line model will be referred to as

$$\begin{aligned} \dot{x}_{b_1} &= f_{b_1}(x_{b_1}, x_{tl}, y_{b_1}) \\ \dot{x}_{b_2} &= f_{b_2}(x_{b_2}, x_{tl}, y_{b_2}) \\ \dot{x}_{tl} &= f_{tl}(x_{tl}, x_{b_1}, x_{b_2}, y_f) \end{aligned} \tag{3.48}$$

where $x_{tl} = [I_{tlD}\ I_{tlQ}]^T$, $x_{b_1} = [V_{b_1D}\ V_{b_1Q}]^T$ and $x_{b_2} = [V_{b_2D}\ V_{b_2Q}]^T$ are the vectors of transmission line states. Vectors $y_{b_1} = [I_{1D}\ I_{1Q}]^T$ and $y_{b_2} = [I_{2D}\ I_{2Q}]^T$ are the coupling vectors with other devices. Vector $y_f = [V_D\ V_Q]^T$ is the coupling vector with the FACTS device, if one is located at the transmission line.

Although fairly simple, this model provides sufficient accuracy. Reference [21] warns about the accuracy of this model for very fast transients but the experimental validation remains an open question which goes beyond the scope of this thesis.

An energy function of the transmission line described by the model in Equation (3.46) is

$$\begin{aligned} E_{tl} &= \frac{1}{2} L_{tl}(I_{tlD}^2 + I_{tlQ}^2) \\ E_{b_1} &= \frac{1}{2} C_{ch_1}(V_{b_1D}^2 + V_{b_1Q}^2) \\ E_{b_2} &= \frac{1}{2} C_{ch_2}(V_{b_2D}^2 + V_{b_2Q}^2) \end{aligned} \tag{3.49}$$

3.2.3 Load

If a transmission grid is modeled using time-varying phasors then the interconnected system model takes the form of coupled nonlinear ODEs, regardless of the load model one chooses. Therefore, loads can be represented either using nonlinear dynamic models or as constant power or constant impedance loads. We use the constant power load representation.

If a load is to be represented as a constant impedance load shown in Figure 3.11, its

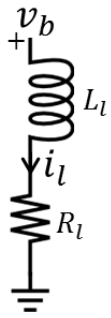

Figure 3.11: Load represented as a constant impedance.

dynamic model would take the form

$$\begin{aligned} \dot{I}_{lD} &= \frac{1}{L_l}(V_{bD} - R_l I_{lD}) + \omega I_{lQ} \\ \dot{I}_{lQ} &= \frac{1}{L_l}(V_{bQ} - R_l I_{lQ}) - \omega I_{lD} \end{aligned} \tag{3.50}$$

To ease the notation, the constant impedance load model will be referred to as

$$\dot{x}_l = f_l(x_l, y_l) \tag{3.51}$$

where $x_l = [I_{lD}\ I_{lQ}]^T$ is the state vector of the load and $y_l = [V_{bD}\ V_{bQ}]^T$ is the vector of load couplings with the node.

An energy function of the constant impedance load described by the model in Equation (3.50) is

$$E_l = \frac{1}{2} L_l (I_{lD}^2 + I_{lQ}^2) \tag{3.52}$$

3.2.4 Generator

Generators are usually modeled as synchronous machines in power system stability studies. Exceptional is the wind turbine which can be modeled as an induction machine depending on its internal structure. The synchronous machine models are well-studied and known

[43, 44] and some references [30, 32] show how they can be altered into the forms more appropriate for power system stability studies. The model of an induction machine can be put in a similar form as well [45].

We avoid using compact forms of generator models in this thesis, as these models partially approximate generator dynamics as instantaneous. Instead, we use the synchronous and induction generator models which preserve dynamics of rotation and dynamics of all windings. These models are taken from [32] and only their final forms are presented here. The reader is encouraged to look at [32] for the full derivation of the models which will be shown next.

It is important to emphasize that the generator models used in this thesis do not neglect any generator dynamics by approximating it as instantaneous.

The synchronous generator model expressed using flux linkages as state variables is

$$\begin{aligned}
\dot{\psi}_d &= -i_d r_s - v_d + \omega_e \psi_q \\
\dot{\psi}_D &= -i_D r_D \\
\dot{\psi}_f &= -i_f r_f + v_f \\
\dot{\psi}_q &= -i_q r_s - v_q - \omega_e \psi_d \\
\dot{\psi}_Q &= -i_Q r_Q \\
\dot{\theta} &= \omega \\
\dot{\omega} &= \frac{1}{2H}(T_m - T_e)
\end{aligned} \tag{3.53}$$

In this equation, flux linkages ψ_d and ψ_q are the flux linkages of the stator winding. Flux linkages ψ_D and ψ_Q are the flux linkages of the rotor damper winding. Flux linkage ψ_f is the flux linkage of the rotor field excitation winding. Currents i_d, i_q, i_D, i_Q and i_f correspond to these flux linkages. Electrical torque T_e is created by the load while mechanical torque T_m is provided through the governor of the generator. Excitation voltage is denoted with

v_f.

To complete the model, the connection between currents and flux linkages is given by the relationship

$$\begin{bmatrix} \psi_d \\ \psi_D \\ \psi_f \\ \psi_q \\ \psi_Q \end{bmatrix} = \begin{bmatrix} L_d & L_{AD} & L_{AF} & 0 & 0 \\ L_{AD} & L_D & L_{DF} & 0 & 0 \\ L_{AF} & L_{DF} & L_F & 0 & 0 \\ 0 & 0 & 0 & L_q & L_{AQ} \\ 0 & 0 & 0 & L_{AQ} & L_Q \end{bmatrix} \begin{bmatrix} i_d \\ i_D \\ i_f \\ i_q \\ i_Q \end{bmatrix} \tag{3.54}$$

or in compact form

$$[\psi_d\, \psi_D\, \psi_f\, \psi_q\, \psi_Q]^T = \mathbf{L_g}[i_d\, i_D\, i_f\, i_q\, i_Q]^T \tag{3.55}$$

where $\mathbf{L_g}$ is the machine inductance matrix relating the flux linkages and the currents in the coils. The electrical torque T_e is equal to

$$T_e = \psi_q i_d - \psi_d i_q \tag{3.56}$$

The induction generator model can also be stated using flux linkages as state variables

$$\begin{aligned} \dot{\psi}_d &= -i_d r_s - v_d + \omega_e \psi_q \\ \dot{\psi}_D &= -i_D r_D - v_D + (\omega_e - \omega)\psi_Q \\ \dot{\psi}_q &= -i_q r_s - v_q - \omega_e \psi_d \\ \dot{\psi}_Q &= -i_Q r_Q - v_Q - (\omega_e - \omega)\psi_D \\ \dot{\theta} &= \omega \\ \dot{\omega} &= \frac{1}{2H}(T_m - T_e) \\ T_e &= \psi_D i_Q - \psi_Q i_D \\ [\psi_d\, \psi_q\, \psi_D\, \psi_Q]^T &= \mathbf{L_g}[i_d\, i_q\, i_D\, i_Q]^T \end{aligned} \tag{3.57}$$

As the synchronous and induction generator models are very similar, we will continue

with derivations using the synchronous generator model. Everything that is derived in this section can also be done in the case of the induction generator whose final model will take a slightly different form from the synchronous generator form.

The dynamic model in Equation (3.53) can be rewritten using currents as states, as shown in [32]. The change of states is simply obtained by using the relationship (3.55) as the mapping between states. The newly obtained dynamic model is

$$\begin{aligned}
\dot{i}_d &= -l_d r_s i_d - l_{AD} r_r i_D - l_{AF} r_f i_f + \omega_e l_d L_q i_q + \omega_e l_d L_{AQ} i_Q - l_d v_d - l_{AF} v_f \\
\dot{i}_D &= -l_{AD} r_s i_d - l_D r_r i_D - l_{DF} r_f i_f + \omega_e l_{AD} L_q i_q + \omega_e l_{AD} L_{AQ} i_Q - l_{AD} v_d - l_{AF} v_f \\
\dot{i}_f &= -l_{AF} r_s i_d - l_{DF} r_r i_D - l_F r_f i_f + \omega_e l_{AF} L_q i_q + \omega_e l_{AF} L_{AQ} i_Q - l_{AF} v_d - l_F v_f \\
\dot{i}_q &= -\omega_e l_q L_d i_d - \omega_e l_q L_{AD} i_D - \omega_e l_q L_{AF} i_f - l_q r_s i_q - l_{AQ} r_r i_Q - l_q v_q \\
\dot{i}_Q &= -\omega_e l_{AQ} L_d i_d - \omega_e l_{AQ} L_{AD} i_D - \omega_e l_{AQ} L_{AF} i_f - l_{AQ} r_s i_q - l_Q r_r i_Q - l_{AQ} v_q \\
\dot{\theta} &= \omega \\
\dot{\omega} &= \frac{1}{2H}(T_m - T_e)
\end{aligned} \tag{3.58}$$

where

$$\mathbf{l} = \mathbf{L}^{-1} = \begin{bmatrix} l_d & l_{AD} & l_{AF} & 0 & 0 \\ l_{AD} & l_D & l_{DF} & 0 & 0 \\ l_{AF} & l_{DF} & l_F & 0 & 0 \\ 0 & 0 & 0 & l_q & l_{AQ} \\ 0 & 0 & 0 & l_{AQ} & l_Q \end{bmatrix} \tag{3.59}$$

is the inverse of the generator inductance matrix $\mathbf{L}$. The electrical torque can be expressed using currents as

$$T_e = (L_q - L_d) i_d i_q + L_{AQ} i_Q i_d - L_{AD} i_D i_q - L_{AF} i_f i_q \tag{3.60}$$

The excitation system and governors are not modeled although the inclusion of these models is simple. Instead, mechanical input power is assumed constant. This way, only the effect of faster controllers, FACTS and excitation, to interconnected system dynamics

is observed.

Energy accumulated in a generator is the sum of kinetic energy of rotation E_{rot} and electromagnetic energy of stator and rotor coils E_{em}.

$$E_g = E_{rot} + E_{em} = H\omega^2 + \frac{1}{2}\mathbf{I_g^T L I_g} \tag{3.61}$$

Control of generator acceleration

Next, we show how generator acceleration can be controlled using the excitation voltage. The controller derived here is used in the following chapters to ensure interconnected system stability.

In order to control generator acceleration, we create a control Lyapunov function-like controller and define the objective manifold as

$$\nu(x_g) = \frac{1}{2}(\alpha - \alpha^*)^2 \tag{3.62}$$

where α is the acceleration of the generator.

Function from (3.62) satisfies the first two properties of CLF: $\nu(x_g) \geq 0,\ \forall x_g \in \mathcal{R}^7$ and $\nu(x_g) = 0,\ \alpha = \alpha^*$. The third property of the CLF, $\dot{\nu}(x_g) \leq 0,\ \forall x_g \in \mathcal{R}^7$, is guaranteed by the controller. The first derivative of the energy function is

$$\dot{\nu}(x_g) = (\alpha - \alpha^*)\dot{\alpha} \tag{3.63}$$

If the generator damping is neglected, the generator acceleration is defined as

$$\alpha = \frac{1}{2H}(T_M - T_e) = \frac{1}{2H}(T_M - \mathbf{I_g^T N I_g}) \tag{3.64}$$

The first derivative of acceleration is then

$$\dot{\alpha} = -\frac{\dot{T}_e}{2H} = \frac{1}{2H}(\omega(\Psi_d i_d + \Psi_q i_q) + Q_e - (\Psi_q \dot{i}_d - \Psi_d \dot{i}_q)) \tag{3.65}$$

where $\Psi_d = L_d i_d + L_{AD} i_D + L_{AF} i_F$ and $\Psi_q = L_q i_q + L_{AQ} i_Q$. In the last equation $\dot{i}_d$ depends on the excitation voltage v_f while $\dot{i}_q$ does not. This is due to the fact that the excitation winding is aligned with $d - axis$ of the rotor.

By choosing the exciter voltage as

$$v_f = \frac{1}{l_{AF}\Psi_q}(-\omega(\Psi_d i_d + \Psi_q i_q) - Q_e - \Psi_q(\dot{i}_d - l_{AF} v_f) + \Psi_d \dot{i}_q - \beta) \tag{3.66}$$

we obtain $\dot{\alpha} = -\beta$. The term β is specified by the designer and in our case we choose it to be

$$\beta = K_P(\alpha - \alpha^*) \tag{3.67}$$

where $K_P > 0$ is the gain of the controller. This controller will ensure that the generator states reach desired objective manifold.

3.3 Modeling of an Interconnected Power System

In order to introduce a model of an interconnected power system, we take a step back and define a common reference. Each device model is represented in terms of dynamics of phasors. The D and Q components of these phasors are given with respect to a reference axis. The reference axis has to be the same for all the devices in the system if we are to combine their models together. Therefore, we first introduce a unique reference. Next, we show how generator states are mapped from their local reference frames into this common

reference frame. Finally, the interconnected system model is shown.

3.3.1 The choice of phase angle reference

A reference angle has to exist in an interconnected power system if we wish to represent voltages and currents in terms of phasors. The phase angle of each phasor is measured relative to this common reference angle. Another way to think about the phase angle reference is to consider it as the time-zero marker for the time domain sin-wave voltages and currents.

At the same time, rotor position angles of all synchronous generators can be expressed as the deviations from this common reference, denoted by δ, instead of the absolute value of the rotor position angle θ. An advantage of capturing dynamics of rotor position deviation over rotor angle absolute value is that it tells more about dynamic stability of the interconnected system. Rotor angle deviations show if the synchronization between generators is lost and preserving the synchronization between generators is the main transient stabilization objective.

The common reference angle is defined by the frequency it rotates at, notably called reference frequency. The choice of the reference frequency is not unique and a few most common references are described next. Three ways of assigning the frequency reference are commonly used: nominal steady state frequency, frequency of a large machine, or center of inertia frequency.

Nominal Steady State Frequency as the Reference Frequency

The reference frequency can be chosen as the nominal steady state frequency of all synchronous machines. The nominal frequency, which is denoted by ω_0, is a constant value for the entire simulation time and equal to $377 rad/s (60 Hz)$. The steady state frequency is not physical and does not belong to any of the generators nor devices in the system.

Therefore, it is more often used in power system simulation tools than for control design purposes, e.g. MATLAB SimPowerSystems Toolbox uses this reference.

If nominal steady state frequency is used as a reference, then the dynamic equations describing rotation of all synchronous generators in the system are modified in the following way

$$\begin{aligned} \dot{\delta} &= \omega - \omega_0 \\ \dot{\omega} &= \frac{1}{2H}(T_m - \mathbf{I_g^T N I_g}) \end{aligned} \tag{3.68}$$

where δ represents the deviation of the generator's rotor angle position from the reference angle.

Frequency of a Large Generator as Reference

Frequency of a very large generator can be taken as the reference frequency. This is usually the generator with the largest inertia. Additionally, it is assumed that this generator is equipped with a governor controller whose set-point is set to the nominal frequency of the system $\omega_0 = 377 rad/s$.

If a generator is chosen as the reference generator then its frequency and phase angle are removed from the set of system states. This is done because the reference frequency has to be known at all times and cannot depend on other states. Therefore, this approach somewhat changes the overall dynamic response of the interconnected power system because it neglects the dynamics of frequency which, although slow, might still exist. Note that the current dynamics of this generator are kept in the system model.

Additionally, if the voltage is perfectly controlled to a desired value, dynamic equations for voltage can be removed from the system model. If this assumption is made we arrive at the infinite bus approximation of a large generator. An infinite bus can be considered as an exceptionally large generator whose frequency is always constant and equal to ω_0 and

whose voltage is controlled to its set-point E.

The dynamic equations describing rotation of all synchronous generators in the system except of the reference generator will be modified in the same way as shown in (3.68). The difference between this reference and the nominal steady state frequency is in the number of states kept in the interconnected system model.

Center of Inertia Frequency as the Reference Frequency

Center of inertia (COI) frequency is the scaled weighted sum of the frequencies of all generators in the system [31]. The weights are the inertias of all generators and the scaling factor is the sum of all inertias. Therefore, center of inertia frequency and center of inertia phase angle are given by

$$\begin{aligned} \omega_{COI} &= \frac{1}{\sum_{k=0}^{n_g} H_k} \sum_{k=0}^{n_g} H_k \omega_k \\ \theta_{COI} &= \frac{1}{\sum_{k=0}^{n_g} H_k} \sum_{k=0}^{n_g} H_k \theta_k \end{aligned} \tag{3.69}$$

The dynamic behavior of center of inertia reference is obtained by taking the first derivative of expressions in Equation (3.69) and is given by

$$\begin{aligned} \omega_{COI} &= \frac{1}{2H_T} T_{COI} \\ \theta_{COI} &= \omega_{COI} \end{aligned} \tag{3.70}$$

where T_{COI} and H_T are defined as

$$\begin{aligned} T_{COI} &= \sum_{k=0}^{n_g} T_{m_k} - T_{e_k} \\ H_T &= \sum_{k=0}^{n_g} H_k \end{aligned} \tag{3.71}$$

The dynamic equations describing rotation of all synchronous generators in the system are modified in the following way

$$\begin{aligned}\dot{\delta} &= \tilde{\omega} = \omega - \omega_{COI} \\ \dot{\tilde{\omega}} &= \frac{1}{2H}(T_m - \mathbf{I_g^T N I_g}) - \frac{1}{2H_T}T_{COI}\end{aligned} \tag{3.72}$$

This reference is a moving reference which is not fixed by any constraint. In other words, this kind of reference allows for mechanical frequencies of synchronous generators to settle at any value without specifying what that value should be. One way to avoid floating frequency is to model governors as dynamic and use frequency control to ensure that the frequency of all generators is controlled toward ω_0 and therefore $\omega_{COI} = \omega_0$. If this is not done, then the value of the frequency of center of inertia is unknown using this model.

Frequency Reference and the Electrical Frequency

All the reference frames presented in this section convert the dynamic system model into a form in which all the state variables converge to constants in steady state and in which deviations in rotation are captured as dynamic states.

In all three cases, the dynamics of currents and voltages should be interpreted relative to the corresponding reference frequency. Therefore we define electrical frequency as

$$\omega_e = \omega_0 \tag{3.73}$$

if the reference frequency is chosen as the nominal steady state frequency or the frequency of a large generator and

$$\omega_e = \omega_{COI} \tag{3.74}$$

if the electrical frequency is chosen as the center of inertia frequency.

It is important to mention that the induction generator model is also modified to describe deviations in frequency and rotor position angle. However, this modification does not provide any new insight into system stability due to the existence of an induction machine's slip frequency.

Center of inertia phase angle reference is used in this thesis.

3.3.2 Mapping Generator States into Network Reference Frame

Generator equations (3.53) and (3.57) are given in the rotating reference frame. The rotating reference frame is aligned with the rotor of the generator, and notably, it spins with the velocity equal to the mechanical frequency of the generator. D and Q component of the stator and rotor flux in these equations are given relative to the rotating reference frame.

On the other hand, a reference frame rotating together with the electrical frequency of the network is called network reference frame.

In order to put a model of an interconnected system together, multiple generators have to be interconnected. In order to do so, the states of these generators should be mapped into the same reference frame. We choose this common reference frame as explained in the previous section and we name it network reference frame.

The Park-Blondel transform is used to map the states of generators from their respective rotating reference frames into the common network reference frame. The Park-Blondel transform which maps the states of the generator from the rotating into network reference

frame is given as

$$\begin{bmatrix} I_D \\ \\ I_Q \end{bmatrix} = \begin{bmatrix} sin(\delta) & cos(\delta) \\ \\ -cos(\delta) & sin(\delta) \end{bmatrix} \begin{bmatrix} i_d \\ \\ i_q \end{bmatrix} = \mathbf{P_B}(\delta) \begin{bmatrix} i_d \\ \\ i_q \end{bmatrix} \tag{3.75}$$

where (i_d, i_q) is the phasor of stator current of the generator in rotating reference frame, (I_D, I_Q) is the phasor of the same current in the network reference frame and δ is deviation of the rotor position angle of the generator.

The inverse transform which maps the generator stator current from the network to the rotating reference frame is given as

$$\begin{bmatrix} i_d \\ \\ i_q \end{bmatrix} = \begin{bmatrix} sin(\delta) & -cos(\delta) \\ \\ cos(\delta) & sin(\delta) \end{bmatrix} \begin{bmatrix} I_D \\ \\ I_Q \end{bmatrix} = \mathbf{P_B^{-1}}(\delta) \begin{bmatrix} I_D \\ \\ I_Q \end{bmatrix} \tag{3.76}$$

Now that the transform has been introduced, it is convenient to rewrite the generator model in the network reference frame. The obtained generator model describes dynamics of the phasor of stator current in the network reference frame (I_D, I_Q).

Reference [31] explains how this change of states is performed on the system whose generators are represented using two-axis generator model. Derivation in this thesis follows the same steps, and therefore, it will not be described in details.

The dynamical equations of the generator given in (3.58) can be rewritten as

$$\begin{aligned} \dot{I}_D = & - c_1 r_s I_D + c_2 r_s (I_D cos(2\delta) + I_Q sin(2\delta)) \\ & + \omega_e d_1 I_Q + \omega_e d_2 (I_D sin(2\delta) - I_Q cos(2\delta)) \\ & - l_{AD} r_r i_D sin(\delta) - l_{AF} r_f i_f sin(\delta) + \omega_e l_d L_{AQ} i_Q sin(\delta) \\ & - \omega_e l_q L_{AD} i_D cos(\delta) - \omega_e l_q L_{AF} i_f cos(\delta) - l_{AQ} r_r i_Q cos(\delta) \end{aligned}$$

$$
\begin{aligned}
&- c_1 V_D + c_2(V_D cos(2\delta) + V_Q sin(2\delta)) - l_{AF} v_f sin(\delta) - (\omega - \omega_e) I_Q \\
\dot{i}_D =& - l_{AD} r_s (I_D sin(\delta) - I_Q cos(\delta)) - l_D r_r i_D - l_{DF} r_f i_f \\
&+ \omega_e l_{AD} L_q (I_D cos(\delta) + I_Q sin(\delta)) + \omega_e l_{AD} L_{AQ} i_Q - l_{AD} v_d - l_{AF} v_f \\
\dot{i}_f =& - l_{AF} r_s (I_D sin(\delta) - I_Q cos(\delta)) - l_{DF} r_r i_D - l_F r_f i_f \\
&+ \omega_e l_{AF} L_q (I_D cos(\delta) + I_Q sin(\delta)) + \omega_e l_{AF} L_{AQ} i_Q - l_{AF} v_d - l_F v_f \\
\dot{I}_Q =& - c_1 r_s I_Q + c_2 r_s (I_D sin(2\delta) - I_Q cos(2\delta)) \\
&- \omega_e d_1 I_D - \omega_e d_2 (I_D cos(2\delta) + I_Q sin(2\delta)) \\
&+ l_{AD} r_r i_D cos(\delta) + l_{AF} r_f i_f cos(\delta) - \omega_e l_d L_{AQ} i_Q cos(\delta) \\
&- \omega_e l_q L_{AD} i_D sin(\delta) - \omega_e l_q L_{AF} i_f sin(\delta) - l_{AQ} r_r i_Q sin(\delta) \\
&- c_1 V_Q + c_2 (V_D sin(2\delta) - V_Q cos(2\delta)) + l_{AF} v_f cos(\delta) + (\omega - \omega_e) I_D \\
\dot{i}_Q =& - \omega_e l_{AQ} L_d (I_D sin(\delta) - I_Q cos(\delta)) - \omega_e l_{AQ} L_{AD} i_D - \omega_e l_{AQ} L_{AF} i_f \\
&- l_{AQ} r_s (I_D cos(\delta) + I_Q sin(\delta)) - l_Q r_r i_Q - l_{AQ} v_q \\
\dot{\delta} =& \omega - \omega_e \\
\dot{\omega} =& \frac{1}{2H}(T_m - T_e)
\end{aligned}
\tag{3.77}
$$

where,

$$
\begin{aligned}
c_1 &= \frac{1}{2}(l_d + l_q), \quad d_1 = \frac{1}{2}(l_d L_q + l_q L_d) \\
c_2 &= \frac{1}{2}(l_d - l_q), \quad d_2 = \frac{1}{2}(l_d L_q - l_q L_d)
\end{aligned}
\tag{3.78}
$$

Next, we rewrite Equation (3.77) in the compact matrix form as

$$\begin{aligned}
\dot{\mathbf{I}}_{\mathbf{g}} =& \mathbf{A_{ss}}(\delta,\omega)\mathbf{I_g} + \mathbf{A_{sr}}(\delta,\omega)\mathbf{i_g} + \mathbf{B_{ss}}(\delta)\mathbf{V} + \mathbf{B_{sr}}(\delta)v_f \\
\dot{\mathbf{i}}_{\mathbf{g}} =& \mathbf{A_{rs}}(\delta,\omega)\mathbf{I_g} + \mathbf{A_{rr}}(\omega)\mathbf{i_g} + \mathbf{B_{rs}}(\delta)\mathbf{V} + \mathbf{B_{rr}}v_f \\
\dot{\delta} =& \omega - \omega_e \\
\dot{\omega} =& \frac{1}{2H}(T_m - \mathbf{I_g^T N I_g})
\end{aligned} \tag{3.79}$$

where

$$\begin{aligned}
\mathbf{A_{ss}}(\delta,\omega) =& \mathbf{A_1} + \mathbf{B_1 W} + \mathbf{C_1 R}(2\delta) + \mathbf{D_1 W R}(2\delta) - \tilde{\mathbf{W}} \\
\mathbf{A_{sr}}(\delta,\omega) =& \mathbf{P_B}(\delta)\mathbf{F_1} + \mathbf{P_B}(\delta)\mathbf{W H_1} \\
\mathbf{B_{ss}}(\delta) =& \mathbf{M_1} + \mathbf{N_1 R}(2\delta) \\
\mathbf{B_{sr}}(\delta) =& \mathbf{K_1 U}(\delta) \\
\mathbf{A_{rs}}(\delta,\omega) =& \mathbf{C_2 P_B^{-1}}(\delta) + \mathbf{W_3 D_2 P_B^{-1}}(\delta) \\
\mathbf{A_{rr}}(\omega) =& \mathbf{F_2} + \mathbf{W_3 H_2} \\
\mathbf{B_{rs}}(\delta) =& \mathbf{N_2 P_B^{-1}}(\delta) \\
\mathbf{B_{rr}} =& \mathbf{K_2}
\end{aligned} \tag{3.80}$$

and $\mathbf{I_g}$ is the vector of stator current in the network reference frame and $\mathbf{i_g}$ is the vector of rotor currents in the rotating reference frame

$$\mathbf{I_g} = [I_D\ I_Q]^T, \quad \mathbf{i_g} = [i_D\ i_F\ i_Q]^T \tag{3.81}$$

and $\mathbf{V}$ is the vector of the generator terminal voltage in the network reference frame

$$\mathbf{V} = [V_D\ V_Q]^T \tag{3.82}$$

Matrix $\mathbf{P_B}(\delta)$ in Equation (3.80) is the Park-Blondel transform matrix and $\mathbf{P_B^{-1}}(\delta)$ is its inverse. Matrices $\mathbf{R}(2\delta)$, $\mathbf{W}$, $\mathbf{W_3}$, $\tilde{\mathbf{W}}$ and $\mathbf{U}(\delta)$ are

$$\begin{aligned} \mathbf{R}(2\delta) &= \begin{bmatrix} cos(2\delta) & sin(2\delta) \\ sin(2\delta) & -cos(2\delta) \end{bmatrix} \quad \mathbf{W} = \begin{bmatrix} 0 & \omega \\ -\omega & 0 \end{bmatrix} \quad \mathbf{W_3} = \begin{bmatrix} 0 & \omega & 0 \\ 0 & 0 & \omega \\ -\omega & 0 & 0 \end{bmatrix} \\ \tilde{\mathbf{W}} &= \begin{bmatrix} 0 & \omega-\omega_e \\ -(\omega-\omega_e) & 0 \end{bmatrix} \quad \mathbf{U}(\delta) = \begin{bmatrix} sin(\delta) \\ -cos(\delta) \end{bmatrix} \end{aligned} \tag{3.83}$$

Parameter matrices in Equation (3.80) are

$$\begin{aligned} \mathbf{A_1} &= \begin{bmatrix} -r_s c_1 & 0 \\ 0 & -r_s c_1 \end{bmatrix} \quad \mathbf{B_1} = \begin{bmatrix} d_1 & 0 \\ 0 & d_1 \end{bmatrix} \quad \mathbf{C_1} = \begin{bmatrix} r_s c_2 & 0 \\ 0 & r_s c_2 \end{bmatrix} \quad \mathbf{D_1} = \begin{bmatrix} d_2 & 0 \\ 0 & d_2 \end{bmatrix} \\ \mathbf{F_1} &= \begin{bmatrix} -l_{AD} r_r & -l_{AF} r_f & 0 \\ 0 & 0 & -l_{AQ} r_r \end{bmatrix} \quad \mathbf{H_1} = \begin{bmatrix} l_q L_{AD} & l_q L_{AF} & 0 \\ 0 & 0 & l_d L_{AQ} \end{bmatrix} \\ \mathbf{M_1} &= \begin{bmatrix} -c_1 & 0 \\ 0 & -c_1 \end{bmatrix} \quad \mathbf{N_1} = \begin{bmatrix} c_2 & 0 \\ 0 & c_2 \end{bmatrix} \quad \mathbf{K_1} = \begin{bmatrix} -l_{AF} & 0 \\ 0 & -l_{AF} \end{bmatrix} \\ \mathbf{C_2} &= \begin{bmatrix} -l_{AD} r_s & 0 \\ -l_{AF} r_s & 0 \\ 0 & -l_{AQ} r_s \end{bmatrix} \quad \mathbf{D_2} = \begin{bmatrix} l_{AQ} L_d & 0 \\ 0 & l_{AD} L_q \\ 0 & l_{AF} L_q \end{bmatrix} \quad \mathbf{N_2} = \begin{bmatrix} -l_{AD} & 0 \\ -l_{AF} & 0 \\ 0 & -l_{AQ} \end{bmatrix} \quad \mathbf{K_2} = \begin{bmatrix} -l_{DF} \\ -l_{AF} \\ 0 \end{bmatrix} \\ \mathbf{F_2} &= \begin{bmatrix} -l_D r_r & -l_{DF} r_f & 0 \\ -l_{DF} r_r & -l_F r_f & 0 \\ 0 & 0 & -l_Q r_r \end{bmatrix} \quad \mathbf{H_2} = \begin{bmatrix} l_{AQ} L_{AD} & l_{AQ} L_{AF} & 0 \\ 0 & 0 & l_{AD} L_{AQ} \\ 0 & 0 & l_{AF} L_{AQ} \end{bmatrix} \end{aligned} \tag{3.84}$$

Finally, to ease the notation, generator model (3.79) will be referred to as

$$\dot{x}_g = f_g(x_g, y_g, u_g) \tag{3.85}$$

where $x_g = [I_D \ I_Q \ i_D \ i_F \ i_Q \ \delta \ \omega]^T$ is the vector of generator states and $y_g = [V_D \ V_Q]^T$ is the coupling vector with the transmission line model. The set of dynamic equations f_g will vary between the synchronous and induction machine equations depending on the type of generator. The governor mechanical input torque is considered as a parameter while the excitation is considered as a control input. Therefore, $u_g = v_f$.

3.3.3 Dynamic Model of an Interconnected Power System

An interconnected system model is obtained by combining the full dynamic models of induction and/or synchronous generators shown in Equation (3.85); with transmission line

time-varying phasor model shown in Equation (3.48); and the FACTS time-varying phasor model shown in Equation (3.23).

Consider a power system with n_b nodes, n_{tl} transmission lines, n_g generators and n_f FACTS devices. For $i = 1...n_b$, $j = 1...n_{tl}$, $k = 1...n_g$ and $m = 1...n_f$, the interconnected power system model is

$$
\begin{aligned}
\dot{\mathbf{I}}_{\mathbf{g}_k} =& \mathbf{A}_{\mathbf{ss}_k}(\delta_k, \omega_k)\mathbf{I}_{\mathbf{g}_k} + \mathbf{A}_{\mathbf{sr}_k}(\delta_k, \omega_k)\mathbf{i}_{\mathbf{g}_k} + \mathbf{B}_{\mathbf{ss}_k}(\delta_k)\mathbf{S_g}[k,i]\mathbf{V_i} + \mathbf{B}_{\mathbf{sr}_k}(\delta_k)v_{f_k} \\
\dot{\mathbf{i}}_{\mathbf{g}_k} =& \mathbf{A}_{\mathbf{rs}_k}(\delta_k, \omega_k)\mathbf{I}_{\mathbf{g}_k} + \mathbf{A}_{\mathbf{rr}_k}(\omega_k)\mathbf{i}_{\mathbf{g}_k} + \mathbf{B}_{\mathbf{rs}_k}(\delta_k)\mathbf{S_g}[k,i]\mathbf{V_i} + \mathbf{B}_{\mathbf{rr}_k}v_{f_k} \\
\dot{\delta}_k =& \omega_b\tilde{\omega}_k \\
\dot{\tilde{\omega}}_k =& \frac{1}{2H_k}(T_{M_k} - \mathbf{I}_{\mathbf{g}_k}^T\mathbf{N}_k\mathbf{I}_{\mathbf{g}_k} - D_k\tilde{\omega}_k) - \frac{1}{2H_T}T_{COI} \\
\dot{V}_{b_iD} =& \frac{\omega_b}{C_{ch_i}}\left(\sum_{j=1}^{n_{tl}}\mathbf{S_{tl}}[i,j]I_{tl_jD} + \mathbf{S_g}[i,k]\mathbf{I}_{\mathbf{g}_k} - \frac{P_{l_i}V_{b_iD} + Q_{l_i}V_{b_iQ}}{V_{b_iD}^2 + V_{b_iQ}^2}\right) + \omega_b\omega V_{b_iQ} \\
\dot{V}_{b_iQ} =& \frac{\omega_b}{C_{ch_i}}\left(\sum_{j=1}^{n_{tl}}\mathbf{S_{tl}}[i,j]I_{tl_jQ} + \mathbf{S_g}[i,k]\mathbf{I}_{\mathbf{g}_k} - \frac{P_{l_i}V_{b_iQ} - Q_{l_i}V_{b_iD}}{V_{b_iD}^2 + V_{b_iQ}^2}\right) - \omega_b\omega V_{b_iD} \\
\dot{I}_{tl_jD} =& \frac{\omega_b}{L_{tl_j}}\left(-\sum_{i=1}^{n_b}\mathbf{S_{tl}}[j,i]V_{b_iD} - \mathbf{S_f}[j,m]V_{mD} - \omega_b\frac{R_{tl_j}}{L_{tl_j}}I_{tl_jD}\right) + \omega_b\omega I_{tl_jQ} \\
\dot{I}_{tl_jQ} =& \frac{\omega_b}{L_{tl_j}}\left(-\sum_{i=1}^{n_b}\mathbf{S_{tl}}[j,i]V_{b_iQ} - \mathbf{S_f}[j,m]V_{mQ} - \omega_b\frac{R_{tl_j}}{L_{tl_j}}I_{tl_jQ}\right) - \omega_b\omega I_{tl_jD} \\
\dot{V}_{mD} =& \frac{\omega_b}{C_m}\left(\mathbf{S_f}[m,j]I_{tlD} - I_{mD}\right) + \omega_b\omega V_{mQ} \\
\dot{V}_{mQ} =& \frac{\omega_b}{C_m}\left(\mathbf{S_f}[m,j]I_{tlQ} - I_{mQ}\right) - \omega_b\omega V_{mD} \\
\dot{I}_{mD} =& \frac{\alpha_m\omega_b}{L_m}V_{mD} + \omega_b\omega I_{mQ} \\
\dot{I}_{mQ} =& \frac{\alpha_m\omega_b}{L_m}V_{mQ} - \omega_b\omega I_{mD}
\end{aligned}
\tag{3.86}
$$

where $\mathbf{I_{g_k}}$ is the vector of coil currents of generator k, δ_k its rotor angle deviation and $\tilde{\omega}_k$ frequency deviation. Node voltages are denoted by V_{b_i} and transmission line currents by I_{tl_j}. FACTS states are V_m and I_m. Parameter ω_b is the base frequency of the system.

Matrix $\mathbf{B}_\delta(\delta_k)$ is the Park-Blondel transform which is introduced to convert the generator stator currents from the rotating into the network reference frame.

Matrices $\mathbf{S_{tl}} \in \mathcal{R}^{n_b \times n_{tl}}$, $\mathbf{S_g} \in \mathcal{R}^{n_b \times n_g}$ and $\mathbf{S_f} \in \mathcal{R}^{n_{tl} \times n_f}$ are incidence matrices which show the connectivity between devices in the grid. Matrix $\mathbf{S_{tl}}$ shows the connectivity between transmission lines and nodes. Entry $\mathbf{S_{tl}}[i,j]$ is equal to one if the current of transmission line j is directed into bus i, minus one if directed from the bus, or zero if the two are not connected. Matrix $\mathbf{S_g}$ shows the connectivity between generators and nodes. Entry $\mathbf{S_g}[i,k]$ is equal to one if generator k and bus i are connected or zero otherwise. Matrix $\mathbf{S_f}$ shows the connectivity between FACTS and transmission lines. Entry $\mathbf{S_f}[j,m]$ is equal to one if FACTS device m and transmission line j are connected or zero otherwise.

This approach to interconnected system modeling can exhibit a problem in the modeling of transmission lines which connect buses with no external injection (generation and/or demand). If all transmission lines have particularly small charging capacitances, or no charging capacitances at all, then one of the transmission line currents will be an algebraic function of all other currents coming into or going out from that node. In order to avoid choosing one current as algebraic when building the model, charging capacitances are modeled for each transmission line. Another possible solution for this problem is the transmission line transformation through the network topology reduction [31]. A drawback of this method is that the newly obtained transmission lines do not resemble physical topology and have no physical parameters.

The coupled set of ODEs from Equation (3.86) can be rewritten as

$$\begin{aligned}
\dot{\mathbf{x}}_\mathbf{g} &= \mathbf{f_g}(\mathbf{x_g}, \mathbf{x_b}) \\
\dot{\mathbf{x}}_\mathbf{b} &= \mathbf{f_b}(\mathbf{x_b}, \mathbf{x_{tl}}, \mathbf{x_g}) \\
\dot{\mathbf{x}}_\mathbf{tl} &= \mathbf{f_{tl}}(\mathbf{x_{tl}}, \mathbf{x_b}, \mathbf{x_f}) \\
\dot{\mathbf{x}}_\mathbf{f} &= \mathbf{f_f}(\mathbf{x_f}, \mathbf{x_{tl}}, \mathbf{u})
\end{aligned} \tag{3.87}$$

In this model, $\mathbf{x_g} \in \mathcal{R}^{7n_g}$ is the vector of states of all generators, $\mathbf{x_{tl}} \in \mathcal{R}^{2n_{tl}}$ is the vector of states of all transmission line currents, $\mathbf{x_b} \in \mathcal{R}^{2n_b}$ is the vector of states of all node voltages, and $\mathbf{x_f} \in \mathcal{R}^{4n_f}$ is the vector of states of all FACTS devices. Input $\mathbf{u} \in \mathcal{R}^{n_f}$ is the vector of firing angles of all FACTS devices. Notably, new proposed representation is modular because each device can be though of as a separate module.

Another way to describe the same system would be to distinguish between its mechanical and electrical parts as in Equation (3.88).

$$\begin{aligned} \dot{\mathbf{x}}_{\mathbf{rot}} &= \mathbf{f}_{\mathbf{rot}}(\mathbf{x}_{\mathbf{rot}}, \mathbf{x}_{\mathbf{em}}) \\ \dot{\mathbf{x}}_{\mathbf{em}} &= \mathbf{f}_{\mathbf{em}}(\mathbf{x}_{\mathbf{rot}}, \mathbf{x}_{\mathbf{em}}, \mathbf{u}) \end{aligned} \tag{3.88}$$

where $\mathbf{x_{rot}} \in \mathcal{R}^{n_{rot}}$ is the vector of the states of rotation and $\mathbf{x_{em}} \in \mathcal{R}^{n_{em}}$ is the vector of the electromagnetic states belonging to generator windings, transmission line and FACTS inductances and capacitances. Parameters $n_{rot} = 2n_g$ and $n_{em} = 5n_g + 2n_b + 2n_{tl} + 4n_f$ are the numbers of the mechanical states of rotation and the electromagnetic states in wires, respectively. Both representations will be used to design different controllers.

The accumulated energy of the interconnected system is equal to the sum of accumulated energies in all devices.

$$E_{tot} = \sum_{k=1}^{n_g} E_{rot_k} + \sum_{k=1}^{n_g} E_{em_k} + \sum_{i=1}^{n_b} E_{b_i} + \sum_{j=1}^{n_{tl}} E_{tl_j} + \sum_{m=1}^{n_f} E_{f_m} \tag{3.89}$$

3.4 Example of a Three-bus System

The new approach to modeling is illustrated on the example of a three-bus system. The controllers which are introduced in the following chapters are simulated on this system.

The three-bus system, given in Figure 3.12, is an interconnected system of three generators and one FACTS device. This system first appeared in [66] and later in [31]. The

Table 3.1: Parameters of the transmission system in the three-bus system

Transmission line	1	3	2
Connecting buses	bus 2-1	bus 2-3	Bus 1-3
$L_{tl}[pu]$	0.46	0.108	0.26
$R_{tl}[pu]$	0.01	0.012	0.01

nominal active power injections and demand values at the time instance of interest are shown in the figure. A TCSC has been added to the original system from [66], but the parameters of the line were changed so that the equilibrium of the system remained unchanged. The TCSC compensates for one third of the transmission line impedance at the given operating point.

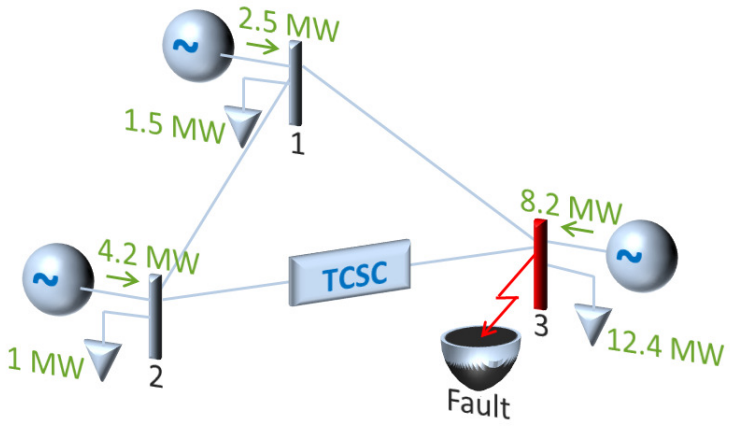

Figure 3.12: Three bus test system.

Parameters of the generators in the three-bus system are given in Table 3.2. Parameters of the transmission system in the three-bus system are given in Table 3.1. The inductor and the capacitor of the TCSC have the values $L = 0.0332pu$ and $C = 45.2489pu$.

Table 3.2: Parameters of the generators in the three-bus system

Parameter	Gen 1	Gen 2	Gen 3
$H[s]$	10	15	60
$D[pu]$	0	0	0
$L_d[pu]$	0.44	0.25	0.075
$L_D[pu]$	0.44	0.25	0.075
$L_F[pu]$	0.4462	0.2535	0.076
$L_q[pu]$	0.44	0.25	0.075
$L_Q[pu]$	0.44	0.25	0.075
$L_{ad}[pu]$	0.396	0.225	0.0675
$L_{AF}[pu]$	0.396	0.225	0.0675
$L_{DF}[pu]$	0.396	0.225	0.0675
$L_{aq}[pu]$	0.396	0.225	0.0675
$r_s[pu]$	0.0026	0.0024	0.00028
$r_r[pu]$	0.026	0.024	0.0028
$r_f[pu]$	0.00026	0.00024	0.000028

The model of the three-bus system is given as

$$\begin{aligned}
\dot{x}_{g_1} &= f_g(x_{g_1}, x_{b_1}) \\
\dot{x}_{g_2} &= f_g(x_{g_2}, x_{b_2}) \\
\dot{x}_{g_3} &= f_g(x_{g_3}, x_{b_3}) \\
\dot{x}_{b_1} &= f_b(x_{b_1}, x_{g_1}, x_{tl_1}, x_{tl_2}) \\
\dot{x}_{b_2} &= f_b(x_{b_2}, x_{g_2}, x_{tl_1}, x_{tl_3}) \\
\dot{x}_{b_3} &= f_b(x_{b_3}, x_{g_3}, x_{tl_2}, x_{tl_3}) \\
\dot{x}_{tl_1} &= f_{tl}(x_{tl_1}, x_{b_1}, x_{b_2}) \\
\dot{x}_{tl_2} &= f_{tl}(x_{tl_2}, x_{b_1}, x_{b_3}) \\
\dot{x}_{tl_3} &= f_{tl}(x_{tl_3}, x_{b_2}, x_{b_3}, x_f) \\
\dot{x}_f &= f_f(x_{tl_3}, x_f, u_f)
\end{aligned} \tag{3.90}$$

Simulations in this thesis are always started with the system being at an equilibrium at the beginning of the simulation. Therefore, we denote both, equilibrium of the system and the initial condition with a subscript 0 as $\mathbf{x_0} = \mathbf{x_e}$.

A stable equilibrium of the system is given as

$$
\begin{aligned}
x_{g_10} &= [2.4325 \ -1.0316\ 0 \ -3.8231\ 0\ 0.5822\ 0]^T \\
x_{g_20} &= [4.6730 \ -0.6093\ 0 \ -5.8333\ 0\ 0.7741\ 0]^T \\
x_{g_30} &= [2.2587 \ -8.4402\ 0 \ -21.0000\ 0 \ -0.2887\ 0]^T \\
x_{b_10} &= [0.8043 \ -0.2351]^T \\
x_{b_20} &= [0.7750 \ -0.2493]^T \\
x_{b_30} &= [0.7252 \ -0.5706]^T \\
x_{tl_10} &= [-0.0321\ 0.0629]^T \\
x_{tl_20} &= [1.2999 \ -0.2541]^T \\
x_{tl_30} &= [4.0049 \ -0.1904]^T \\
x_{f0} &= [-0.0052 \ -0.1096 \ -0.9548\ 0.0454]^T \\
u_{f0} &= 0.2892
\end{aligned}
\tag{3.91}
$$

Chapter 4

Energy-based Control of Power Systems

The FACTS controllers proposed in this thesis are motivated by the idea that FACTS devices can stabilize power systems by redirecting energy during large disturbances. Energy and energy-based frameworks are chosen as the basis for the control design for several reasons. First, well-established methods exist for dynamic system controller design, e.g. control Lyapunov function reviewed in Appendix 3. Second, energy functions offer physical interpretation of system dynamics and controller actions. Third, additivity of energy makes it simple to look at the system as an interconnected network of modules. This feature is useful for multi-device systems which change their structure frequently, such as power systems. Fourth and final, energy function is easily partitioned based on location of devices, a feature extremely helpful for decentralization of the controller.

The objective of energy-based approach is to find a monotonically decreasing function along the system trajectories in a certain region around the equilibrium. Existence of such function ensures that the system states will converge to the equilibrium and that the system equilibrium is stable. The function is called energy function due to its properties which are similar to the properties of Hamiltonians of physical systems.

In many cases, controllers can be used to ensure that an energy function of the closed-loop system is monotonically decreasing. These control design methods are called energy shaping methods and the controllers are called energy-based controllers.

This approach to controller design has certain pros and cons with respect to other control design methods. The biggest advantage of energy-based controllers is that they can be applied to large scale physical systems without making any simplifications on the system model. Another advantage of this controller design method is that physical systems with well defined Hamiltonians naturally lend themselves to the control design.

A biggest disadvantage of energy-based controllers is in the high communication requirement. This is particularly inconvenient in the case of highly geographically spread systems such are electric energy grids. Additionally, the entire system equilibrium has to be known by the controllers. These two requirements are hard to meet in practice.

This chapter shows how an energy-based controller for FACTS can be defined. This controller stabilizes the interconnected system dynamics although it suffers from the previously mentioned drawbacks.

4.1 Energy-based full-state FACTS controller

As already explained, FACTS cannot inject or dissipate active power in steady state. Therefore, their impact is limited. At the same time, their performance depends on the way we pose the controller problem. We show that a smart definition of the controller objective will result in better performance.

It was shown in [31] that better performance of energy-based excitation control can be obtained by using an output stabilizing controller over a full-state stabilizing controller. To understand the reason behind it we look at the properties of electric energy grids. First, a power system is transiently stable if its generators are kept synchronized during and after the disturbance. Second, excitation control enters the system as the voltage control which

means that it only indirectly affects the rotation. Therefore, a full-state controller would first stabilize the voltage to an equilibrium and would later barely make an impact at the rotation dynamics. Additionally, this controller would have to be a high-gain controller in order to make a significant impact at the rotation dynamics. This is hardly achievable in practice due to the exciter saturation.

Similarly as excitation control, a FACTS controller has indirect impact on the rotation dynamics. Therefore, we define the objective manifold as an output feedback stabilization manifold in the same way as it was done in [31]. According to this reference, the objective manifold for transient stabilization of the system in Equation (3.88) can be defined as

$$\mathcal{O} = \{ \mathbf{x_{rot}} \in \mathcal{R}^{2n_g} \quad | \quad \dot{\mathbf{x}}_{\mathbf{rot}} = 0 \} \tag{4.1}$$

This objective manifold is the same as the one defined over accumulated energy of rotation

$$\mathcal{O} = \{ \mathbf{x_{rot}} \in \mathcal{R}^{2n_g} \quad | \quad \dot{E}_{rot} = 0 \} \tag{4.2}$$

Next, we observe that for an isolated system during a disturbance of power P_F, it holds that $\dot{E}_{rot} + \dot{E}_{em} = P_F$. Considering this, the objective manifold in Equation (4.2) can be restated in terms of accumulated electromagnetic energy as

$$\mathcal{O} = \{ \mathbf{x_{em}} \in \mathcal{R}^{n-2n_g} \quad | \quad \dot{E}_{em} = P_F^* \} \tag{4.3}$$

At this point, our stabilization objective is reformulated as a tracking objective for which the tracking manifold is given by how much energy we wish to store as electromagnetic. An estimate of the power of disturbance P_F^* has to be made in order to do tracking.

Further, we express this manifold in an incremental way. In other words, we reformulate the tracking objective so that the energy function is equal to zero when the system is at

equilibrium.

$$\tilde{\nu}_{em} = E_{em}(\tilde{\mathbf{x}}_{\mathbf{em}}), \quad \tilde{\mathbf{x}}_{\mathbf{em}} = \mathbf{x}_{\mathbf{em}} - \mathbf{x}_{\mathbf{em0}} \tag{4.4}$$

where $\tilde{\mathbf{x}}_{\mathbf{em}} = \mathbf{x}_{\mathbf{em}} - \mathbf{x}_{\mathbf{em0}}$ is the increment in system states and $\tilde{\nu}_{em}$ is the corresponding increment in electromagnetic energy. We use ν instead of E to mark that we are not dealing with physical energy function anymore, but only with its image which is mapped into the equilibrium of the system.

Next, we arrive to the problem formulation in terms of the incremental energy injected into the system by the disturbance.

$$\mathcal{O} = \{\ \tilde{\mathbf{x}}_{\mathbf{em}} \in \mathcal{R}^{n-2n_g} \quad | \quad \dot{\tilde{\nu}}_{em} = \tilde{P}^*_F\ \} \tag{4.5}$$

The first derivative of the increment in accumulated electromagnetic energy of the system in Equation (3.86) is equal to $\dot{\tilde{\nu}}_{em} = \tilde{P} + \tilde{Q}$, where $\tilde{P}$ and $\tilde{Q}$ correspond to the increment in total system real and reactive power caused by deviations in states and are equal to

$$\begin{aligned}
\tilde{P} =& \sum_{i=1}^{n_b}\sum_{j=1}^{n_{tl}} \mathbf{S_{tl}}[i,j](\tilde{V}_{b_iD}I_{tl_jD} + \tilde{V}_{b_iQ}I_{tl_jQ} + V_{b_iD}\tilde{I}_{tl_jD} + V_{b_iD}\tilde{I}_{tl_jD}) \\
&+ \sum_{m=1}^{n_f}\sum_{j=1}^{n_{tl}} \mathbf{S_f}[m,j](\tilde{V}_{mD}I_{tl_jD} + \tilde{V}_{mQ}I_{tl_jQ} + V_{mD}\tilde{I}_{tl_jD} + V_{mD}\tilde{I}_{tl_jD}) \\
&+ \sum_{m=1}^{n_f}(\tilde{V}_{mD}I_{mD} + \tilde{V}_{mQ}I_{mQ} + V_{mD}\tilde{I}_{mD} + V_{mD}\tilde{I}_{mD}) \\
\tilde{Q} =& \sum_{i=1}^{n_b} C_{ch_i}(\tilde{V}_{b_iD}V_{b_i0Q} - \tilde{V}_{b_iQ}V_{b_i0D}) + \sum_{j=1}^{n_{tl}} L_{tl_j}(\tilde{I}_{tl_jD}I_{tl_j0Q} - \tilde{I}_{tl_jQ}I_{tl_j0D}) \\
&+ \sum_{m=1}^{n_f} C_m(\tilde{V}_{mD}V_{m0Q} - \tilde{V}_{mQ}V_{m0D}) + \sum_{m=1}^{n_f} L_m(\tilde{I}_{mD}I_{m0Q} - \tilde{I}_{mQ}I_{m0D})
\end{aligned} \tag{4.6}$$

Equation (4.6) is not derived in this thesis as this derivation is straightforward and tedious.

Finally, the objective manifold is stated as

$$\mathcal{O} = \{ \tilde{\mathbf{x}}_{\mathbf{em}} \in \mathcal{R}^{n-2n_g} \quad | \quad \tilde{Q} = \tilde{P}_F^* \} \tag{4.7}$$

which reflects our desire to accumulate energy created by a fault inside inductors and capacitors of FACTS devices and transmission system.

The objective manifold given in Equation (4.7) is used to control the system dynamics so that the energy of a disturbance is temporarily accumulated as electromagnetic energy of FACTS. A controller which achieves this is the controller of active power through FACTS given in Equation (3.30) which reference is given as

$$\beta = K_P(P_f - (\tilde{P}_F^* - \tilde{Q})) \tag{4.8}$$

This controller has a few major shortcomings. First, the power of the disturbance has to be known in order to efficiently track its energy. Second, being based on increments, the controller is equilibrium-dependent. Third, all states of all devices need to be communicated to the controller. This has led us to propose an ectropy-based control that does not have these problems as described in the following chapters.

4.2 Stabilization of the Three-bus System

We look at response of the three-bus system, introduced in Section 3.4, to a fault which causes the uncontrolled system to become transiently unstable.

The system is assumed to be in an equilibrium at the beginning of the simulation. The fault is created as a short circuit at Bus 3 at time $t = 0.1s$ from the beginning of the simulations. The short circuit is cleared after $T = 0.33s$ and the system is restored back to

the pre-fault configuration. The critical clearing time of this uncontrolled system for this particular fault is $T_{cct} = 0.25s$. Note that the duration of fault is longer than the critical clearing time of the uncontrolled system.

The response of the uncontrolled system is given in figures 4.1(a) and 4.1(d). Clearly, the system is unstable. Figures 4.1(b) and 4.1(e) show the response of the system when the TCSC is equipped with a linear PI controller taken from [6]. Figures 4.1(c) and 4.1(f) show the response of the system when the TCSC is equipped with a Lyapunov function-based controller from [17]. Both controllers cannot improve the critical clearing time and stabilize the system.

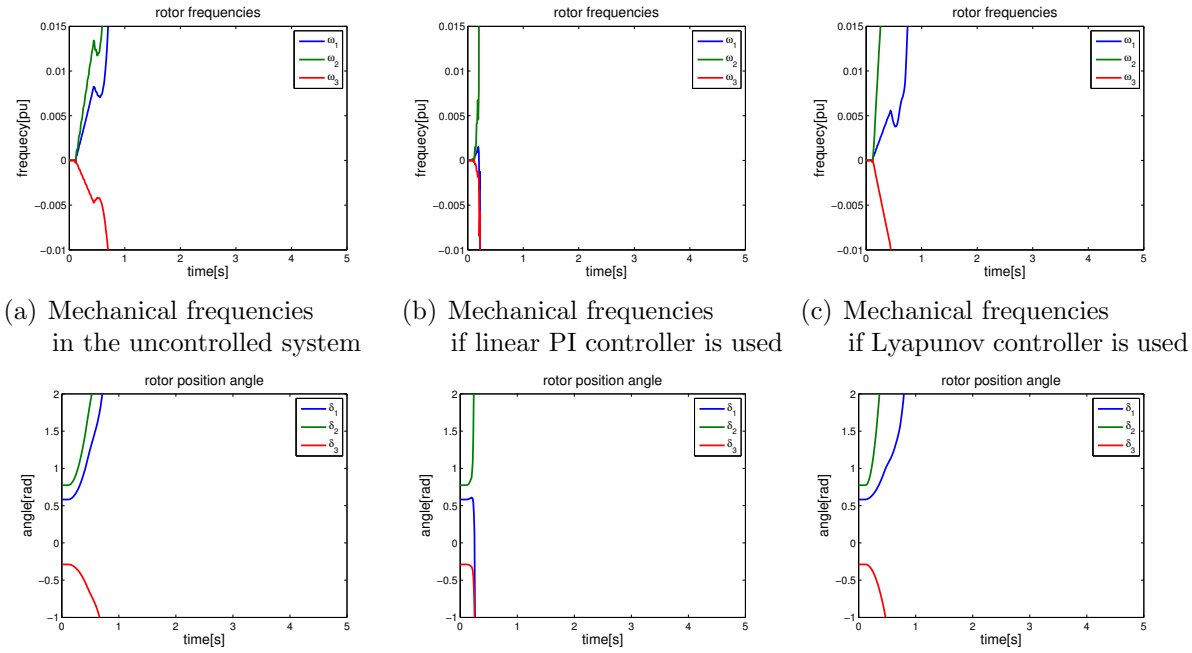

(a) Mechanical frequencies in the uncontrolled system

(b) Mechanical frequencies if linear PI controller is used

(c) Mechanical frequencies if Lyapunov controller is used

(d) Rotor position angles in the uncontrolled system

(e) Rotor position angles if linear PI controller is used

(f) Rotor position angles if Lyapunov controller is used

Figure 4.1: The three bus system response for different unsuccessful controllers.

Next, the energy-based disturbance tracking controller given in Equation (3.30) is used together with the reference from Equation (4.8) to stabilize the system under the described disturbance. The resulting system response is shown in Figure 4.2. The system remains stable for the duration of fault and the critical clearing time is extended. Note from

Figure 4.2(c) that the accumulated energy of the TCSC and wires is rising during the time of fault. This increase in electromagnetic energy is sufficient to slow down the rotation of generators and to extend the critical clearing time.

Figure 4.2(d) shows the switching signal of the TCSC. We observe that the FACTS controller reacts very fast in response to the disturbance. This kind of fast response cannot be obtained with excitation control unless very high-gain controllers are used. High-gain excitation control tends to be ineffective due to saturation of exciters. On the other hand, we observed that the saturation of FACTS switching signal is not reached in this simulation and in the majority of other simulations we performed. One of the reasons for such behavior is that FACTS are able to react fast even without high-gain controllers.

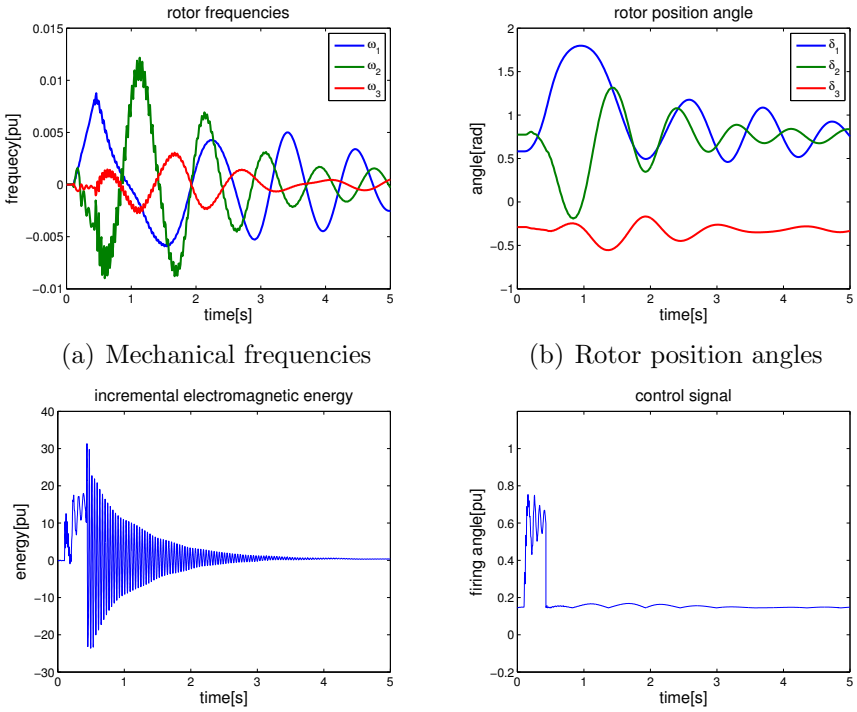

(a) Mechanical frequencies

(b) Rotor position angles

(c) Increment in accumulated energy

(d) Controller signal

Figure 4.2: Three bus test system simulation results for the disturbance tracking TCSC controller.

4.3 Stabilization of the IEEE 14-bus System

One of the contributions of this thesis are controllers which can easily be applied to general large scale systems. As a large scale system example we consider IEEE 14-bus system which is commonly used as a test bench in literature [69, 70]. The parameters of the system are taken from the provided references.

IEEE 14-bus system has five generators as shown in Figure 4.3. Two of these generators, denoted by G, produce active power at the nominal operating point. Other three generators, denoted by C, are operated as synchronous condensers, i.e. they only produce reactive power.

The original system is modified by placing two TCSCs in the transmission grid: TCSC 1 on the transmission line between nodes 4 and 5 and TCSC 2 on the transmission line between nodes 1 and 2.

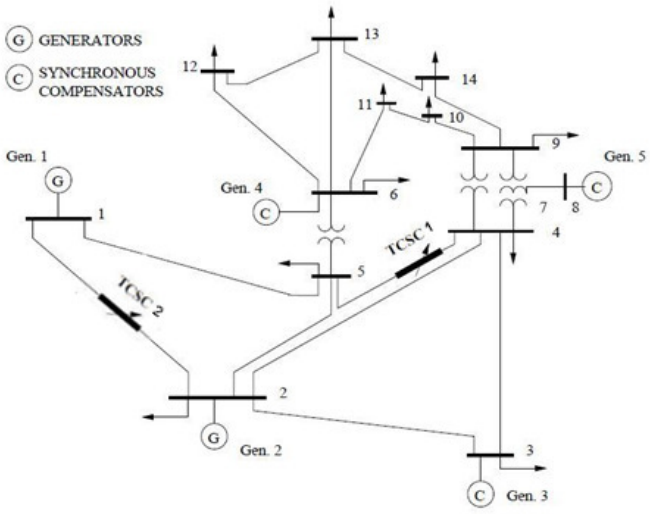

Figure 4.3: IEEE 14 bus system with two TCSCs.

A fault is simulated as a short circuit to the ground at node 4 for a duration of $0.4s$. This fault creates a disturbance which causes transient instability of the system. The stable response of the system with the energy-based TCSC controllers is shown in Figure 4.4.

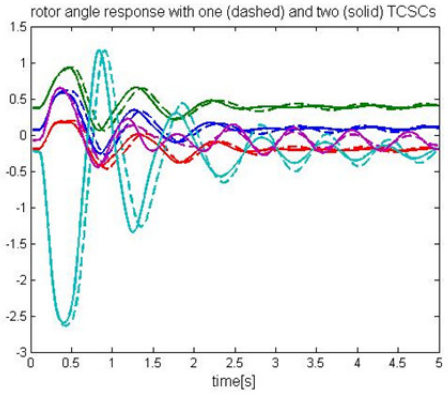

Figure 4.4: Rotor angle position of the generators in the IEEE 14 bus system.

Part II

Two-level Approach to Modeling and Control

Chapter 5

Dynamic Modeling of Power Systems using Interaction Variables

In the remainder of this thesis we introduce the structure-based modeling of general interconnected power systems which would help us with systematic controller design. For this purpose we propose a two-level approach to modeling and control in which lower level captures internal dynamics of components and the higher level captures their interactions.

Interconnected power systems are composed of many different components. Each component participates in the interconnected system dynamics in its own way. With the increased penetration of renewable generation and responsive demand, the dynamic behavior of interconnected power systems becomes more complex than it used to be, while the interconnected system stability remains a high priority objective.

Stability of interconnected power systems is hard to guarantee due to several reasons. The most important reason is that the dynamic system model is extremely complex because of highly nonlinear states evolving at vastly different rates. Further, dynamic models of some devices, sometimes even whole system areas, might be unavailable. Common unwillingness of utilities to share information about the system states reduces observability of states across areas. Therefore, the only practical way to access interconnected power

system stability is to look at the stability of its parts, devices and/or areas, and to pose the stability conditions in such a way to guarantee that once these parts are interconnected the system will remain stable. In this thesis, we propose a modeling approach which represents the power system as an interconnected network of modules.

Different approaches to access dynamical stability of modular systems are proposed in control system theory. Reference [46] introduces stability conditions on module dynamics in terms of interconnection strength which guarantee interconnected stability of complex large-scale dynamical systems. Reference [47] shows how these conditions can be adopted to the systems with nonlinear dynamics. Many practical examples in these references are taken from the domain of power systems. Although mathematically correct, these references do not offer a physical interpretation of the stability conditions. In this thesis, we propose an approach to accessing dynamical stability of power systems using variables which have physical interpretation. We refer to these variables as the interaction variables.

Interaction variables are introduced to explicitly capture how one part of the system affects other parts of the same system. They show interactions between any module and the rest of the system as the change in dynamic states whose observation leads to better understanding of physical phenomena and whose control leads to stability of interconnected systems. The notion of interaction variables for electric power systems was first proposed in [48]. Their physical interpretation is the accumulated energy inside control areas. An extensive use of linearized interaction variables was made in [49] for hierarchical modeling and control in large-scale electric power systems. This notion of interaction variables was used to propose stabilizing controllers for FACTS devices for preventing inter-area oscillations between control areas [50, 51]. Recently, further use of the linearized interaction variables was made for governor control needed to ensure quality of frequency response in the electric power systems [52, 53].

One of the main contributions of this thesis is a further generalization of the interac-

tion variables concepts to modeling and control for very fast power-electronically switched stabilization of electric power system dynamics following major equipment faults.

In this section, the concept of interaction variables is generalized to the nonlinear stabilization problem in power systems. As in the linear case, the physical interpretation of interaction variables is the accumulated energy in different devices. The accumulated energy is a good indicator of stability [19] and can be used to design Lyapunov-based controllers [54]. Ultimately, we show that the interaction variable-based control design ensures stabilization of the interconnected power systems under certain conditions.

5.1 Modularity in Power Systems

A power system is a dynamic system completely made of interconnected modules, where each module has its internal inputs, states which govern its dynamics, and couplings with other modules in the system.

A module i is defined as a part of the interconnected system which can be described by a set of dynamic equations

$$\dot{x}_i = f_i(x_i, y_i, u_i), \quad x_i(t_0) = x_{i0},\ u_i(t_0) = u_{i0},\ y_i(t_0) = y_{i0}, \quad f_i(x_{i0}, y_{i0}, u_{i0}) = 0 \tag{5.1}$$

where $x_i \in \mathcal{R}^{n_i}$ is the vector of states of module i, $y_i \in \mathcal{R}^{n_i^c}$ is the coupling vector of module i, and $u_i \in \mathcal{R}^{m_i}$ is the vector of control inputs of module i. The coupling variables of module i contained in vector y_i are those states on the ports of all other modules directly connected to module i which contribute to its dynamics.

$$y_i = \{\ y_{ij} \mid y_{ij} = \mathbf{C_{ij}^T} x_j\ ,\ j = 1...n_i^c\} \tag{5.2}$$

Note that the connections between modules have no memory.

We observe next that there exist multiple, non-unique, ways to partition any given system into its interconnected modules. For the purpose of designing controllers for dynamical stabilization we introduce the choice of modules as shown in Figure 5.1. Each generator is represented as a separate module. All transmission lines, excluding FACTS devices, are grouped into one module. We avoid representing FACTS as modules because we wish to use them as dynamic controllers.

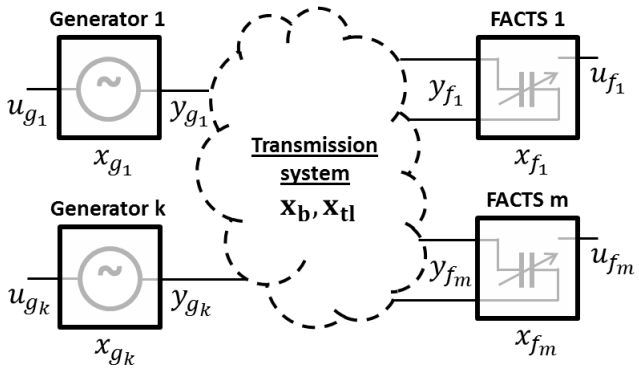

Figure 5.1: Modularity in power systems.

Further, we assume that $n_g \geq n_f$ and that each FACTS device is used to control one generator. First n_f generators are controlled by FACTS, the rest is controlled by their own exciters. The excitation voltage on the generators which are controlled by FACTS is fixed and constant.

Finally, a general electric power system whose model is given in (3.87) is represented by $(n_g + 1)$ modules in total and each of the modules, except of the transmission system module, is controlled either by a FACTS device or by the corresponding local exciter.

$$\begin{aligned} &\text{generator modules 1 through n}_\text{g}: && \dot{x}_{g_k} = f_g(x_{g_k}, \mathbf{x_b}) \\ &\text{transmission system module}: && \dot{\mathbf{x}}_\mathbf{b} = \mathbf{f_b}(\mathbf{x_b}, \mathbf{x_{tl}}, \mathbf{x_g}), \quad \dot{\mathbf{x}}_\mathbf{tl} = \mathbf{f_{tl}}(\mathbf{x_{tl}}, \mathbf{x_b}, \mathbf{x_f}) \\ &\text{dynamic FACTS controllers}: && \dot{\mathbf{x}}_\mathbf{f} = \mathbf{f_f}(\mathbf{x_f}, \mathbf{x_{tl}}, \mathbf{u}) \end{aligned} \tag{5.3}$$

5.2 Nonlinear Interaction Variables

Nonlinear interaction variables are defined for each stand-alone module. The choice of interaction variables is non-unique but it should be made wisely in order to reflect the physical state of the system.

An interaction variable of module i has the following properties:

- It is a function of module's internal states.
- Its dynamics are governed by module's own inputs, and disturbances, and by the couplings with other modules.

We define an interaction variable of module i as a scalar energy function of the following form

$$z_i = \nu_i(x_i) \tag{5.4}$$

whose dynamic behavior is described by

$$\dot{z}_i = \dot{\nu}_i(x_i) = -h_i(x_i) + g_i(x_i, y_i) + b_i(x_i, u_i) \tag{5.5}$$

Function h_i is always positive semi-definite for physical modules whose entire source of energy is coming from inputs (passive modules). Function g_i can be either positive or negative definite and it represents the rate of change of the interaction variable governed by the dynamics of all neighboring modules. Finally, function b_i captures the effect of inputs on dynamics of the interaction variable.

For physical systems, the interaction variable can be chosen as the Hamiltonian $\mathcal{H}_i$ or the total accumulated energy E_i inside the module. We choose the Hamiltonian as the

working definition of interaction variable.

$$z_i = \nu_i(x_i) = \mathcal{H}_i(x_i) = E_i(x_i) \tag{5.6}$$

The dynamics of the accumulated energy of module i, i.e. its interaction variable, are governed by its internal active power dissipation, active power injection through the inputs of the module, and the exchange of active power between module i and the rest of the system.

In particular, the interaction variable belonging to a generator module is its energy given in (3.61) and rewritten here for completeness.

$$z_k(x_{g_k}) = E_g = H_k\omega_k + \frac{1}{2}\mathbf{I}_{\mathbf{g_k}}^{\mathbf{T}}\mathbf{L_k}\mathbf{I}_{\mathbf{g_k}} \tag{5.7}$$

For the transmission system module, the interaction variable is equal to the sum of energies, given in (3.49), of all transmission line inductors and charging capacitors

$$z_{tl}(\mathbf{x_b}, \mathbf{x_{tl}}) = \sum_{i=1}^{n_b} E_{b_i} + \sum_{j=1}^{n_{tl}} E_{tl_j} = \sum_{i=1}^{n_b} \frac{1}{2} C_{ch_i} V_{b_i}^2 + \sum_{j=1}^{n_{tl}} \frac{1}{2} L_{tl_j} I_{tl_j}^2 \tag{5.8}$$

As these interaction variables represent the accumulated energy, their first derivatives will represent power exchange between the modules and the rest of the world. In particular, the first derivative of the interaction variable belonging to a generator module is

$$\dot{z}_k = P_{M_k} - P_{e_k}(x_{g_k}, \mathbf{x_b}) - P_{D_k}(x_{g_k}) \tag{5.9}$$

where P_{M_k} is the mechanical power input of generator k, $P_{e_k}(x_{g_k}, \mathbf{x_b})$ is its electrical active power output and $P_{D_k}(x_{g_k})$ its dissipation.

For the transmission system module, the interaction variable is equal to

$$\begin{aligned}\dot{z}_{ts} = &\sum_{k=1}^{n_g} P_{e_k}(x_{g_k}, \mathbf{x_b}) - \sum_{i=1}^{n_b} P_{l_i} \\ &- \sum_{m=1}^{n_f} P_{f_m}(\mathbf{x_{tl}}, x_{f_m}) - P_{D_{ts}}(\mathbf{x_b}, \mathbf{x_{tl}})\end{aligned} \tag{5.10}$$

where $P_{f_m}(\mathbf{x_{tl}}, x_{f_m})$ is the active power through FACTS m and $P_{D_{ts}}(\mathbf{x_b}, \mathbf{x_{tl}})$ is the cumulative dissipation of the transmission system.

5.3 Proposed Interaction Variable-based Model

Next, we replace one of the original states of module i by its interaction variable. This is done to obtain a single state of module i which carries the information about its interactions with other modules.

The dynamical model of module i, given in (5.1) can be rewritten using interaction variables as states

$$\begin{aligned}\dot{\bar{x}}_i &= \bar{f}_i(\bar{x}_i, z_i, y_i, u_i) \\ \dot{z}_i &= -h_i(x_i) + g_i(x_i, y_i) + b_i(x_i, u_i)\end{aligned} \tag{5.11}$$

where $\bar{x}_i \in \mathcal{R}^{n_i - 1}$ is the vector of all original module states except one. This one particular state is substituted by the interaction variable. The newly obtained dynamical model of module i describes behavior of its internal states and its interaction variable.

One state has to be removed from the original set of states in order to avoid state redundancy. Although this state can be chosen arbitrarily, it has to satisfy one property. Due to the fact that an energy function is usually of quadratic form, the replaced state has to always be positive so that the inverse of energy function would exist over the entire state trajectory.

Therefore, we choose frequency of the generator ω_k as the state to be removed for the generator module and replaced by z_k. In the case of the transmission system we choose magnitude of one of the bus voltages V_{b_i} to be replaced by z_{ts}. The reduced vectors of generator states is

$$\bar{x}_{g_k} = [I_{D_k}\ I_{Q_k}\ i_{D_k}\ i_{F_k}\ i_{Q_k}\ \delta]^T \tag{5.12}$$

and the reduced vector of transmission system states is

$$\bar{x}_{ts} = [\theta_{b_1}, V_{b_2}, \theta_{b_2}, ..., V_{b_{n_b}}, \theta_{b_{n_b}}, \mathbf{x_{tl}}^T]^T \tag{5.13}$$

Note that the newly obtained model has the same behavior in terms of stability.

As an illustration, the power system dynamical model given in Equation (3.87) can be rewritten using interaction variables as states. The newly obtained model is

$$\begin{aligned}
\dot{\bar{x}}_{g_k} &= \bar{f}_{g_k}(\bar{x}_{g_k}, z_k, \bar{\mathbf{x}}_\mathbf{b}, u_{g_k}) \\
\dot{z}_k &= P_{M_k} - P_{e_k}(x_{g_k}, \mathbf{x_b}) - P_{D_k}(x_{g_k}) \\
\dot{\bar{\mathbf{x}}}_\mathbf{b} &= \bar{\mathbf{f}}_\mathbf{b}(\bar{\mathbf{x}}_\mathbf{b}, z_{ts}, \mathbf{x_{tl}}, \bar{\mathbf{x}}_\mathbf{g}, \mathbf{x_f}) \\
\dot{\mathbf{x}}_\mathbf{tl} &= \mathbf{f_{tl}}(\mathbf{x_{tl}}, z_{ts}, \bar{\mathbf{x}}_\mathbf{b}, \mathbf{x_f}) \\
\dot{z}_{ts} &= \sum_{k=1}^{n_g} P_{e_k}(x_{g_k}, \mathbf{x_b}) - \sum_{i=1}^{n_b} P_{l_i} \\
&\quad - \sum_{m=1}^{n_f} P_{f_m}(\mathbf{x_{tl}}, x_{f_m}) - P_{D_{ts}}(\mathbf{x_b}, \mathbf{x_{tl}}) \\
\dot{\mathbf{x}}_\mathbf{f} &= \mathbf{f_f}(\mathbf{x_f}, \mathbf{x_{tl}}, \mathbf{u_f})
\end{aligned} \tag{5.14}$$

5.4 Dynamic Model Reduction Using Singular Perturbation

Singular perturbation theory, reviewed in Appendix 3, is used to reduce the order of a dynamical model by approximating the fast system dynamics as instantaneous. In order to distinguish between fast and slow dynamics, we compare time constants of different states.

For the typical values of parameters in per unit, it holds that $L_{tl} >> C_{ch}$, $L_{tl}C_{facts} > 2$ and $L_{facts}C_{facts} \approx 0.2$ [29, 37]. Assuming these typical parameter values, the dynamics of transmission lines are an order of magnitude faster than the dynamics of FACTS. The relationship between time constants, given in seconds, is the following

$$2H_k > \frac{C_m}{\omega_b}, \frac{L_m}{\omega_b}, \frac{\mathbf{L}_k}{\omega_b} >> \frac{L_{tl_j}}{\omega_b} > \frac{C_{ch_i}}{\omega_b} \tag{5.15}$$

Therefore, the fastest dynamics belong to the inductors and capacitors of the transmission system. We reduce the model by looking at the time scale separation between transmission system and other devices, FACTS and generators.

To start, we rewrite the equations of the transmission grid given in model (3.86)

$$\begin{aligned}
\dot{V}_{b_iD} =& \frac{\omega_b}{C_{ch_i}} \left(\sum_{j=1}^{n_{tl}} \mathbf{S_{tl}}[i,j] I_{tl_jD} + \sum_{k=1}^{n_g} \mathbf{S_g}[i,k] \mathbf{I_g}_k - \frac{P_{l_i} V_{b_iD} + Q_{l_i} V_{b_iQ}}{V_{b_iD}^2 + V_{b_iQ}^2} \right) + \omega_b \omega V_{b_iQ} \\
\dot{V}_{b_iQ} =& \frac{\omega_b}{C_{ch_i}} \left(\sum_{j=1}^{n_{tl}} \mathbf{S_{tl}}[i,j] I_{tl_jQ} + \sum_{k=1}^{n_g} \mathbf{S_g}[i,k] \mathbf{I_g}_k - \frac{P_{l_i} V_{b_iQ} - Q_{l_i} V_{b_iD}}{V_{b_iD}^2 + V_{b_iQ}^2} \right) - \omega_b \omega V_{b_iD} \\
\dot{I}_{tl_jD} =& \frac{\omega_b}{L_{tl_j}} \left(- \sum_{i=1}^{n_b} \mathbf{S_{tl}}[j,i] V_{b_iD} - \sum_{m=1}^{n_f} \mathbf{S_f}[j,m] V_{mD} - R_{tl_j} I_{tl_jD} \right) + \omega_b \omega I_{tl_jQ} \\
\dot{I}_{tl_jQ} =& \frac{\omega_b}{L_{tl_j}} \left(- \sum_{i=1}^{n_b} \mathbf{S_{tl}}[j,i] V_{b_iQ} - \sum_{m=1}^{n_f} \mathbf{S_f}[j,m] V_{mQ} - R_{tl_j} I_{tl_jQ} \right) - \omega_b \omega I_{tl_jD}
\end{aligned} \tag{5.16}$$

To simplify the derivation we rewrite these equations in polar coordinates as

$$\begin{aligned}
\dot{V}_{b_i} =& \frac{\omega_b}{C_{ch_i}} \left(\sum_{j=1}^{n_{tl}} \mathbf{S_{tl}}[i,j] I_{tl_j} cos(\theta_{b_i} - \psi_{tl_j}) + \sum_{k=1}^{n_g} \mathbf{S_g}[i,k] \mathbf{I_{g_k}} cos(\theta_{b_i} - \mathbf{I_{g_k}}) - \frac{P_{l_i}}{V_{b_i}} \right) \\
\dot{\theta}_{b_i} =& \frac{-\omega_b}{C_{ch_i} V_{b_i}} \left(\sum_{j=1}^{n_{tl}} \mathbf{S_{tl}}[i,j] I_{tl_j} sin(\theta_{b_i} - \psi_{tl_j}) + \sum_{k=1}^{n_g} \mathbf{S_g}[i,k] \mathbf{I_{g_k}} sin(\theta_{b_i} - \mathbf{I_{g_k}}) - \frac{Q_{l_i}}{V_{b_i}} \right) - \omega \\
\dot{I}_{tl_j} =& \frac{\omega_b}{L_{tl_j}} \left(- \sum_{i=1}^{n_b} \mathbf{S_{tl}}[j,i] V_{b_i} cos(\theta_{b_i} - \psi_{tl_j}) - \sum_{m=1}^{n_f} \mathbf{S_f}[j,m] V_m cos(\theta_m - \psi_{tl_j}) - R_{tl_j} I_{tl_j} \right) \\
\dot{\psi}_{tl_j} =& \frac{\omega_b}{L_{tl_j} I_{tl_j}} \left(- \sum_{i=1}^{n_b} \mathbf{S_{tl}}[j,i] V_{b_i} sin(\theta_{b_i} - \psi_{tl_j}) - \sum_{m=1}^{n_f} \mathbf{S_f}[j,m] V_m sin(\theta_{b_i} - \psi_{tl_j}) \right) - \omega
\end{aligned}$$

By using the singular perturbation argument we set $\frac{C_{ch_i}}{\omega_b} = 0$ and $\frac{L_{tl_j}}{\omega_b} = 0$ and rewrite the previous equations as

$$\begin{aligned}
0 =& \left(\sum_{j=1}^{n_{tl}} \mathbf{S_{tl}}[i,j] I_{tl_j} cos(\theta_{b_i} - \psi_{tl_j}) + \sum_{k=1}^{n_g} \mathbf{S_g}[i,k] \mathbf{I_{g_k}} cos(\theta_{b_i} - \mathbf{I_{g_k}}) - \frac{P_{l_i}}{V_{b_i}} \right) \\
0 =& \frac{-1}{V_{b_i}} \left(\sum_{j=1}^{n_{tl}} \mathbf{S_{tl}}[i,j] I_{tl_j} sin(\theta_{b_i} - \psi_{tl_j}) + \sum_{k=1}^{n_g} \mathbf{S_g}[i,k] \mathbf{I_{g_k}} sin(\theta_{b_i} - \mathbf{I_{g_k}}) - \frac{Q_{l_i}}{V_{b_i}} \right) \\
0 =& \left(- \sum_{i=1}^{n_b} \mathbf{S_{tl}}[j,i] V_{b_i} cos(\theta_{b_i} - \psi_{tl_j}) - \sum_{m=1}^{n_f} \mathbf{S_f}[j,m] V_m cos(\theta_m - \psi_{tl_j}) - R_{tl_j} I_{tl_j} \right) \\
0 =& \frac{1}{I_{tl_j}} \left(- \sum_{i=1}^{n_b} \mathbf{S_{tl}}[j,i] V_{b_i} sin(\theta_{b_i} - \psi_{tl_j}) - \sum_{m=1}^{n_f} \mathbf{S_f}[j,m] V_m sin(\theta_{b_i} - \psi_{tl_j}) \right)
\end{aligned} \tag{5.17}$$

By multiplying the equations by V_{b_i}, $V_{b_i}^2$, I_{tl_j} and $I_{tl_j}^2$, respectively, we get

$$\begin{aligned}
0 =& \sum_{j=1}^{n_{tl}} \mathbf{S_{tl}}[i,j] V_{b_i} I_{tl_j} cos(\theta_{b_i} - \psi_{tl_j}) + \sum_{k=1}^{n_g} \mathbf{S_g}[i,k] P_{g_k} - P_{l_i} \\
0 =& \sum_{j=1}^{n_{tl}} \mathbf{S_{tl}}[i,j] V_{b_i} I_{tl_j} sin(\theta_{b_i} - \psi_{tl_j}) + \sum_{k=1}^{n_g} \mathbf{S_g}[i,k] Q_{g_k} - Q_{l_i} \\
0 =& - \sum_{i=1}^{n_b} \mathbf{S_{tl}}[j,i] I_{tl_j} V_{b_i} cos(\theta_{b_i} - \psi_{tl_j}) - \sum_{m=1}^{n_f} \mathbf{S_f}[j,m] P_{f_m} - P_{D_j}
\end{aligned} \tag{5.18}$$

$$0 = -\sum_{i=1}^{n_b} \mathbf{S_{tl}}[j,i] I_{tl_j} V_{b_i} sin(\theta_{b_i} - \psi_{tl_j}) - \sum_{m=1}^{n_f} \mathbf{S_f}[j,m] Q_{f_m}$$

where $P_{D_j} = R_{tl_j} I_{tl_j}^2$ is the dissipation of active power in the transmission line.

The first two equations of (5.18) show that active and reactive power of shunt capacitors is always equal to zero, while the second two equations show that active and reactive power of transmission line inductors is always equal to zero. The equations show this for each transmission line reactance and each shunt capacitance separately. By adding the first and the third equation together, and the second and the fourth equation together, for all nodes and all edges we get

$$\begin{aligned} 0 &= \sum_{k=1}^{n_g} P_{g_k} - \sum_{m=1}^{n_f} P_{f_m} - \sum_{j=1}^{n_{tl}} P_{D_j} - \sum_{i=1}^{n_b} P_{l_i} \\ 0 &= \sum_{k=1}^{n_g} Q_{g_k} - \sum_{m=1}^{n_f} Q_{f_m} - \sum_{i=1}^{n_b} Q_{l_i} \end{aligned} \tag{5.19}$$

At this point we assume that the dissipation of active power inside the transmission system is small compared to the total power injected by generators and consumed by loads. Thus,

$$\sum_{j=1}^{n_{tl}} P_{D_j} = 0 \tag{5.20}$$

Finally, Equation (5.21) shows the relationship between active power of generators, FACTS and loads assuming the lossless transmission system and very fast dynamics of transmission line inductors and shunt capacitors

$$0 = \sum_{k=1}^{n_g} P_{g_k} - \sum_{m=1}^{n_f} P_{f_m} - \sum_{i=1}^{n_b} P_{l_i} \tag{5.21}$$

and Equation (5.22) shows the relationship between reactive power of generators, FACTS

and loads under the same assumptions

$$0 = \sum_{k=1}^{n_g} Q_{g_k} - \sum_{m=1}^{n_f} Q_{f_m} - \sum_{i=1}^{n_b} Q_{l_i} \tag{5.22}$$

The last two equations show not only that dynamics of the transmission system are instantaneous under the singular perturbation assumption, but that the active and the reactive power captured inside the transmission system are both equal to zero. This is a qualitatively different result from the one obtained by assuming the instantaneous transmission system dynamics. According to the assumption of the instantaneous transmission system dynamics, reactive power captured inside the transmission system exists and is different than zero.

Dynamic behavior of the interaction variable of the transmission system z_{ts} is governed by the change of active power inside the transmission system. By comparing (5.14) and (5.21) we can conclude that the dynamic behavior of this state is instantaneous as well as a consequence of the instantaneous dynamics of the transmission lines.

$$\dot{z}_{ts} = \sum_{k=1}^{n_g} P_{e_k}(x_{g_k}, \mathbf{x_b}) - \sum_{i=1}^{n_b} P_{l_i} - \sum_{m=1}^{n_f} P_{f_m}(\mathbf{x_{tl}}, x_{f_m}) = 0 \tag{5.23}$$

In other words, the change of the accumulated energy in all transmission lines is governed by the change of states of generators and FACTS only.

By using algebraic Equations (5.21) and (5.22) we can express active and reactive power output of generator k as

$$\begin{aligned} P_{e_k} &= -\sum_{l=1, l\neq k}^{n_g} P_{e_l} + \sum_{i=1}^{n_b} P_{l_i} + \sum_{m=1}^{n_f} P_{f_m} \\ Q_{e_k} &= -\sum_{l=1, l\neq k}^{n_g} Q_{e_l} + \sum_{i=1}^{n_b} Q_{l_i} + \sum_{m=1}^{n_f} P_{f_m} \end{aligned} \tag{5.24}$$

and rewrite the system model from Equation (5.14) as

$$\begin{aligned}
\dot{\bar{x}}_{g_k} &= \bar{f}_{g_k}(\bar{\mathbf{x}}_\mathbf{g}, z_k, \mathbf{x_f}, u_{g_k}) \\
\dot{z}_k &= P_{M_k} + \sum_{l=1, l\neq k}^{n_g} P_{e_l} - \sum_{i=1}^{n_b} P_{l_i} - P_{D_k}(x_{g_k}) - \sum_{m=1}^{n_f} P_{f_m} \\
\dot{\mathbf{x}}_\mathbf{f} &= \mathbf{f_f}(\mathbf{x_f}, \bar{\mathbf{x}}_\mathbf{g}, \mathbf{u_f})
\end{aligned} \tag{5.25}$$

The model relevant for assessing stability of an interconnected system given in (5.25) has $7n_g$ dynamic equations of modules and $4n_f$ equations of dynamic controllers.

5.5 Interaction Variable-based Model of the Three-bus System

The three-bus system is divided into modules as shown in Figure 5.2. In this particular case, we decide to group generators 1 and 2 into one single module in order to reduce the total number of equations and simplify this illustration.

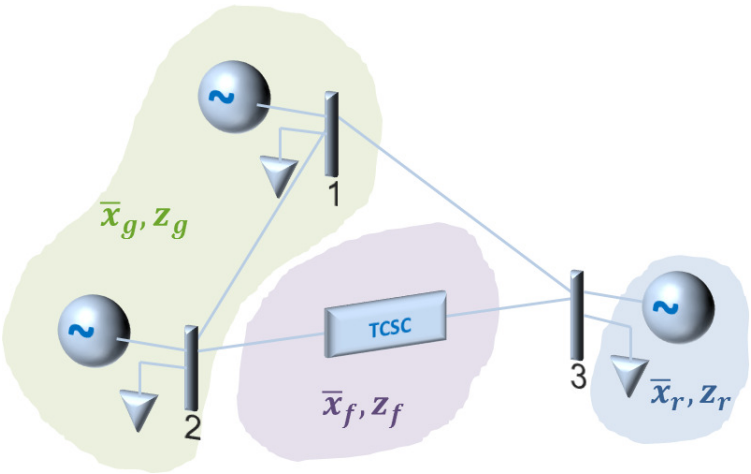

Figure 5.2: Three bus test system.

The model of the three-bus system expressed using physical states is given in (3.90). Based on the explanation in this chapter, we rewrite the model using interaction variables

as

$$
\begin{aligned}
\dot{\bar{x}}_g &= \bar{f}_g(\bar{x}_g, z_g, P_{e_1} + P_{e_2}) \\
\dot{\bar{x}}_r &= \bar{f}_r(\bar{x}_r, z_r, P_{e_3}) \\
\dot{z}_g &= P_{M_1} + P_{M_2} + P_{e_3} - P_{l_1} - P_{l_2} - P_{l_3} - P_{D_g} - P_f \\
\dot{z}_r &= P_{M_3} + P_{e_1} + P_{e_2} - P_{l_1} - P_{l_2} - P_{l_3} - P_{D_r} - P_f \\
\dot{x}_f &= f_f(P_f, x_f, u_f)
\end{aligned}
\tag{5.26}
$$

Chapter 6

Ectropy-based Control of Power Systems

Although the energy-based controller has shown good performance, its implementation in practice is questionable due to the high level of required communications. The high level of communication comes from the need to stabilize a large number of states toward a desired path as shown in Equation (4.6).

The need for communication is reduced by designing an ectropy-based controller. This controller stabilizes the energy of the critical generators toward their equilibrium. A fewer states need to be measured to stabilize energy and thus the need for communication reduces.

The proposed controller is based on the notion of ectropy. Ectropy is a measure of order in the system [26] and it has been used to design governor controllers [56] and FACTS controllers [57] in the past. The controller is designed for the power system modeled using interaction variables as it was shown in the previous chapter.

The ectropy-based controller suffers from its own limitation. It will be shown in this chapter that this controller guarantees the stability of the power system under the condition that internal dynamics of modules are stable. Therefore, its significant benefit is that it allows for controller to be designed in two stages, internal controller for different devices

and an interaction variable controller.

This chapter shows how an ectropy-based controller for FACTS can be designed.

6.1 Stability Conditions

This section introduces stability conditions for power systems represented in a modular way as given in Equation (5.25). The dynamic two-level model introduced in the previous chapter describes internal dynamics of modules represented by states $\bar{x}_{g_k}$ and the dynamics of interactions represented by states z_k. Note that states x_f belong to the dynamic controllers. Our goal is to express the stability conditions in a two-level form as well.

There are two ways we can approach this problem. One way is to pose stability conditions in a modular form, i.e. proving stability for each module individually will guarantee stability of the interconnected systems under certain conditions. These conditions relate strength of connections between modules with internal dynamics of modules. If the conditions are satisfied, one can claim that the interconnected system is stable just by looking at the strength of connections and by assessing stability of each module individually. If the stability conditions are not satisfied by some modules, the internal dynamics of those modules can be altered by using local controllers so that the desired properties are obtained in the closed loop. This approach is introduced in [46] for linear systems and later generalized for nonlinear systems in [47].

However, this approach is not the most convenient one as the connections between modules defined in the previous chapter are strong. Generators are greatly affected by large disturbances and they will exchange a lot of energy with other devices in the system. Therefore, the modules would need to be equipped with high gain controllers to satisfy the conditions described in the previous paragraph. This is a requirement hardly achievable in practice. Instead, we approach the problem from a different perspective.

At this point we acknowledge the difference between time scales of interaction variables

z_k and the internal generator states $\bar{x}_{g_k}$. The internal generator states evolve at the much faster time scale than the accumulated energy of the generator, i.e. interaction variable. Therefore, we pose stability conditions in the form of conditions for singularly perturbed systems as explained in [55].

According to this reference, an equilibrium of a singularly perturbed system is stable if a Lypunov function exists for each of the subsystems, slow and fast. Additionally, the time scales of the two subsystems need to differ sufficiently.

In our case, the fast states $\bar{x}_{g_k}$ need to be in transition all the time in order to have active power through FACTS different than zero. Therefore, we don't pose the condition of asymptotic stability on internal states. We assume these states to be bounded, while slow, interaction variable dynamics need to be stabilized.

Assuming that internal dynamical states $\bar{x}_{g_k}$ are bounded, we design the controller to ensure stability of the interaction variables of the interconnected power system in the following section.

6.2 Ectropy Definition

Ectropy is a dual notion to entropy. It is a measure of order in the system.

It is important to make a distinction between ectropy for deterministic and stochastic systems. We are dealing with power systems modeled using ODEs and as such they are deterministic. Therefore, we use the notion of ectropy as it is defined in classical thermodynamics [26], and not statistical thermodynamics [58].

The most important property of ectropy is that it is represented by a monotonically decreasing function for any isolated physical system. An isolated system in thermodynamics does not exchange energy or matter with its surroundings. We refer to an electric energy system or a module as isolated if it has a constant net power exchange with other systems/modules. In other words, an isolated module exchanges energy with the rest of

the world always at the same rate. Notably, any excess energy that appears inside the module does not propagate out and thus the name isolated.

For example, an electric energy system described by (5.25) is an isolated system because $\sum_{k=1}^{n_g} P_{M_k} - \sum_{l=1}^{n_l} P_{L_l} = 0$, while a single generator described by the generator equations from (5.25) is not because $P_{M_k} - P_{e_k} \neq 0$ for all t.

For an isolated large-scale dynamical system given in (5.25), a function ε satisfying

$$\varepsilon(\mathbf{z}(\mathbf{t_2})) \leq \varepsilon(\mathbf{z}(\mathbf{t_1})) + \int_{t_1}^{t_2} \sum_{k=1}^{n_g} z_k(t)[P_{M_k} - P_{e_k}(x_{g_k}) - P_{D_k}(x_{g_k})]dt \tag{6.1}$$

for any $t_2 \geq t_1 \geq t_0$ is called ectropy function of the system given in (5.25).

A function ε which satisfies (6.1) for the system given in Equation (5.25) is

$$\varepsilon = \frac{1}{2} \sum_{k=1}^{n_g} (z_k - z_{k0})^2 \tag{6.2}$$

Note that the energy of FACTS is not included in this definition. This is because we consider FACTS as exogenous dynamic controllers. Also, the control objective for transient stabilization of power systems is to keep the mechanical frequencies of the generators synchronized. This is best achieved if only the generator energy is stabilized while FACTS energy is left to adjust and compensate for the intake in disturbance energy.

6.3 Ectropy-based Controller

In this section we design excitation and FACTS controllers which will stabilize the interconnected system dynamics. The controllers are based on ectropy.

An ectropy-based controller is used to guarantee that the ectropy of the system is always

decreasing, i.e.

$$\dot{\varepsilon} = \sum_{k=1}^{n_g}(z_k - z_{k0}) \left(P_{M_k} + \sum_{l=1,l\neq k}^{n_g-1} P_{e_l}(x_{g_l}, \mathbf{x_b}) - P_{D_k}(x_{g_k}) - \sum_{m=1}^{n_f} P_{f_m}(\mathbf{x_{tl}}, x_{f_m}) - \sum_{i=1}^{n_b} P_{l_i} \right) \leq 0 \tag{6.3}$$

This condition is satisfied by controlling the electrical power of FACTS devices P_{f_m}, or the electrical power of generators P_{e_k}. At this time we assume that the number of controllers in the system is the same as the number of generators. Further we assume that first $n_g - n_f$ generators are controlled by the excitation voltage while the rest of them are controlled by the FACTS devices.

By looking at the previous equation, we can see that a FACTS device needs the information about the electrical power output of all generators in the system in order to stabilize the system ectropy. Additionally, it needs to have the information about active power P_f of other FACTS devices. This condition requires very fast communication channels to be placed in the system, which is not acceptable in practice.

To overcome this problem, we introduce another change of states as

$$\bar{z}_k = z - z_k - \mathcal{H}_{facts}(x_{f_m}) \tag{6.4}$$

for generators controlled by FACTS and

$$\bar{z}_k = z - z_k \tag{6.5}$$

for generators controlled by the excitation voltage, where

$$z = \sum_{k=1}^{n_g} z_k + \mathcal{H}_{facts}(\mathbf{x_f}) + z_{ts0} \tag{6.6}$$

is the total accumulated energy in the system. The new states $\bar{z}_k$ can be considered as the energy of the rest of the system without module k. Stabilization of this complementary interaction variable can be thought of as stabilization of the rest of the system given the local information at module k.

The ectropy function for the newly defined model is

$$\varepsilon = \frac{1}{2}\sum_{k=1}^{n_g}(\bar{z}_k - \bar{z}_{k0})^2 \tag{6.7}$$

The first derivative of ectropy defined in this way is

$$\begin{aligned}\dot{\varepsilon} =& \dot{\varepsilon}_{gen} + \dot{\varepsilon}_{facts} \\ =& -\sum_{k=1}^{n_g-n_f}(\bar{z}_k - \bar{z}_{k0})\left(\sum_{l=1,l\neq k}^{n_g} P_{M_l} - \sum_{l=1}^{n_l} P_{l_l} + P_{e_k}(x_{g_k})\right) \\ & -\sum_{k=n_f+1}^{n_g}(\bar{z}_k - \bar{z}_{k0})\left(\sum_{l=1,l\neq k}^{n_g} P_{M_l} - \sum_{i=1}^{n_b} P_{l_i} + P_{e_k}(x_{g_k}, \mathbf{x_b}) - P_{f_m}(\mathbf{x_{tl}}, x_{f_m})\right)\end{aligned} \tag{6.8}$$

The second part of the ectropy derivative will be less than zero $\dot{\varepsilon} \leq 0$ if the FACTS controller is designed as

$$P^*_{f_m} = \sum_{l=1,l\neq k}^{n_g} P_{M_l} - \sum_{i=1}^{n_b} P_{l_i} + P_{e_k}(x_{g_k}, \mathbf{x_b}) - K_{E_k}(\bar{z}_k - \bar{z}_{k0}) \tag{6.9}$$

Section 3.2.1 shows how to design switching of FACTS in order to control power through FACTS to obtain the reference $P^*_{f_m}$.

In order to see when the first part of the ectropy derivative will be less than zero we need to do some algebra. First, we modify the condition knowing that we are dealing with a closed system and then split the derivative of the energy of generator k to the mechanical

and the electrical part.

$$\begin{aligned}\dot{\varepsilon}_{gen} &= -\sum_{k=1}^{n_g-n_f}(\bar{z}_k-\bar{z}_{k0})(-P_{M_k}+P_{e_k}(x_{g_k},\mathbf{x_b})) \\ &= -\sum_{k=1}^{n_g-n_f}(\bar{z}_k-\bar{z}_{k0})(-2H_k\omega_k\alpha_k-\omega_k T_{e_k}+P_{e_k}(x_{g_k},\mathbf{x_b}))\end{aligned} \tag{6.10}$$

Next, we assume that the generator acceleration α_k can be directly controlled by the excitation voltage as shown in Section 3.2.4. The reference for the acceleration control can be obtained from (6.10) as

$$\alpha_k^* = \frac{1}{2H_k\omega_k}(-\omega_k T_{e_k}+P_{e_k}(x_{g_k},\mathbf{x_b})-K_{E_k}(\bar{z}_k-\bar{z}_{k0})) \tag{6.11}$$

Using the references from equations (6.9) and (6.11) we can stabilize the interconnected power systems in the presence of disturbances.

6.4 Stabilization of the Three-bus System

The three-bus system is divided into modules as shown in Figure 5.2 and described by the dynamic model in Equation (5.26). The disturbance is the same as the one described in Section 3.4. The ectropy-based disturbance stabilizing controller given in Equation (3.30) is used with the reference given in Equation (6.9) to stabilize the three-bus system. The TCSC controller is stabilizing interaction variable z_g of generators 1 and 2 from model (5.26). The inertia of the third generator is much larger than the inertias of the other two generators and therefore this generator is not critical for transient stabilization of the system. Because of this, the module denoted by subscript r can be left uncontrolled.

The resulting system response is shown in Figure 6.1. The critical clearing time is extended and the system remains stable for the duration of fault. Note from Figure 6.1(b)

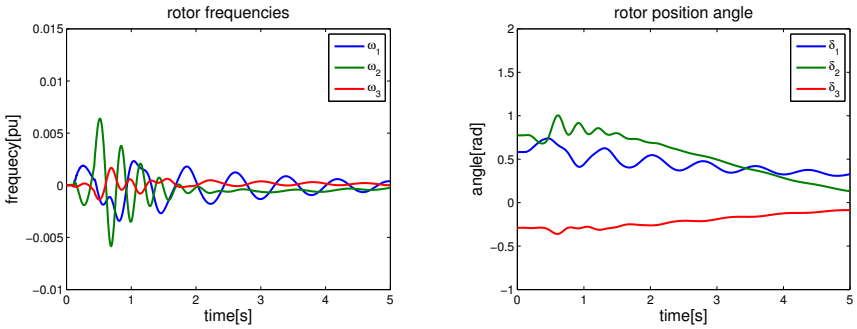

(a) Mechanical frequencies

(b) Rotor position angles

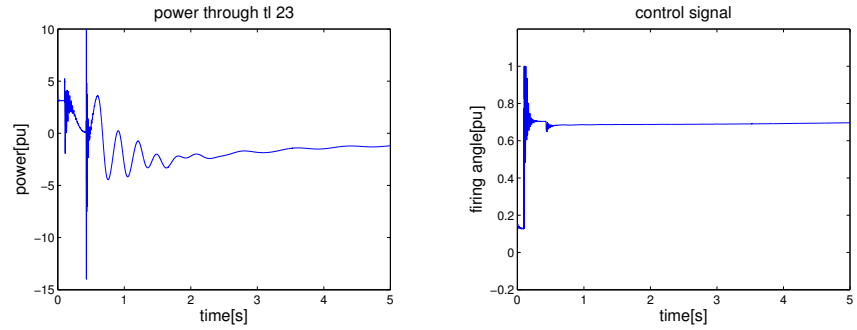

(c) Power through FACTS

(d) Controller signal

Figure 6.1: Three bus test system simulation results for the ectropy stabilization TCSC controller.

that the post-fault system equilibrium is not the same as the pre-fault one. This difference exists because the ectropy-based controller does not control all system states toward their respective equilibria. Instead, the controller allows the internal module states to settle in any equilibrium point as long as the interactions of the modules have settled in the desired equilibrium. Internal dynamics of modules can be controlled to ensure that all system states will reach desired equilibria.

Figure 6.1(c) shows the power through the transmission line with the TCSC. The TCSC keeps this power different from zero by accumulating energy in its inductors and capacitors, while the two generators keep supplying the power without accelerating considerably.

Next, we show how the three-bus system can be stabilized using the converter-based FACTS device. The three-bus system is modified to include a CSC instead of the TCSC. The new system topology is shown in Figure 2.6. A dynamic model of this CSC is derived

in Section 3.2.1. The same disturbance is considered. The response of the system is shown in Figure 6.2.

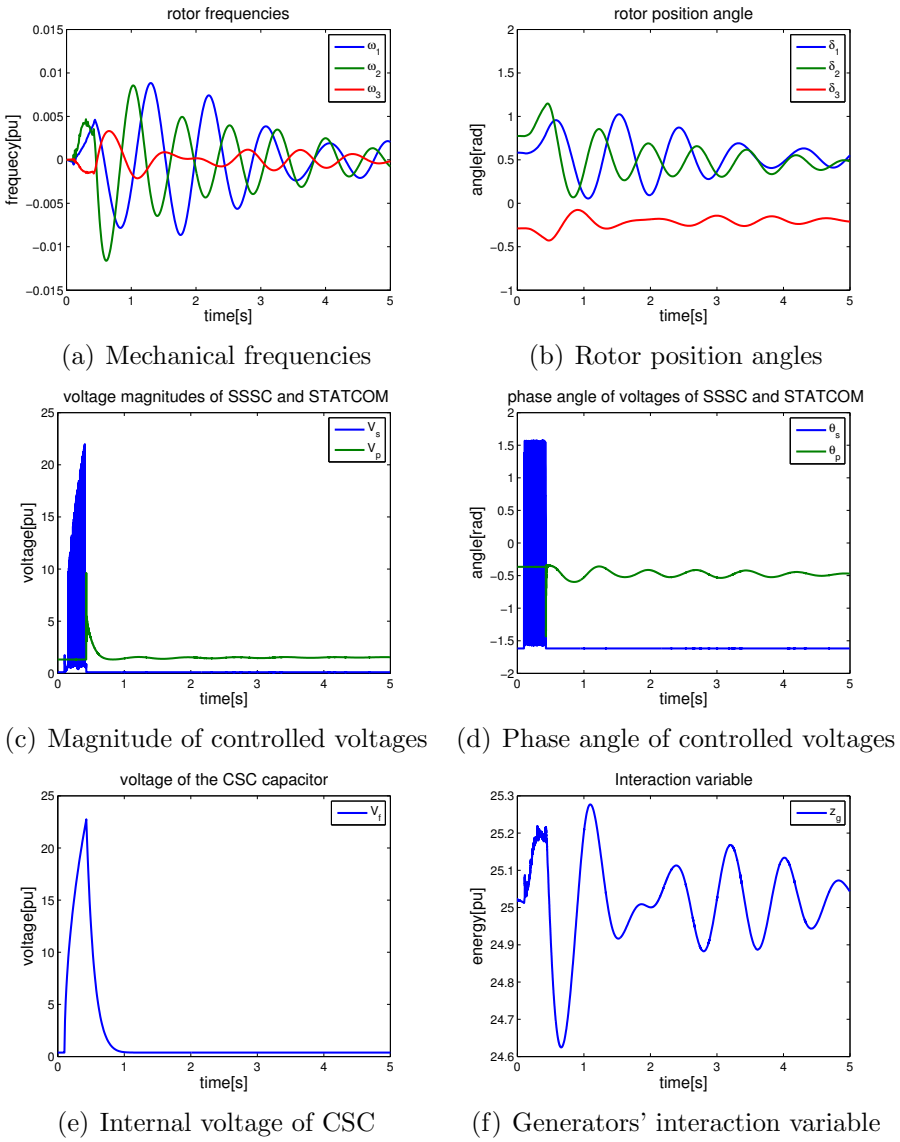

(a) Mechanical frequencies (b) Rotor position angles

(c) Magnitude of controlled voltages (d) Phase angle of controlled voltages

(e) Internal voltage of CSC (f) Generators' interaction variable

Figure 6.2: Three bus test system simulation results for the ectropy stabilization CSC controller.

We observe that the three-bus system is stabilized using the ectropy-based controller on CSC. Also, we observe very high frequency of switching of SSSC while STATCOM controller switches with a slower rate. This behavior is expected as the SSSC is used to stabilize the interaction variable of the generator module z_g while the STATCOM is used

to stabilize internal states of the CSC.

6.5 Stabilization of the IEEE 14-bus System

The stable response of the IEEE 14-bus system from Figure 4.3 with the ectropy-based controller on both TCSCs is shown in Figure 6.3.

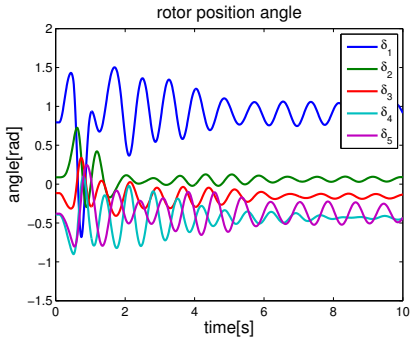

Figure 6.3: Rotor angle position of the generators in the IEEE 14 bus system.

Chapter 7

The Choice of Controller Given Design Specifications

This chapter deals with the question of proposing the best controller given the desired system behavior.

FACTS and other power-electronically-controlled devices are introduced to the grid to obtain benefits by adjusting the nominal working conditions in the grid. Rarely are they placed in the grid with the primary purpose of dynamics stabilization. Therefore, their size and parameters are in practice chosen to satisfy requirements for improved steady state performance and not improved transient behavior. In this chapter we address the question of how to choose the best FACTS device in order to obtain desirable transient performance.

We propose an approach, based on the introduced interaction variable-based model and ectropy-based controller, to select the type and the size of the controller and the minimum information exchange required to guarantee reliability with provable performance for a given topology, a set of disturbances and a range of operating conditions. The approach can be used to guarantee reliability by increasing the critical clearing time and stabilizing the interconnected system. The proposed type and size of controllers would be different in these two cases. It is important to observe that the approach does not use equivalencing to

simplify parts of the system but, instead, it uses the maximum and the minimum bound on energy which needs to be transferred between parts of the system. Also, the approach provides sizing of controllers based on information about energy exchange and does not require detailed information about internal dynamics of devices. Note that the approach does not provide the best location for the controllers but, instead, takes the controller locations as given.

Additionally, we observe administrative boundaries when proposing the controller for an interconnected grid. The power systems are often partitioned into areas by ownership of equipment. While the parameters of devices are usually not shared between areas, disturbances do not recognize man-made boundaries and propagate between areas. In practice, the controllers are tuned without considering dynamics of neighboring areas. In the grid which is increasingly operated as an open access grid, a systematic modular approach to power system controller design which would overcome this constraint is needed.

In this chapter, we use the controller from the previous chapter to determine the size of FACTS assuming their locations are given. We show how the proposed approach can be used to design dynamic controllers which would ensure reliable system operation during disturbances on a simplified example resembling Western Electric Coordinating Council (WECC) power system. A simplified WECC-like power system which captures the oscillations in frequency between Bonneville Power Administration (BPA) and Southern California Edison (SCE) is outlined in Figure 7.1 based on the spring-mass system equivalent given in [60]. Although the parameters of devices in the system from Figure 7.1 are not the actual system parameters, they are chosen to have the same modes as the spring-mass system equivalent in [60] so that our example system would mirror the dynamic behavior of the real-world system during transients.

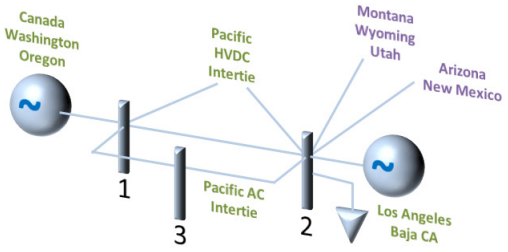

Figure 7.1: A simplified network resembling WECC power system.

7.1 Maximum Power Output of FACTS

We next assume that an interconnected power system is composed of N modules, and that, if put together, their dynamic equations form a dynamic Ordinary Differential Equation (ODE) model of the interconnected power system. Note that the connections between modules do not have memory. They are simply memoryless nodes. Transmission lines, in particular, are modeled as modules.

In our control design approach, we distinguish between two types of modules: Control-modules (C-modules) or the modules with control inputs ($m_i \neq 0$), and Observation-modules (O-modules) or the modules with no inputs ($m_i = 0$). The difference between the two is relevant for proving interconnected system stability in the next section.

The separation of a power system into modules is non unique and it depends on many factors. As it is shown in the subsequent sections, a good approach is to place PE devices into C-modules and critical generators into O-modules because they are the ones which are mostly affected by disturbances. It is also shown later in this thesis that a good approach is to choose the connections between C-modules and O-modules to be strong and to choose the connections in between O-modules and in between C-modules to be weak.

The WECC-like power system is divided into two modules, an O-module i and a C-module j, as shown in Figure 7.2. These two modules belong to the group of modules a and are mutually connected at a single point (bus 1). They are also connected to two other groups of modules, b and d. Note that the Pacific HVDC Intertie is left out of the figure

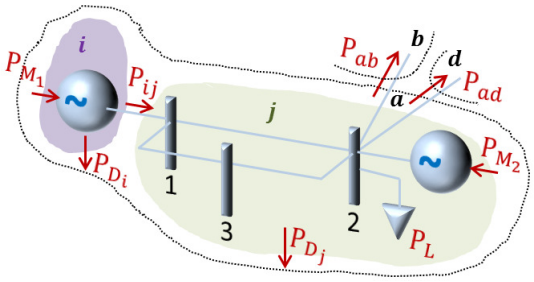

Figure 7.2: A modular representation of the WECC-like power system.

because its constant injections do not change the conclusions in this thesis.

The power flows between the modules are also indicated in Figure 7.2. The active power $P_{ij} = P_{tl_1} + P_{tl_2}$ is the power flow between modules i and j. The active powers P_{ab}, P_{ac} and P_{ad} represent the power flows between group of modules a and groups of modules b and d. The active powers P_{D_i} and P_{D_j} in Equation (5.14) represent the accumulative rate of change of energy dissipation in both modules. Powers P_{M_1} and P_{M_2} are the mechanical power inputs into the two generators and P_L is the power consumption of the load.

It is usually assumed that the mechanical power input to conventional generators is constant for the analysis of transient system behavior on shorter time scales (up to $1min$). We assume the same. Also, we assume that load P_L is a constant power load.

7.1.1 Cooperative control of two interconnected modules

Let us assume that an interconnected system is composed of two modules, an O-module i without a control input and a C-module j with control input u_j. This system is shown in Figure 7.3. The states of each module are x_i and x_j. The energies of modules are E_i and E_j. Dissipated powers in the modules are P_{D_i} and P_{D_j} and they can be functions of states. Power exchanged between the modules P_{ij} is a function of states. Input power P_{in} and output power P_{out} are constant power injections with directions taken as in Figure 7.3. Powers exchanged between the two modules and other modules in the system are P_{ki} and P_{lj} directed as show in the figure. These two powers are functions of states of modules on

both sides of each connection.

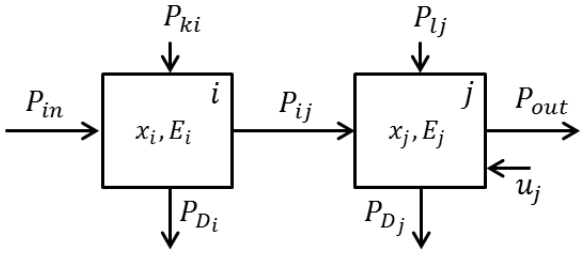

Figure 7.3: An interconnected system of two modules.

In order to control this interconnected system an ectropy function of module i is proposed as

$$\varepsilon_i = \frac{1}{2}(E_i - E_{i0})^2 \geq 0 \tag{7.1}$$

with a property that $\varepsilon_i \geq 0$ over the entire trajectory of states. The first derivative of this function is

$$\dot{\varepsilon}_i = (E_i - E_{i0})(P_{in} - P_{ij} + P_{ki} - P_{D_i}) \tag{7.2}$$

In order to make the first derivative of ectropy function always negative, we assume that power P_{ij} in between modules is controllable using input u_j. In other words, even though the internal structure of module j is unknown at this time, controller u_j has to be able to control P_{ij}. If this condition is satisfied, then power P_{ij} needs to be controlled to be

$$P_{ij} = P_{in} + P_{ki} - P_{D_i} + K_E(E_i - E_{i0}) \tag{7.3}$$

for the first derivative of ectropy of module i to always remain negative, $\dot{\varepsilon}_i \leq 0$. Constant $K_E > 0$ is the controller gain.

The second part of this derivation is meant to determine the minimum and the maxi-

mum value of u_j for which the interconnected system is stabilizable.

We start by writing an ectropy function of module j

$$\varepsilon_j = \frac{1}{2}(E_j - E_{j0})^2 \geq 0 \tag{7.4}$$

with a property that $\varepsilon_j \geq 0$ over the entire trajectory of states. Once the action of controller from Equation (7.3) is included in the expression, the first derivative of ectropy function of module j is

$$\begin{aligned}\dot{\varepsilon}_j =&(E_j - E_{j0})(P_{in} - P_{out} - P_{D_i} - P_{D_j} \\ &+ P_{ki} + P_{lj} + K_E(E_i - E_{i0}) + u_j) \\ =&(E_j - E_{j0})(P_B + u_j)\end{aligned} \tag{7.5}$$

where

$$\begin{aligned}P_B =&P_{in} - P_{out} - P_{D_i} - P_{D_j} + P_{ki0} + P_{ki0} \\ &+ \Delta P_{ki} + \Delta P_{lj} + K_E(E_i - E_{i0})\end{aligned} \tag{7.6}$$

is introduced to simplify the notation. Conditions for u_j so that $\dot{\varepsilon}_j \leq 0$ is true over the entire trajectory of states are obtained from Equation (7.5)

$$\begin{aligned}(E_j - E_{j0}) > 0, \quad u_j < -P_B \\ (E_j - E_{j0}) < 0, \quad u_j > -P_B\end{aligned} \tag{7.7}$$

If we are able to estimate the maximum and the minimum value for P_B then we can calculate lower and upper bound on u_j for which $\dot{\varepsilon}_j \leq 0$ over the entire trajectory of states.

$$P_B^{min} \leq u_j \leq P_B^{max}, \quad \dot{\varepsilon}_j \leq 0 \tag{7.8}$$

Next, we look for maximum and minimum value for P_B.

Based on the interconnected system property 1, we know that

$$P_{D_{i0}} + P_{D_{j0}} - |P_F| \leq P_{D_i} + P_{D_j} \leq P_{D_{i0}} + P_{D_{j0}} + |P_F| \tag{7.9}$$

Using the conservation of power law at the equilibrium and by subtracting Equation (7.9) from $(P_{in} - P_{out} + P_{ki0} + P_{lj0})$ we obtain

$$-|P_F| \leq P_{in} - P_{out} - P_{D_i} - P_{D_j} + P_{ki0} + P_{lj0} \leq |P_F| \tag{7.10}$$

This expression represents the bound on the first four terms of P_B in Equation (7.6).

The bound on the deviations of power ΔP_{ki} and ΔP_{lj} exchanged between modules can be found by recognizing that this is an electric grid. First, we recognize that

$$\begin{aligned} |\Delta P_{ki}| &\leq |P_{ki}| + |P_{ki0}| \\ &\leq 0.25 + P_{ki}^2 + |P_{ki0}| \\ &= 0.25 + V_k^2 I_i^2 cos^2(\theta_k - \psi_i) + |P_{ki0}| \\ &\leq 0.25 + V_k^2 I_i^2 + |P_{ki0}| \end{aligned} \tag{7.11}$$

Next, we recognize that the last expression can be rewritten using energy expressions for inductor and capacitor on the connection between the two modules as

$$|\Delta P_{ki}| \leq 0.25 + \frac{2E_{C_k}}{C_k}\frac{2E_{L_i}}{L_i} + |P_{ki0}| \tag{7.12}$$

Based on the interconnected system property 2, we know that the maximum energy any element can have cannot be higher than the energy of the disturbance added to the equi-

librium energy of that element. Therefore, we can rewrite the last equation as

$$|\Delta P_{ki}| \leq 0.25 + |P_{ki0}| + \{P_{ki}^2\}^{max} \tag{7.13}$$

where $\{P_{ki}^2\}^{max}$ is equal to one of the following two

$$\{P_{ki}^2\}^{max} = \begin{cases} \frac{2(E_{C_{k0}}+|P_F|T_F)}{C_k} \frac{2(E_{L_{i0}}+|P_F|T_F)}{L_i} \\ \\ \frac{2(E_{L_{k0}}+|P_F|T_F)}{L_k} \frac{2(E_{C_{i0}}+|P_F|T_F)}{C_i} \end{cases} \tag{7.14}$$

depending on which module has a through variable and which module has an across variable on its ports.

Equation (7.13) represents the bound on the deviation of power ΔP_{ki} exchanged between modules k and i. The same expression can be derived as a bound for the deviation of power ΔP_{lj}.

We have observed that Equation (7.13) gives a somewhat conservative bound. Further work is needed to determine how this bound can be made less conservative.

The bound on the last term in Equation (7.6) is found using the same system property. Therefore,

$$-K_E|P_F|T_F \leq K_E(E_i - E_{i0}) \leq K_E|P_F|T_F \tag{7.15}$$

The bound on control input u_j is obtained by summing up the bounds in Equations (7.10), (7.13) and (7.15). Therefore, the maximum and minimum bounds on the

controller input are

$$\begin{aligned} P_B^{max} &= -P_B^{min} \\ &= |P_F| + 0.5 + K_E|P_F|T_F + |P_{ki0}| + |P_{lj0}| \\ &+ \frac{2(E_{C_{k0}} + |P_F|T_F)}{C_k}\frac{2(E_{L_{i0}} + |P_F|T_F)}{L_i} \\ &+ \frac{2(E_{C_{l0}} + |P_F|T_F)}{C_l}\frac{2(E_{L_{j0}} + |P_F|T_F)}{L_j} \end{aligned} \tag{7.16}$$

they are guaranteed to stabilize the interconnected system.

7.1.2 The case of multiple interconnected modules

We consider next a group of modules denoted by a with total of n_m modules, n_{Cm} C-modules and n_{Om} O-modules, in Figure 7.4.

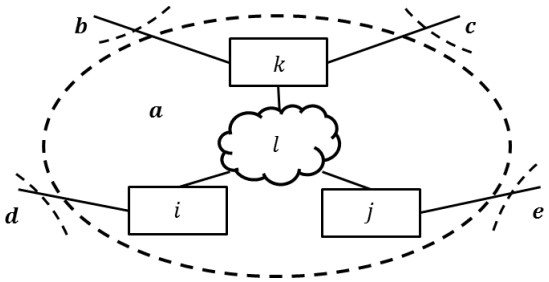

Figure 7.4: A group of interconnected modules.

It can be shown that Equation (7.17) describes the bounds in the case of a group of modules. In this equation, subscript a refers to our group of modules

$$\begin{aligned} P_B^{max} &= -P_B^{min} \\ &= |P_F| + 0.25n_c + \sum_{i=1}^{n_{Cm}} K_{Ei}|P_F|T_F \\ &+ \sum_{i=1}^{n_c} (|P_{ai0}| + \{P_{ai}^2\}^{max}) \end{aligned} \tag{7.17}$$

where n_c is the total number of connections of group of modules a with other modules or

groups of modules and $\{P_{ai}^2\}^{max}$ is given in Equation (7.14).

The derivation of this equation is based on the derivation presented in the previous subsection and it can be found in full in [61].

7.2 The Choice of the Capacitor and the Inductor of FACTS

Choosing a *right* controller to stabilize an interconnected power system in response to selected large disturbances is an important problem. This section explains how a controller can be chosen based on the controller bounds derived in the previous section and what kind of communication architecture is necessary to implement the controller.

We start by providing the design specifications which include the topology of the grid including the locations of controllers, a range of operating conditions $\mathcal{D}$ and a set of disturbances $\mathcal{C}_{\mathcal{F}}$.

A range of operating conditions, for the system given in (5.11), is defined as a union of a range of possible energy levels the modules could find themselves in and a range of possible power exchanges between the group of modules for which the controller type is being considered and other groups of modules.

$$\begin{aligned}\mathcal{D} = \{\ E_i = z_i \in \mathcal{R}^{n_m} \mid E_i^{min} \leq E_i \leq E_i^{max} \cup \\ P_{aj} \in \mathcal{R}^{n_c} \mid P_{aj}^{min} \leq P_{aj} \leq P_{aj}^{max}\ \}\end{aligned} \tag{7.18}$$

A set of disturbances is defined in pairs of time and disturbance power as

$$\mathcal{C}_{\mathcal{F}} = \{\ (P_F, T_F) \in \mathcal{R}^{n_F \times n_F}\ \} \tag{7.19}$$

We choose the right type of controller based on the maximum power that the controller

should be able to inject into the grid. We find maximum u_j by finding the maximum value of the expression in Equation (7.17) for the provided design specifications.

$$\begin{aligned} u_j^{max} &= max(P_B^{max}(P_F, T_F, E_i)), \\ &(P_F, T_F) \in \mathcal{C}_{\mathcal{F}} \ \& \ (E_i) \in \mathcal{D} \end{aligned} \tag{7.20}$$

Note that the P_B^{max} bound will always be maximal for the maximum values of energy and power from the set of operating conditions $\mathcal{D}$. However, maximum P_F will not always result in maximal P_B^{max}, as this bound will depend on the duration of fault T_F as well.

The type of the controller can be determined by comparing u_j^{max} and the maximum power output different technologies are able to provide. For example, FACTS are able to generate higher active power output but for very short periods of time. While still able to react fast, flywheels can provide active power for longer periods of time.

Next, the controller sizing can be done once u_j^{max} is known. Internal structure of the controller needs to be known as well. An example of sizing a controller is given in the next section.

Finally, Equation (7.3) identifies the necessary communication topology. A controller needs to have an information about the interaction variable of the O-module it is controlling. Also, the information about the power this O-module exchanges with its neighboring modules has to be known to the controller. Finally, the controller might have to measure variables internally in order to control the power between its C-module and the O-module.

7.3 An Example of a WECC-like Power System

An WECC-like system is shown in Figure 7.1. The question of interest is how to choose a controller which should be located at bus 3.

Nominal equilibrium values of important variables are given in Table 7.1. All values

are given in per unit. Note that it is not necessary to have knowledge about equilibrium of any other state in the system to select an adequate controller.

Table 7.1: Parameters of the simplified WECC power system

Variable	Nominal Value	Variable	Nominal Value
P_{M_1}	1.3165	P_{tl_1}	0.4353
P_{M_2}	0.1700	P_{tl_2}	0.8812
P_L	1.4765	P_{ab}	0
z_i	0.4212	P_{ac}	0
z_j	0.2871	P_{ad}	0

A large disturbance considered in this example is a short circuit to the ground in the middle of transmission line 2 for duration of $0.9s$. Mathematically, this disturbance is described with a set

$$\mathcal{C}_{\mathcal{F}} = \{\ (P_{M_1}, 0.9s)\ \} = \{\ (1.3165pu, 0.3s)\ \} \tag{7.21}$$

To simplify this illustration, only one operating point from the range of operating conditions is considered. For this operating point,

$$\begin{aligned} \mathcal{D} = \{\ & E_{Ci0} = 0.2871pu\ ,\ E_{Lj0} = 0.0524pu\ , \\ & P_{kj} = 0\ ,\ P_{lj} = 0\ ,\ P_{mj} = 0\ \} \end{aligned} \tag{7.22}$$

The active powers exchanged with other groups of modules are assumed zero in the equilibrium in order to simplify the illustration.

For the disturbance and the operating condition of interest, the system is transiently unstable. This is due to the loss of synchronization between generators.

One possible C-RAS action in this case would be to disconnect transmission line 2 from the rest of the system. Figure 7.5 shows the response of the system frequency when no

action is taken and when C-RAS disconnects transmission line 2. The system is clearly unstable when no action is taken. Also, the C-RAS action will not help because it relies on the existence of equilibrium of the post-fault system, which in this case is nonexistent.

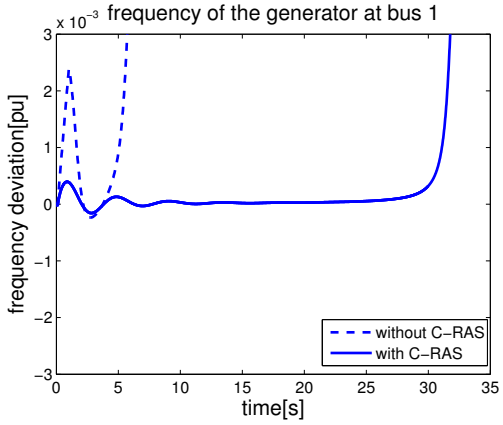

Figure 7.5: Frequency response in the uncontrolled system and in the system with C-RAS.

Therefore, we design a controller which would insure the stability of the system. The bound on maximum power the controller should inject is calculated using Equation (7.17) and is equal to

$$u_j^{max} = P_B^{max} = 2.5013pu \tag{7.23}$$

Next, the controller is proposed to stabilize the system for the projected maximum control input. Both, FACTS and flywheels could be used to stabilize the disturbance on this short time scale. We consider FACTS as a possible solution. A Thyristor Controlled Series Capacitor (TCSC) is placed in the middle of transmission line 1, at Bus 3. This TCSC should be able to provide u_j^{max}. In the following subsection, we select its inductor and capacitor so that stability is guaranteed.

7.3.1 Choosing TCSC parameters

The size of the capacitor can be estimated by exploring Equations (7.13) and (7.14) in a slightly modified form. We start by expressing the maximum power output of the TCSC as the exchanged power between the TCSC capacitor C and the transmission line inductor L_{tl}

$$\begin{aligned} |\Delta P_{tcsc-tl}| = u_j^{max} &= 0.25 + |P_{tcsc-tl0}| \\ &+ \frac{2(E_{C_0} + |P_F|T_F)}{C} \frac{2(E_{L_{tl0}} + |P_F|T_F)}{L_{tl}} \end{aligned} \tag{7.24}$$

This expression can be simplified by knowing that the active power of a TCSC is always equal to zero at the equilibrium $|P_{tcsc-tl0}| = 0$. Energy of the capacitor E_{C_0} is unknown. Therefore, we express this energy as

$$E_{C_0} = \frac{1}{2} C V_0^2 \tag{7.25}$$

By assuming that $V_0^2 \ll 0.25$, which is true for a TCSC because of the small voltage drop across its ends, we estimate capacitance C of the TCSC from Equation (7.24) as

$$C = \frac{2|P_F|T_F}{(u_j^{max} - 0.25)} \frac{2(E_{L_{tl0}} + |P_F|T_F)}{L_{tl}} \tag{7.26}$$

In this particular example,

$$C = 25.6548pu \tag{7.27}$$

The inductance of the TCSC is calculated to obtain a range of nominal compensation levels from 0 to 40% of the transmission line impedance. In this case, the value for the

inductance of the TCSC inductor is

$$L = 0.0292pu \tag{7.28}$$

The proposed TCSC controller has been installed in the system at Bus 3. Figure 7.6 shows the transiently stable frequency response when the system is controlled by the TCSC while C-RAS is assumed inactive.

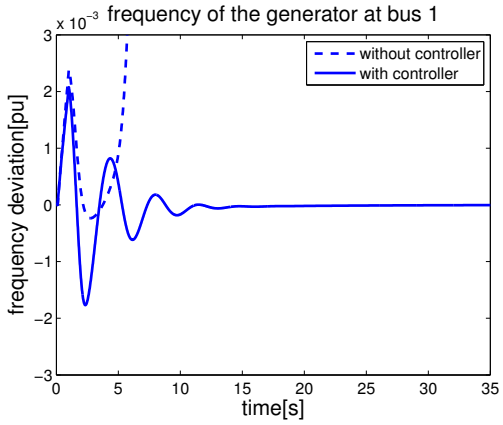

Figure 7.6: Frequency response in the uncontrolled and controlled system without C-RAS.

In the case in which C-RAS disconnects transmission line 2, the system will stay transiently stable in the presence of the TCSC controlled as shown in Figure 7.7.

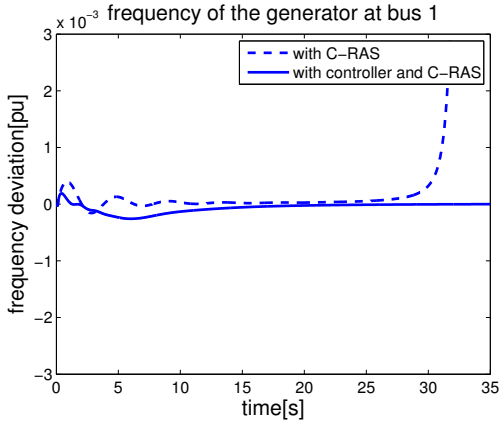

Figure 7.7: Frequency response in the uncontrolled and controlled system with C-RAS.

Chapter 8

Conclusions and Future Work

In this thesis we revisit the problem of transient stabilization in power systems. One of the main motivators to do so comes from the recent transformation of electric energy grids with new technologies. PMUs and fast communications could enable to explore power-electronically-controlled FACTS devices as possible controllers for transient stabilization.

In order to use FACTS devices as controllers of large and fast disturbances, it is necessary to model the dynamics of FACTS devices and the transmission grid. If fast dynamics are not modeled, the potential of FACTS devices to react fast to disturbances will not be exploited. We propose a time-varying phasor model of interconnected power systems which captures relevant fast dynamics of FACTS and allows us to design fast controllers of active power through FACTS. Such controllers are shown to have better performance by being able to stabilize larger disturbances than the earlier proposed FACTS controllers.

To enable the implementation of the proposed controllers, we propose a two-level approach to transient stabilization which minimizes the need for communication between controllers. The main idea behind this approach is to represent a power system as a composition of interconnected modules. Each module is described by its own internal dynamics and the dynamics of an interaction variable. The interaction variable shows how this module interacts with neighboring modules. Using this approach dynamics of the system are

separated in two-levels: internal and interaction level of power system dynamics. It is shown using a singular perturbation argument that controllers for both levels can be designed separately. Additionally, we propose an ectropy-based controller for stabilization of the interaction-level dynamics of the interconnected system. The main characteristic of this controller is that it requires only minimal amount of information to be implemented and therefore the need to communicate measurements reduces.

In this thesis we explain how the controllers are designed assuming the modules are given. Future work should take one step further and introduce systematic methods for decomposing the grid into modules of right size and right internal structure to guarantee the best transient response of the interconnected system. The modules should be selected based on the available components in the grid but also on the requirements for stability and communications; these modules are not necessarily defined by the ownership or organizational boundaries. The requirements for stability and communications can be standardized and imposed to equipment owners through regulatory frameworks so that stability can be guaranteed at the interconnected system level.

The accumulated energy of devices plays an important role in controller design. Naturally, a question of accuracy of the information about accumulated energy arises. The estimate of this energy has to be as good as possible in order to have satisfying controller performance. Further work is needed in order to assess how inaccurate information of interaction variables will impact the controller performance.

Additional research is needed to address the question of controller saturation. The switching on FACTS devices can take values in the range between zero and one. Although the controllers have been constrained to this range in the performed simulations, they are formulated assuming that switching can take values outside of this range. Further analysis is needed to incorporate the saturation limits into the controller logic. On the positive side, we have observed through simulations that the saturation is not reached very often

and for extended periods of time even in cases of very large disturbances.

All real-world implementations of FACTS have protection circuits which disconnect the device from the grid if the current/voltage maximum limits are violated. The proposed controllers are based on the idea that FACTS can accumulate energy. The increment in energy of FACTS brings its internal currents and voltages closer to the point at which protection is triggered. If for selected disturbances the currents and voltages rise significantly, the protection circuits might need to be readjusted to accommodate the use of controllers for transient stabilization.

Another practical issue for controller implementation is the delay in communications. The controller needs to react fast in response to disturbances and the delay which enters through communication channels may or may not have a significant impact. Further analysis is needed in order to address this question.

Finally, in Chapter 7 we show how dimensioning of FACTS can be done if given a set of disturbances and a range of operating conditions. However, we only scratch the surface with the proposed method. A more thorough research should be conducted to observe how FACTS dimensions change if modules are chosen differently. Additionally, future research should focus on obtaining less conservative values for the inductor and the capacitor of FACTS.

Appendix

1 Traditional Approach to Designing Transient Stabilizing Controllers

The dynamics of an interconnected electric power system are commonly modeled using a nonlinear Differential Algebraic Equation (DAE) model [30]:

$$\begin{aligned} \dot{x}(t) &= f\left(x(t), y(t), u(t)\right) \\ 0 &= g\left(x(t), y(t)\right) \end{aligned} \tag{1}$$

In this formulation, $g(x(t), y(t))$ represents power flow equations and $f(x(t), y(t))$ represents dynamics of components connected to nodes, such as generators and/or loads. Vector $x(t)$ is the vector of internal states of generators and vector $y(t)$ is the vector of nodal voltage magnitudes and phase angles. The set of algebraic equations $g(x(t), y(t))$ does not have a closed-form solution if loads are modeled as constant power nonlinear loads. Only if the loads are modeled as constant impedance loads a closed-form solution can be found by relating algebraic states $y(t)$ to dynamic states $x(t)$ as

$$y(t) = h\left(x(t)\right) \tag{2}$$

In this case, Equation (1) can be rewritten in the Ordinary Differential Equation (ODE)

form as

$$\dot{x}(t) = f\left(x(t), h(x(t)), u(t)\right) \tag{3}$$

The equilibrium of the system is any point $(x_0\, y_0\, u_0)$ which satisfies

$$0 = f\left(x_0, y_0, u_0\right) \tag{4}$$

In the general case, there exists more than one equilibrium point in the system [62]. Therefore, the stability is assessed with respect to each specific equilibrium point. Stability of an equilibrium point can be defined in many different ways [63]. Asymptotic stability definition is used here unless stated otherwise. An equilibrium point is considered to be asymptotically stable if the system trajectory returns to it from any point in a small region around it. In other words, if the perturbations caused by disturbances are sufficiently small the system states will return to the stable equilibrium point as the time approaches infinity. The largest region for which this holds is called Region Of Attraction (ROA) of the stable equilibrium point.

2 Singular Perturbation Theory

In order to analyze the power system models introduced later in this thesis, we intensively use the singular perturbation theory. Therefore, we review the main concepts of the singular perturbation theory in this section.

Singular perturbation is an approach used to simplify dynamical model of a system whose dynamics evolve on considerably different time scales. It was introduced in [55] and later applied to power systems in [64] and [65].

The basic idea underlying the singular perturbation theory is to separate the dynamical

system model into two models which evolve on different timescales.

We start by assuming that the nonlinear system model given in (3) can be rewritten in the form

$$\begin{aligned} \dot{x}_1 &= f_1(x_1, x_2, \xi, t), \quad x_1(t_0) = x_{10}, \quad x_1 \in \mathcal{R}^n, \\ \xi\dot{x}_2 &= f_2(x_1, x_2, \xi, t), \quad x_2(t_0) = x_{20}, \quad x_2 \in \mathcal{R}^m, \end{aligned} \tag{5}$$

In this equation, states x_1 are the slow and states x_2 are the fast states. Parameter ξ is a small parameter which separates the two time scales. The order reduction of model (5) is converted into a parameter perturbation called *singular*. When $\xi = 0$, the dimension of the original state space reduces from $n + m$ to n because the differential equation describing dynamics of x_2 degenerates into the algebraic equation

$$0 = f_2(\underline{x}_1, \underline{x}_2, 0, t) \tag{6}$$

where the underline is used to indicate that the variables belong to a system with $\xi = 0$.

If we solve (6) for $\underline{x}_2 = f_2^{-1}(\underline{x}_1, t)$, we obtain the model which describes the dynamics of the system on the slower time scale.

$$\dot{\underline{x}}_1 = f_1(\underline{x}_1, f_2^{-1}(\underline{x}_1, t), 0, t) \tag{7}$$

This model is referred to as a *quasi-steady-state model*. The singular perturbation theory shows next how the model of the fast subsystem is obtained.

A time variable τ is assigned to the fast time scale so that

$$\xi\frac{dx_2}{dt} = \frac{dx_2}{d\tau}, \quad \text{hence} \quad \frac{d\tau}{dt} = \frac{1}{\xi} \tag{8}$$

Using the new time variable, a differential equation describing fast dynamics can be rewrit-

ten as

$$\frac{d\tilde{x}_2}{d\tau} = f_2(x_{10}, \underline{x}_{20} + \tilde{x}_2, 0, t_0), \quad \tilde{x}_{20} = x_{20} - \underline{x}_{20} \tag{9}$$

This model is referred to as a *boundary layer model*.

Once the quasi-steady-state and boundary layer models are created, Equations (7) and (9), we can analyze them separately or even design the controllers for each of the models independently. This property will be highly exploited in the sections to follow.

3 Control Lyapunov Function

The controllers presented in this thesis are based on Lyapunov approach. Therefore, we review the Control Lyapunov Function approach to controller design.

Lyapunov-based controllers have had a long history of being used for stability assessment in electric power systems [1, 19, 66]. It was further used in general systems theory to create Control Lyapunov Function (CLF) to design nonlinear controllers [54, 67, 68]. Naturally, a systematic use of CLF was proposed for transient stabilization of electric power systems in [5, 17].

The basic idea underlying the CLF is to find a function of states $\nu(x)$, for any given nonlinear system modeled in the standard state space form given in (3), with the following three properties

$$\begin{aligned} &\nu(x) \geq 0 \quad \forall x \in \mathcal{R}^n \\ &\nu(x) = 0 \quad \forall x \in \mathcal{O} \\ &\dot{\nu}(x) \leq 0 \quad \forall x \in \mathcal{R}^n \end{aligned} \tag{10}$$

The third property is secured by the proper design of a controller. Therefore, energy

function $\nu(x)$ is an energy function of the closed-loop system.

If one wishes to stabilize the system back to an equilibrium then the objective manifold $\mathcal{O}$ will be defined as

$$\mathcal{O} = \{\ x \in \mathcal{R}^n \quad | \quad x = x_0\ \} \tag{11}$$

where x_0 is an equilibrium of the system given in (3). A controller designed for this objective manifold is a stabilizing controller. If the stabilization is done over the full set of states, then the controller is said to be full-state feedback controller. If the stabilization is done only over certain states whose number is $m < n$, then the controller is said to be output feedback controller.

If, however, one wishes for the system to follow a certain trajectory in state space then the objective manifold can be defined accordingly

$$\mathcal{O} = \{\ x \in \mathcal{R}^n \quad | \quad g(x) = 0\ \} \tag{12}$$

where $g(x)$ is a trajectory manifold. References [5, 31] show how objective manifold can be defined for excitation control. A controller designed for this kind of objective manifold is a tracking controller. Full state and output feedback definitions hold in this case too.

Bibliography

[1] M. Pavella, D. Ernst, D. Ruiz-Vega, *Transient Stability of Power Systems: A Unified Approach to Assessment and Control*, Kluwer Academic Publishers, 2000.

[2] P. Kundur, G. K. Morison, L. Wang, *Techniques for On-line Transient Stability Assessment and Control*, IEEE Power Engineering Society Winter Meeting, 2000.

[3] P. Arons, *SCE Pilots the Next Level of Grid of Grid Protection*, Transmission & Distribution World, December 2007.

[4] J. Wen, P. Arons, *Implementation of Centralized Remedial Action Scheme-An Important Step towards WAMPAC*, IEEE Power and Engineering Society General Meeting, July 2011.

[5] J. W. Chapman, M. D. Ilic, C. A. King, L. Eng, H. Kaufman, *Stabilizing a Multimachine Power System via Decentralized Feedback Linearizing Excitation Control*, IEEE Transactions on Power System, Vol.8, No.3, 1993, pp.830-839.

[6] L. Angquist, C. Gama, *Damping Algorithm Based on Phasor Estimation*, IEEE Power Engineering Society Winter Meeting, 2001.

[7] M. Noroozian, C. W. Taylor, *Benefits of SVC and STATCOM for Electric Utility Application*, IEEE Power and Energy Society Transmission and Distribution Conference and Exposition, 2003.

[8] A. Oskoui, B. Mathew, J. P. Hasler, M. Oliveira, T. Larsson, A. Petersson, E. John, *Holly STATCOM - FACTS to Replace Critical Generation, Operational Experience*, IEEE Power and Energy Society Transmission and Distribution Conference and Exposition, 2005.

[9] C. Gama, L. Angquist, G. Ingestrom, M. Noroozian, *Commissioning and Operative Experience of TCSC for Damping Power Oscillation in the Brazilian North-south Interconnection*, Cigre, ref. 14-104. 2000.

[10] E. Uzunovic, B. Fardanesh, S. Zelingher, S. J. Macdonald, C. D. Schauder, *Interline Power Flow Controller (IPFC): A Part of Convertible Static Compensator (CSC)*, North American Power Symposium, October 2000.

[11] S. Arabi, H. Hamadanizadeh, B. Fardanesh, *Convertible Static Compensator Performance Studies on the NY State Transmission System*, IEEE Transactions on Power Systems, Vol.17, No.3, pp.701-706, August 2002.

[12] J. F. Gronquist, W. A. Sethares, F. L. Alvarado, R. H. Lasseter, *Power Oscillation*

Damping Control Strategies for FACTS Devices Using Locally Measurable Quantities, IEEE Transactions on Power Systems, Vol.10, No.3, August 1995, pp.1598-1605.

[13] X. Yu, H. Sira-Ramirez, G. Ledwich, *Switching Control Strategy for the Power System Stabilization Problem*, International Journal of Control, Vol. 62, No. 5, 1995, pp.1021-1036.

[14] C. Yu, C. Liu, *A Practical Design of TCSC Controllers for the Inter-area Transient Stability Control Using Real-time Measurements*, Power Engineering Society Winter Meeting, January 1999.

[15] G. Escobar, A. M. Stankovic, P. Mattavelli, R. Ortega *On the Nonlinear Control of TCSC*, Hawaii International Conference on Systems Sciences, January 2002.

[16] A. M. Stankovic, P. C. Stefanov, G. Tadmor, D. J. Sobajic *Dissipativity as a Unifying Control Design Framework for Suppression of Low Frequency Oscillations in Power Systems*, IEEE Transactions on Power Systems, Vol.14, No.1, February 1999, pp.192-199.

[17] M. Ghandhari, G. Andersson, I. A. Hiskens, *Control Lyapunov Functions for Controllable Series Devices*, IEEE Transactions on Power Systems, Vol.16, August 2001, pp.689-694.

[18] N. A. Tsolas, A. Arapostathis, P. P. Varaiya, *A Structure Preserving Energy Function for Power System Transient Stability Analysis*, IEEE Transactions on Circuits and Systems, Vol.32, No.10, October 1985, pp.1041-1049.

[19] M. A. Pai, *Energy Function Analysis for Power System Stability*, Kluwer Academic Publishers, 1989.

[20] H. F. Latorre, M. Ghandhari, L. Soder, *Application of Control Lyapunov Functions to Voltage Source Converters-based High Voltage Direct Current for Improving Transient Stability*, Power Tech, Lausanne, Switzerland, July 2007.

[21] V. Venkatasubramanian, H. Schattler, J. Zaborszky, *Fast Time-varying Pahsor Analysis in the Balanced Three-phase Large Electric Power System*, IEEE Transactions on Automatic Control, Vol.40, No.11, November 1995, pp.1975-1982.

[22] P. Mattavelli, G. C. Verghese, A. M. Stankovic, *Phasor Dynamics of Thyristor-Controlled Series Capacitor Systems*, IEEE Transactions on Power Systems, Vol.12, 1997, pp.1259-1267.

[23] T. H. Demiray, *Simulation of Power System Dynamics using Dynamic Phasor Models*, Ph.D. Dissertation at ETH Zurich, 2008.

[24] M. Cvetkovic, M. Ilic, *PMU Based Transient Stabilization Using FACTS*, IEEE Power System Conference and Exposition, March 2011.

[25] M. Ilic, J. Zaborszky, *Dynamics and Control of Large Electric Power Systems*, John Wiley & Sons, Inc, 2000.

[26] W. M. Haddad, V. Chellaboina, S. G. Nersesov, *Thermodynamics: A Dynamical Systems Approach*, Princeton University Press, 2005.

[27] M. Cvetkovic, M. Ilic, *Energy-Based Transient Stabilization Using FACTS in Systems With Wind Power*, IEEE Power and Energy Society General Meeting, July 2012.

[28] H. D. Chiang, F. Wu, P. Varaiya, *Foundations of Direct Methods for Power System Transient Stability Analysis*, IEEE Transactions on Circuits and Systems, Vol.34, No.2, February 1987, pp.160-173.

[29] P. Kundur, *Power System Stability and Control*, McGraw-Hill, 1997.

[30] P. W. Sauer, M. A. Pai, *Power System Dynamics and Stability*, Prentice-Hall, 1998.

[31] J. W. Chapman *Power System Control for Large Disturbance Stability: Security, Robustness and Transient Energy*, Ph.D. Thesis: Massachusetts Institute of Technology, 1996.

[32] P. M. Anderson, A. A. Fouad, *Power System Control and Stability*, Iowa State University Press, 1977.

[33] V. Venkatasubramanian, *Tools for Dynamic Analysis of the General Large Power System Using Time-varying Phasors*, International Journal of Electrical Power and Energy Systems, Vol.16, No.6, January 1994, pp.365-376.

[34] A. M. Stankovic, T. Aydin, *Analysis of Asymmetrical Faults in Power Systems Using Dynamic Phasors*, IEEE Transactions on Power Systems, Vol.15, No.3, August 2000, pp.1062-1068.

[35] E. Allen, M. Ilic, *Interaction of Transmission Network and Load Phasor Dynamics in Electric Power Systems*, IEEE Transactions on Circuits and Systems - I, Fundamental Theory and Applications, Vol.47, No.11, November 2000, pp.1613-1620.

[36] N. G. Hingorani, L. Gyugyi, *Understanding FACTS Concepts and Technology of Flexible AC Transmission Systems*, IEEE Press, 2000.

[37] K. R. Padiyar, *FACTS Controllers in Power Transmission and Distribution*, Anshan Pub, 2009.

[38] P. Moore, *Flexible AC Transmission Systems*, Power Engineering Journal, 1995.

[39] M. H. Rashid, *Power Electronics: Circuits, Devices, and Applications*, Pearson/Prentice Hall, 2004.

[40] J. G. Kassakian, M. F. Schlecht, G. C. Verghese, *Principles of Power Electronics*, Addison-Wesley, 1991.

[41] J. Vasca, L. Iannelli, *Dynamics and Control of Switched Electronic Systems* , Springer, 2012.

[42] S. R. Sanders, J. M. Noworolski, X. Z. Liu, G. C. Verghese, *Generalized Averaging Method for Power Conversion Circuits*, IEEE Power Electronics Specialists Conference, 1991, pp.333-340.

[43] S. J. Chapman, *Electric Machinery Fundamentals*, McGraw-Hill, 2005.

[44] I. Boldea, *Synchronous Generators*, Taylor & Francis, 2006.

[45] H. A. Pulgar-Painemal, P. W. Sauer, *Dynamic Modeling of Wind Power Generation*, North American Power Symposium, 2009.

[46] D. D. Siljak, *Large-scale Dynamic Systems: Stability and Structure*, North-Holland, 1978.

[47] H. K. Khalil, *Nonlinear Systems*, Prentice Hall, 1991.

[48] M. Ilic, S. Liu, *A Simple Structural Approach to Modeling and Analysis of the Inter-area Dynamics of the Large Electric Power Systems: Part I– Linearized Models of Frequency Dynamics; Part II– Nonlinear Models of Frequency and Voltage Dynamics*, Proceedings of the North American Power Symposium, Washington, DC, October 1993, pp. 560-569.

[49] M. Ilic, S. Liu, *Hierarchical Power Systems Control: Its Value in a Changing Industry (Advances in Industrial Control)*, Springer, 1996.

[50] M. Ilic, S. Liu, J. W. Chapman, *Control of the Inter-Area Dynamics Using FACTS Technologies in Large Electric Power Systems*, Proceedings of the 32nd IEEE Conference on Decision and Control, San Antonio, TX, December, 1993.

[51] M. Ilic, S. Liu, *Direct Control of Inter-area Dynamics in Large Power Systems Using Flexible AC Transmission Systems (FACTS) Technology*, U.S. patent 5 517 422, 1996.

[52] M. Ilic, Q. Liu, *Toward Standards for Model-Based Control of Dynamic Interactions in Large Electric Power Grids*, Asia Pacific Signal and Information Processing Association (APSIPA) Annual Summit and Conference 2012, Dec 2012, California, USA.

[53] Q. Liu, *A Large-Scale Systems Framework for Coordinated Frequency Control of Electric Power Systems*, Ph.D. Dissertation, August, 2013.

[54] J. E. Slotine, W. Li, *Applied Nonlinear Control*, Prentice Hall, 1991.

[55] P. V. Kokotovic, H. K. Khali, J. O'Reilly, *Singular Perturbation Methods in Control: Analysis and Design*, SIAM, 1987.

[56] J. Liu, B. H. Krogh, B. E. Ydstie, *Decentralized Robust Frequency Control for Power Systems Subject to Wind Power Variability*, IEEE Power and Energy Society General Meeting, July 2011.

[57] M. Cvetkovic, M. Ilic, *Ectropy-based Nonlinear Control of FACTS for Transient Stabilization*, IEEE Transactions on Power Systems, submitted October 2013.

[58] E. Schrdinger, *Statistical Thermodynamics*, Cambridge University Press, 1989.

[59] L. Wang, M. Klein, S. Yirga, P. Kundur, *Dynamic Reduction of Large Power Systems for Stability Studies*, IEEE Transactions on Power Systems, Vol.12, No.2, pp.889-895, May 1997.

[60] J. Ballance, B. Bhargava, G. D. Rodriguez, *Use of Synchronized Phasor Measurement System for Enhancing AC-DC Power System Transmission Reliability and Capability* Cigre, ref. C1-210, 2004.

[61] M. Cvetkovic, M. Ilic, *Interaction Variable-based Cooperative Stabilization of Interconnected Nonlinear Dynamic Systems* to be submitted 2014.

[62] S. X. Guo, *The Number of (Equilibrium) Steady-state Solutions of Models of Power Systems*, IEEE Transactions on Circuits and Systems I: Fundamental Theory and Ap-

plications, Vol.41, 1994, pp.584-600.

[63] M. Vidyasagar, *Nonlinear System Analysis*, Prentice-Hall, 1993.

[64] P. V. Kokotovic, J. J. Allemong, J. R. Winkelman, J. H. Chow, *Singular Perturbation and Iterative Separation of Time Scales*, Automatica, Vol.16, 1980, pp.23-33.

[65] M. A. Pai, P. W. Sauer, K. Khorasani, *Singular Perturbation and Large Scale Power System Stability*, Conference on Decision and Control, December 1984.

[66] T. Athay, R. Podmore, S. Virmani, *A Practical Method for the Direct Analysis of Transient Stability*, IEEE Transactions on Power Apparatus and Systems, PAS-98(2):573-584, March 1979.

[67] V. Jurdjevic, J. P. Quinn, *Controllability and stability*, Journal of Differential Equations 28, 1978, pp. 381389.

[68] R. A. Freeman, P. V. Kokotovic, *Robust Nonlinear Control Design*, Birkhuser, 1996.

[69] P. K. Iyambo, R. Tzoneva, *Transient Stability Analysis of the IEEE 14-Bus Electric Power System* AFRICON, 2007.

[70] S. K. M. Kodsi, C. A. Canizares, *Modeling and Simulation of IEEE 14 Bus System with FACTS Controllers*, University of Waterloo Technical Report #2003-3.